A role for hippocampal sharp-wave ripples in active visual search

Timothy Leonard

A DISSERTATION SUBMITTED TO THE
FACULTY OF GRADUATE STUDIES
IN PARTIAL FULFILLMENT OF THE REQUIREMENTS
FOR THE DEGREE OF
DOCTOR OF PHILOSOPHY

GRADUATE PROGRAM IN PSYCHOLOGY
YORK UNIVERSITY
TORONTO, ONTARIO

January 2017

Abstract

Sharp-wave ripples (SWRs) in the hippocampus are thought to contribute to memory formation, though this effect has only been demonstrated in rodents.

The SWR, a large deflection in the hippocampal LFP (local field potential), is known to occur primarily during slow wave sleep and during immobility and consummator behaviors. SWRs have widespread effects throughout the cortex, and are directly implicated in memory formation — their occurrence correlates with correct performance, and their ablation impairs memory in spatial memory tasks.

Though SWRs have been reported in primates, their role is poorly understood. In macaques, SWRs have been observed during quiescent states, anesthesia, and awake behavior, however whether or not SWRs play a role in memory formation, as they do in rodents, has yet to be confirmed.

This work encompasses three separate studies with the goal of determining whether there is a link between SWR occurrence and memory formation in the macaque. The first experiment (Chapter 2) first establishes the validity of the modified Change Blindness task as a memory task which is sensitive to normal hippocampal function in monkeys. The work reports behavioral performance differences for hippocampal-lesioned subjects compared to a control group. In this experiment, the hippocampal lesioned animals did not improve at the same rate, over days, as the control group, confirming that the modified Change Blindness task is indeed reliant on hippocampal function in the macaque.

Chapter 3 establishes that SWR events occur during waking (and stationary) activity, during visual search, in the macaque. Until this work, the prevalence of SWRs in macaques

during waking exploration was unknown. Additionally, analysis was performed to help confirm that the detected events were indeed SWR and not other high frequency phenomena found in the brain.

Chapter 4 shows that gaze during SWRs was more likely to be near the target object on repeated than on novel presentations, even after accounting for overall differences in gaze location with scene repetition. The increase in ripple likelihood near remembered visual objects suggests a link between ripples and memory in primates; specifically, SWRs may reflect part of a mechanism supporting the guidance of search based on experience.

The amalgamation of this work reveals several novel findings and establishes an important step towards understanding the role that SWRs play in memory formation in predominantly-visual primate brains.

Dedication

For Joanna, who has supported me every step of the way.

Acknowledgments

Please see Appendix A for a full statement of contributions.

Kari Hoffman, for her contributions and supervision throughout.

Funding: National Science and Engineering Research Council (NSERC) Discovery Grant, NSERC CREATE Vision Science and Applications, Alfred P. Sloan Foundation, Ontario Ministry for Research and Innovation Early Researcher Award, Canada Foundation for Innovation, the Krembil Foundation, Brain Canada

Chapter 2

Robert Hampton, Tom Hassett, and the Laboratory of Comparative Primate Cognition for contribution of data

Chapter 3

Jonathan M. Mikkila

Emad Eskandar, Jason L. Gerrard and Shaun R. Patel for contribution of data

Thilo Womelsdorf and Daniel Kaping for contribution of data

Table of Contents

List of Tables

List of Figures

Chapter 1 – Introduction

Sharp-wave ripples (SWRs) in the hippocampus are thought to contribute to memory formation. SWRs have been studied primarily in rodents, where they were characteristically observed during quiescent states, and more recently during ambulatory exploration where they are thought to contribute to rapid learning and decision-making. However, whether SWRs in the macaque play a role in memory formation remains unknown.

1.1 Ripple Generation

The sharp-wave ripple (SWR; ripple), the most synchronous event in the mammalian brain (Buzsáki, 1986), is a large deflection in the hippocampal LFP (local field potential), brief in duration (50-100ms), consisting of fast LFP oscillations (rodent: 130-200 Hz; see figure 2), associated with higher incidence of spike bursts in both CA1 and CA3 areas (Buzsáki, 1986). Much like the hippocampal sharpwave (SPW), the SWR occurs primarily during slow wave sleep (SWS), LIA (large irregular state) state (Vanderwolf, 1969), or in absence of theta rhythm, such as during immobility and consummator behaviors (Buzsáki, Leung & Vanderwolf, 1983; Buzsáki, 1986; Buzsáki, Horváth, Urioste, Hetke & Wise, 1992).

Both the SWR and SPW originate in the network of CA3 neurons (Buzsáki, Leung & Vanderwolf, 1983; Buzsáki, 1986). Co-participation between pyramidal cells and interneurons is through to elicit the ripple — large populations of synchronously excited CA3 cells recruit CA1 pyramidal cells, and CA1 basket and chandelier cells are also recruited that, critically, in turn promote the fast oscillatory activity in the pyramidal layer (Buzsáki, 1986; Buzsáki, Horváth, Urioste, Hetke & Wise, 1992; Ylinen et al., 1995; Csicsvari, Hirase, Mamiya & Buzsáki, 2000;

Schlingloff, Káli, Freund, Hájos & Gulyás, 2014). In transgenic mice, blocking CA3 output reduces frequency of CA1 ripple events, and experience dependent reactivation of CA1 cell pairs (Nakashiba, Buhl, McHugh & Tonegawa, 2009). It has been suggested that gap junctions, between pyramidal neurons also play a role in generating fast oscillatory activity (Draguhn, Traub, Schmitz & Jefferys, 1998). However, in contrast, it has been proposed that excitatory and inhibitory basket cells are the minimal circuitry required to induce SWRs (Schlingloff, Káli, Freund, Hájos & Gulyás, 2014).

1.2 Impact beyond hippocampus

SWRs are huge population events with widespread effects. Within the hippocampus (CA3, CA1, Subiculum, Entorhinal Cortex), 10-18% of neurons discharge synchronously during the SWR event (Csicsvari, Hirase, Czurkó, Mamiya & Buzsáki, 1999); additionally, a bursting state in CA3 cells is more common during the SWR event (Buzsáki, Leung & Vanderwolf, 1983; Mizuseki & Buzsáki, 2013). Within CA1, the SWR moves across the septotemporal axis, with the constraint that SWRs originating in the temporal segment tend to remain isolated (Patel, Schomburg, Berényi, Fujisawa & Buzsáki, 2013). From CA3 to CA1, the SWR transfers to other regions of the hippocampus in vivo (Chrobak & Buzsáki, 1996) and in vitro (Maier, Nimmrich & Draguhn, 2003). Beyond the hippocampus, SWRs have been shown to be biased by neocortical slow oscillations in rodents and humans (Siapas & Wilson, 1998; Sirota, Csicsvari, Buhl & Buzsáki, 2003; Battaglia, Sutherland & McNaughton, 2004; Wolansky, Clement, Peters, Palczak & Dickson, 2006; Isomura et al., 2006; Mölle, Yeshenko, Marshall, Sara & Born, 2006; Clemens et al., 2007; Wierzynski, Lubenov, Gu & Siapas, 2009), additionally SWR events are correlated with spindles in the somatosensory and visual areas (Ji & Wilson, 2007), reward-related activity

in the striatum (Lansink, Goltstein, Lankelma, McNaughton & Pennartz, 2009) and activity associated with rule learning in the prefrontal cortex (Wierzynski, Lubenov, Gu & Siapas, 2009; Peyrache, Khamassi, Benchenane, Wiener & Battaglia, 2009).

1.2 Replay

The widespread activation, within the hippocampus, and across the neocortex, during SWR events, has been theorized as a mechanism for synaptic plasticity, that is, strengthening the association between synaptic connections, through the repetition of firing (Hebb, 1949). The hippocampus has several features, along with SWR, making it a tantalizing brain area to consider as a possible hub of memory. For example, it has been suggested that the CA3, rich in recurrent connections (Ishizuka, Weber & Amaral, 1990) is physically wired to perform as an auto associative network able to commit associations through LTP (long-term potentiation), and pattern complete incomplete input patterns (McNaughton & Morris, 1987), which could support memory retrieval, including offline 'completion' of patterns, such as recently encoded memory traces.

Arguably one of the most important and well-studied properties of the hippocampus is the coding of location with hippocampal place cells, creating a foundation for spatial memory representations (O'Keefe J, 1971). At first, it was found that cell pairs active during waking behavior were also active during rest (Pavlides & Winson, 1989). Furthermore, patterns of cell activity, during waking activity, have been shown to reactivate in same sequence during sleep in the rat (Wilson & McNaughton, 1994; Qin, McNaughton, Skaggs & Barnes, 1997; Nádasdy, Hirase, Czurkó, Csicsvari & Buzsáki, 1999) – that is, the spatial properties, encoded into these cell sequences, are preserved during slow wave sleep. Furthermore, these reactivated

sequences are a temporally compressed version of the firing patterns observed during waking (Wilson & McNaughton, 1994), by about 10 to 20 times faster than the average travel speed of the rat through place fields (Nádasdy, Hirase, Czurkó, Csicsvari & Buzsáki, 1999; Lee & Wilson, 2002) and preferentially occur during SWR events (Nádasdy, Hirase, Czurkó, Csicsvari & Buzsáki, 1999; Kudrimoti, Barnes & McNaughton, 1999; Louie & Wilson, 2001; Lee & Wilson, 2002; Foster & Wilson, 2006; Csicsvari, O'Neill, Allen & Senior, 2007; Diba & Buzsáki, 2007). This replay, during sleep, has been shown to extend beyond the hippocampus, where cell pairs, in the hippocampus and cortex, which fired together during behavior, have also shown correlated firing activity during subsequent sleep (Qin, McNaughton, Skaggs & Barnes, 1997). Pairwise firing-rate correlations have also shown a biasing of pairwise cell activity during SWS prior to experience (Kudrimoti, Barnes & McNaughton, 1999) – that is, cell sequences that fire prior to experience, can bias population discharge which occurs during subsequent experience by the animal. Evidence of replay also extends to much larger cell ensembles, encompassing large windows of time (seconds to minutes) during REM (rapid eye movement) sleep (Louie & Wilson, 2001).

SWS replay, primarily occurring during SWR events, has been shown to occur in the same temporal order as which cell activations were experienced (Lee & Wilson, 2002) (figure 1 middle). Intriguingly, SWR replay has been found to occur not just during SWS events, but also during non-exploratory waking periods (Foster & Wilson, 2006; Csicsvari, O'Neill, Allen & Senior, 2007; Diba & Buzsáki, 2007; Davidson, Kloosterman & Wilson, 2009; Karlsson & Frank, 2009). This awake SWR replay does not have a constraint on temporal order, the replay being played

out in the same order in which the cells were activated during experience, or played out in reverse order, possibly linking trajectories to outcomes (Foster & Wilson, 2006; figure 1 right).

Though a bias exists for local events to be replayed – for example, in an open field maze, SWR replay occurred preferentially for place cells near the animals current location (Csicsvari, O'Neill, Allen & Senior, 2007) – the replayed event can be non-local, that is, not reflective of recent experience or current location (Karlsson & Frank, 2009). Furthermore, there is some degree of flexibility in how information is encoded and replay; for example, long bouts of experience may be split over several SWR events (Davidson, Kloosterman & Wilson, 2009). Additionally, replay events can even encompass non-experienced activity, depicting novel combinations of previous experience (Gupta, van der Meer, Touretzky & Redish, 2010).

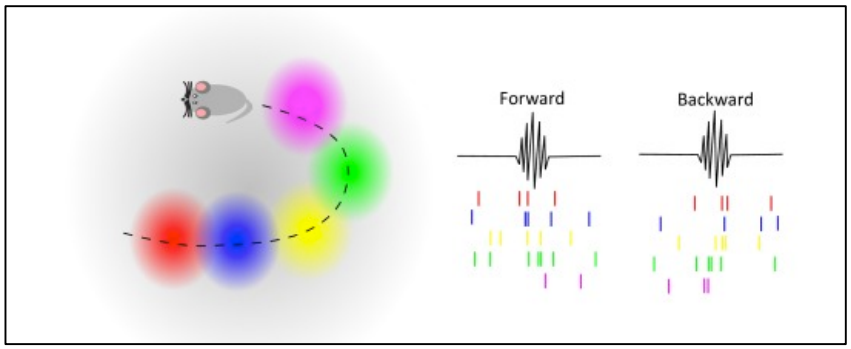

Figure 1. Illustration of forward and reverse (backward) replay in sharp wave ripples.
Adapted from (Atherton, Dupret & Mellor, 2015).

1.5 SWRs and learning

In rodents, sleep reactivation of cell ensembles active during familiar waking behavior, has been found to occur during SWR events (Gerrard, Kudrimoti, McNaughton & Barnes, 2001), increasing in rate, during SWS, after learning (Eschenko, Ramadan, Mölle, Born & Sara, 2008). Furthermore, SWRs during waking states also reflects previous experience, increasing in rate

with experience (Jackson, Johnson & Redish, 2006)(however, for examples where replay events happened preferentially on novel trials see (Foster & Wilson, 2006; Csicsvari, O'Neill, Allen & Senior, 2007). In humans, SWR rates also increase after learning, though the effect was prominent in the rhinal cortex, and not the hippocampus (Axmacher, Elger & Fell, 2008). In addition to experience, reward enhances reactivation, that is, in CA3 pyramidal cells increased participation during SWR events following reward (Ramadan, Eschenko & Sara, 2009; Singer & Frank, 2009).

SWR are directly implicated in memory formation. Occurrence of SWR during goal-directed task predicts correct performance/memory (Dupret, O'Neill, Pleydell-Bouverie & Csicsvari, 2010; Singer, Carr, Karlsson & Frank, 2013) and foreshadow future decisions (Pfeiffer & Foster, 2013). Additionally, interruption of SWRs impairs memory in spatial memory tasks, when SWRs are interrupted, post-learning, during sleep (Girardeau, Benchenane, Wiener, Buzsáki & Zugaro, 2009; Ego-Stengel & Wilson, 2010) or during waking periods (Jadhav, Kemere, German & Frank, 2012).

1.6 SWR in primates

SWR have been reported in primates, but their role is poorly characterized and poorly understood. SWR have been observed in humans, recorded from brains of epileptic patients, described with a power between 80hz – 140hz (Bragin, Engel, Wilson, Fried & Buzsáki, 1999; Bragin, Engel, Wilson, Fried & Mathern, 1999; see figure 2). Additionally, in humans, learning is followed by increase in SWR events in the rhinal cortex (Axmacher, Elger & Fell, 2008). In macaque, SWRs have been observed during quiescent states (Skaggs et al., 2007), and

anesthesia (Logothetis et al., 2012), however whether SWR play a role in memory formation, as they do in rodents, has yet to be confirmed.

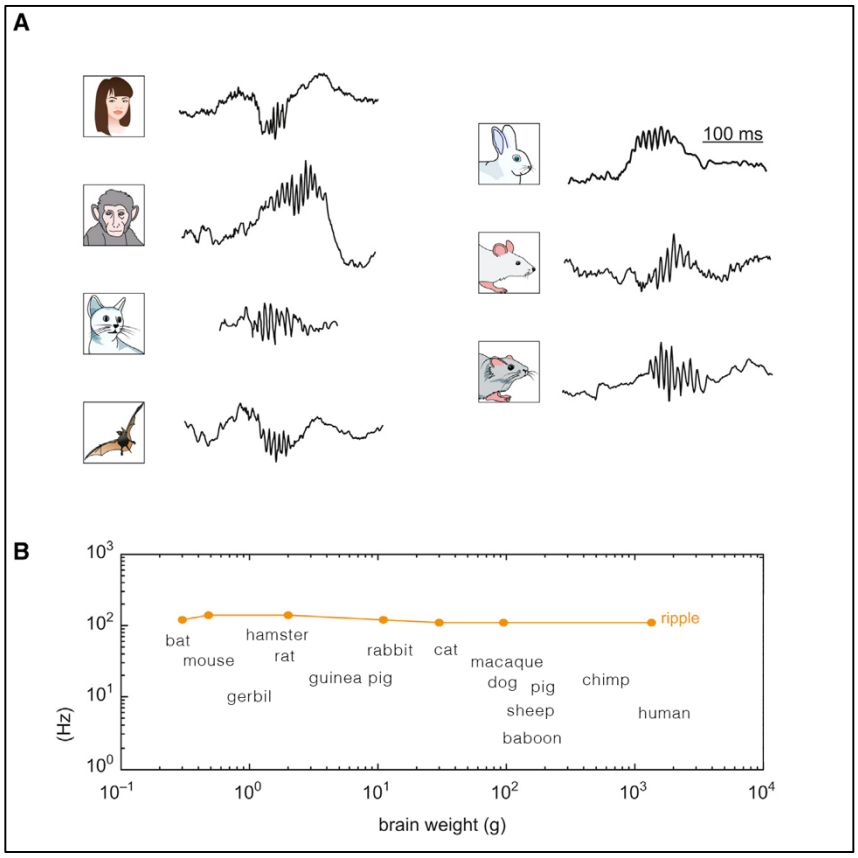

Figure 2. CA1 ripples across species.

A. Hippocampal CA1 ripples in various species. B. Brain weight vs. SWR frequency on log-log scale. There is small variation in frequency despite large change in brain size. Adapted from (Buzsáki, Logothetis & Singer, 2013).

1.7 Summary of Experiments

Chapters 2 through 4 describe three studies, with the ultimate goal of establishing if waking SWRs play a role in memory formation in the macaque. In order to do so, first an appropriate task must be established. The task must be relevant to hippocampal memory formation in the macaque, be experimentally appropriate for the macaque (locomotion type studies are not typical) for this group, and implicitly test memory. The flicker detection task,

designed to test episodic memory, requires participants to search for a changing object ('target') embedded within a scene (Chau, Murphy, Rosenbaum, Ryan & Hoffman, 2011). Shown to be an appropriate implicit test of episodic memory in macaque, the task fits the experimental requirements. However, data is lacking on the extent to which the hippocampus is required for success in this task for macaques. However, in human, successful memory formation on this task is known to require intact human medial temporal lobe (Chau, Murphy, Rosenbaum, Ryan & Hoffman, 2011), and can be used to track deficits due to Alzheimer's disease (Dragan et al., 2016). Chapter 2 reports the data from running this task with hippocampal-lesioned macaques, comparing performance over days to a control group, confirming that performance, over multiple trial repetitions on the flicker detection task, is indeed sensitive to hippocampal damage or malfunction.

Next, chapter 3 involves establishing if SWR events occur during waking (and stationary) activity, during visual search, in the macaque. In primates, SWRs have only been described during sleep (Bragin, Engel, Wilson, Fried & Buzsáki, 1999; Axmacher, Elger & Fell, 2008), quiescent wakefulness (Skaggs et al., 2007), and under anesthesia (Logothetis et al., 2012); their prevalence in waking exploration is unknown. Additionally, the detection of SWRs during exploration is complicated by non-SWR activity that occurs in overlapping 'epsilon' oscillatory bands (Freeman, 2007) ('high gamma', 'high-frequency oscillations' or HFOs (Tort, Scheffer-Teixeira, Souza, Draguhn & Brankačk, 2013). For SWRs to play a role in this task they would need to occur either during offline periods, or during search, or both. But for exploratory SWRs to be detected, we would also need to demonstrate that they were distinct from other high-frequency events associated with exploratory activity in rats.

Having established the flicker detection task does show performance differences between healthy and hippocampal lesioned macaques, and that SWR events are indeed present during macaque visual search, chapter 4 addresses the final question — whether SWR, during visual search, correlate with memory formation in the macaque. If true, this would be a completely novel finding, opening the way for many future studies around visual search, hippocampus, SWR and memory.

1.8 References

Atherton, L. A., Dupret, D., & Mellor, J. R. (2015). Memory trace replay: The shaping of memory consolidation by neuromodulation. *Trends Neurosci, 38*(9), 560-570.

Axmacher, N., Elger, C. E., & Fell, J. (2008). Ripples in the medial temporal lobe are relevant for human memory consolidation. *Brain, 131*(Pt 7), 1806-1817. doi:10.1093/brain/awn103

Battaglia, F. P., Sutherland, G. R., & McNaughton, B. L. (2004). Hippocampal sharp wave bursts coincide with neocortical "up-state" transitions. *Learn Mem, 11*(6), 697-704. doi:10.1101/lm.73504

Bragin, A., Engel, J., Wilson, C. L., Fried, I., & Buzsáki, G. (1999). High-frequency oscillations in human brain. *Hippocampus, 9*(2), 137-142. doi:10.1002/(SICI)1098-1063(1999)9:2<137::AID-HIPO5>3.0.CO;2-0

Bragin, A., Engel, J., Wilson, C., Fried, I., & Mathern, G. (1999). Hippocampal and entorhinal cortex high-frequency oscillations (100--500 Hz) in human epileptic brain and in kainic acid--treated rats with chronic seizures. *Epilepsia., 40*(2), 127-137.

Buzsáki, G. (1986). Hippocampal sharp waves: their origin and significance. *Brain Res, 398*(2), 242-252.

Buzsáki, G., Horváth, Z., Urioste, R., Hetke, J., & Wise, K. (1992). High-frequency network oscillation in the hippocampus. *Science, 256*(5059), 1025-1027.

Buzsáki, G., Leung, L. W., & Vanderwolf, C. H. (1983). Cellular bases of hippocampal EEG in the behaving rat. *Brain Res, 287*(2), 139-171.

Buzsáki, G., Logothetis, N., & Singer, W. (2013). Scaling brain size, keeping timing: evolutionary preservation of brain rhythms. *Neuron, 80*(3), 751-764. doi:10.1016/j.neuron.2013.10.002

Chau, V. L., Murphy, E. F., Rosenbaum, R. S., Ryan, J. D., & Hoffman, K. L. (2011). A Flicker Change Detection Task Reveals Object-in-Scene Memory Across Species. *Front Behav Neurosci, 5*, 58. doi:10.3389/fnbeh.2011.00058

Chrobak, J. J., & Buzsáki, G. (1996). High-frequency oscillations in the output networks of the hippocampal-entorhinal axis of the freely behaving rat. *J Neurosci, 16*(9), 3056-3066.

Clemens, Z., Molle, M., Eross, L., Barsi, P., Halasz, P., & Born, J., et al. (2007). Temporal coupling of parahippocampal ripples, sleep spindles and slow oscillations in humans. *Brain, 130*(11), 2868-2878. doi:10.1093/brain/awm146

Csicsvari, J., O'Neill, J., Allen, K., & Senior, T. (2007). Place-selective firing contributes to the reverse-order reactivation of CA1 pyramidal cells during sharp waves in open-field exploration. *Endocrinol Metab Clin North Am, 26*(3), 704-716.

Csicsvari, J., Hirase, H., Czurkó, A., Mamiya, A., & Buzsáki, G. (1999). Fast network oscillations in the hippocampal CA1 region of the behaving rat. *J Neurosci, 19*(16), RC20.

Csicsvari, J., Hirase, H., Mamiya, A., & Buzsáki, G. (2000). Ensemble patterns of hippocampal CA3-CA1 neurons during sharp wave-associated population events. *Neuron, 28*(2), 585-594.

Davidson, T. J., Kloosterman, F., & Wilson, M. A. (2009). Hippocampal replay of extended experience. *Neuron, 63*(4), 497-507. doi:10.1016/j.neuron.2009.07.027

Diba, K., & Buzsáki, G. (2007). Forward and reverse hippocampal place-cell sequences during ripples. *Nat Neurosci, 10*(10), 1241-1242. doi:10.1038/nn1961

Dragan, M. C., Leonard, T. K., Lozano, A. M., McAndrews, M. P., Ng, K., & Ryan, J. D., et al. (2016). Pupillary responses and memory-guided visual search reveal age-related and Alzheimer's-related memory decline. *Behav Brain Res, , in press* doi:10.1016/j.bbr.2016.09.014

Draguhn, A., Traub, R. D., Schmitz, D., & Jefferys, J. G. (1998). Electrical coupling underlies high-frequency oscillations in the hippocampus in vitro. *Nature, 394*(6689), 189-192.

Dupret, D., O'Neill, J., Pleydell-Bouverie, B., & Csicsvari, J. (2010). The reorganization and reactivation of hippocampal maps predict spatial memory performance. *Nat Neurosci, 13*(8), 995-1002. doi:10.1038/nn.2599

Ego-Stengel, V., & Wilson, M. A. (2010). Disruption of ripple-associated hippocampal activity during rest impairs spatial learning in the rat. *Hippocampus, 20*(1), 1-10. doi:10.1002/hipo.20707

Eschenko, O., Ramadan, W., Mölle, M., Born, J., & Sara, S. J. (2008). Sustained increase in hippocampal sharp-wave ripple activity during slow-wave sleep after learning. *Learning & Memory, 15*(4), 222-228. doi:10.1101/lm.726008

Foster, D. J., & Wilson, M. A. (2006). Reverse replay of behavioural sequences in hippocampal place cells during the awake state. *Nature, 440*(7084), 680-683. doi:10.1038/nature04587

Freeman, W. J. (2007). Definitions of state variables and state space for brain-computer interface : Part 1. Multiple hierarchical levels of brain function. *Cognitive neurodynamics, 1*(1), 3-14. doi:10.1007/s11571-006-9001-x

Gerrard, J. L., Kudrimoti, H., McNaughton, B. L., & Barnes, C. A. (2001). Reactivation of hippocampal ensemble activity patterns in the aging rat. *Behav Neurosci, 115*(6), 1180-1192.

Girardeau, G., Benchenane, K., Wiener, S. I., Buzsáki, G., & Zugaro, M. B. (2009). Selective suppression of hippocampal ripples impairs spatial memory. *Nat Neurosci, 12*(10), 1222-1223. doi:10.1038/nn.2384

Gupta, A. S., van der Meer, M. A. A., Touretzky, D. S., & Redish, A. D. (2010). Hippocampal replay is not a simple function of experience. *Neuron, 65*(5), 695-705. doi:10.1016/j.neuron.2010.01.034

Hebb, D. O. (1949). The organization of behavior. *Endocrinol Metab Clin North Am, 911*(1), 335-335.

Ishizuka, N., Weber, J., & Amaral, D. G. (1990). Organization of intrahippocampal projections originating from CA3 pyramidal cells in the rat. *J. Comp. Neurol., 295*(4), 580-623.

Isomura, Y., Sirota, A., Özen, S., Montgomery, S., Mizuseki, K., & Henze, D. A., et al. (2006). Integration and segregation of activity in entorhinal-hippocampal subregions by neocortical slow oscillations. *Neuron, 52*(5), 871-882. doi:10.1016/j.neuron.2006.10.023

Jackson, J. C., Johnson, A., & Redish, A. D. (2006). Hippocampal sharp waves and reactivation during awake states depend on repeated sequential experience. *J Neurosci, 26*(48), 12415-12426. doi:10.1523/JNEUROSCI.4118-06.2006

Jadhav, S. P., Kemere, C., German, P. W., & Frank, L. M. (2012). Awake hippocampal sharp-wave ripples support spatial memory. *Science, 336*(6087), 1454-1458. doi:10.1126/science.1217230

Ji, D., & Wilson, M. A. (2007). Coordinated memory replay in the visual cortex and hippocampus during sleep. *Nat Neurosci, 10*(1), 100-107. doi:10.1038/nn1825

Karlsson, M. P., & Frank, L. M. (2009). Awake replay of remote experiences in the hippocampus. *Nat Neurosci, 12*(7), 913-918.

Kudrimoti, H. S., Barnes, C. A., & McNaughton, B. L. (1999). Reactivation of hippocampal cell assemblies: effects of behavioral state, experience, and EEG dynamics. *The Journal of neuroscience, 19*(10), 4090-4101.

Lansink, C. S., Goltstein, P. M., Lankelma, J. V., McNaughton, B. L., & Pennartz, C. M. A. (2009). Hippocampus leads ventral striatum in replay of place-reward information. *PLoS Biol, 7*(8)

Lee, A. K., & Wilson, M. A. (2002). Memory of sequential experience in the hippocampus during slow wave sleep. *Neuron, 36*(6), 1183-1194.

Logothetis, N. K., Eschenko, O., Murayama, Y., Augath, M., Steudel, T., & Evrard, H. C., et al. (2012). Hippocampal-cortical interaction during periods of subcortical silence. *Nature, 491*(7425), 547-553. doi:10.1038/nature11618

Louie, K., & Wilson, M. A. (2001). Temporally structured replay of awake hippocampal ensemble activity during rapid eye movement sleep. *Neuron, 29*(1), 145-156.

Maier, N., Nimmrich, V., & Draguhn, A. (2003). Cellular and network mechanisms underlying spontaneous sharp wave-ripple complexes in mouse hippocampal slices. *J Physiol, 550*(Pt 3), 873-887. doi:10.1113/jphysiol.2003.044602

McNaughton, B. L., & Morris, R. G. M. (1987). Hippocampal synaptic enhancement and information storage within a distributed memory system. *Trends in Neuroscience, 10*(10), 408-415.

Mizuseki, K., & Buzsáki, G. (2013). Preconfigured, skewed distribution of firing rates in the hippocampus and entorhinal cortex. *Endocrinol Metab Clin North Am, 4*(5), 1010-1021.

Mölle, M., Yeshenko, O., Marshall, L., Sara, S. J., & Born, J. (2006). Hippocampal sharp wave-ripples linked to slow oscillations in rat slow-wave sleep. *J Neurophysiol, 96*(1), 62-70. doi:10.1152/jn.00014.2006

Nádasdy, Z., Hirase, H., Czurkó, A., Csicsvari, J., & Buzsáki, G. (1999). Replay and time compression of recurring spike sequences in the hippocampus. *J Neurosci, 19*(21), 9497-9507.

Nakashiba, T., Buhl, D. L., McHugh, T. J., & Tonegawa, S. (2009). Hippocampal CA3 Output Is Crucial for Ripple-Associated Reactivation and Consolidation of Memory. *Neuron, 62*(6), 781-787. doi:10.1016/j.neuron.2009.05.013

O'Keefe J, D. J. (1971). The hippocampus as a spatial map. Preliminary evidence from unit activity in the freely-moving rat. *Brain Res., 34*(1), 171-175.

Patel, J., Schomburg, E. W., Berényi, A., Fujisawa, S., & Buzsáki, G. (2013). Local generation and propagation of ripples along the septotemporal axis of the hippocampus. *J Neurosci, 33*(43), 17029-17041. doi:10.1523/JNEUROSCI.2036-13.2013

Pavlides, C., & Winson, J. (1989). Influences of hippocampal place cell firing in the awake state on the activity of these cells during subsequent sleep episodes. *The Journal of neuroscience, 9*(8), 2907-2918.

Peyrache, A., Khamassi, M., Benchenane, K., Wiener, S. I., & Battaglia, F. P. (2009). Replay of rule-learning related neural patterns in the prefrontal cortex during sleep. *Nat Neurosci, 12*(7), 919-926. doi:10.1038/nn.2337

Pfeiffer, B. E., & Foster, D. J. (2013). Hippocampal place-cell sequences depict future paths to remembered goals. *Nature, 497*(7447), 74-79. doi:10.1038/nature12112

Qin, Y. L., McNaughton, B. L., Skaggs, W. E., & Barnes, C. A. (1997). Memory reprocessing in corticocortical and hippocampocortical neuronal ensembles. *Philos Trans R Soc Lond B Biol Sci, 352*(1360), 1525-1533. doi:10.1098/rstb.1997.0139

Ramadan, W., Eschenko, O., & Sara, S. J. (2009). Hippocampal sharp wave/ripples during sleep for consolidation of associative memory. *PloS one, 4*(8), e6697. doi:10.1371/journal.pone.0006697

Schlingloff, D., Káli, S., Freund, T. F., Hájos, N., & Gulyás, A. I. (2014). Mechanisms of sharp wave initiation and ripple generation. *J Neurosci, 34*(34), 11385-11398. doi:10.1523/JNEUROSCI.0867-14.2014

Siapas, A. G., & Wilson, M. A. (1998). Coordinated interactions between hippocampal ripples and cortical spindles during slow-wave sleep. *Neuron, 21*(5), 1123-1128.

Singer, A. C., Carr, M. F., Karlsson, M. P., & Frank, L. M. (2013). Hippocampal SWR activity predicts correct decisions during the initial learning of an alternation task. *Neuron, 77*(6), 1163-1173. doi:10.1016/j.neuron.2013.01.027

Singer, A. C., & Frank, L. M. (2009). Rewarded outcomes enhance reactivation of experience in the hippocampus. *Neuron, 64*(6), 910-921. doi:10.1016/j.neuron.2009.11.016

Sirota, A., Csicsvari, J., Buhl, D., & Buzsáki, G. (2003). Communication between neocortex and hippocampus during sleep in rodents. *Proc Natl Acad Sci U S A, 100*(4), 2065-2069. doi:10.1073/pnas.0437938100

Skaggs, W. E., McNaughton, B. L., Permenter, M., Archibeque, M., Vogt, J., & Amaral, D. G., et al. (2007). EEG sharp waves and sparse ensemble unit activity in the macaque hippocampus. *J Neurophysiol, 98*(2), 898-910. doi:10.1152/jn.00401.2007

Tort, A. B. L., Scheffer-Teixeira, R., Souza, B. C., Draguhn, A., & Brankačk, J. (2013). Theta-associated high-frequency oscillations (110-160Hz) in the hippocampus and neocortex. *Prog Neurobiol, 100*, 1-14. doi:10.1016/j.pneurobio.2012.09.002

Vanderwolf, C. H. (1969). Hippocampal electrical activity and voluntary movement in the rat. *Electroencephalogr Clin Neurophysiol, 26*(4), 407-418.

Wierzynski, C. M., Lubenov, E. V., Gu, M., & Siapas, A. G. (2009). State-Dependent Spike-Timing Relationships between Hippocampal and Prefrontal Circuits during Sleep. *Neuron, 61*(4), 587-596.

Wilson, M. A., & McNaughton, B. L. (1994). Reactivation of Hippocampal Ensemble Memories During Sleep. *Science, 265*(5172), 676-679.

Wilson, M. A., & McNaughton, B. L. (1993). Dynamics of the hippocampal ensemble code for space. *Science, 261*(5124), 1055-1058.

Wolansky, T., Clement, E. A., Peters, S. R., Palczak, M. A., & Dickson, C. T. (2006). Hippocampal Slow Oscillation: A Novel EEG State and Its Coordination with Ongoing Neocortical Activity. *Endocrinol Metab Clin North Am, 26*(23), 6213-6229.

Ylinen, A., Bragin, A., Nádasdy, Z., Jandó, G., Szabó, I., & Sik, A., et al. (1995). Sharp wave-associated high-frequency oscillation (200 Hz) in the intact hippocampus: network and intracellular mechanisms. *J Neurosci, 15*(1 Pt 1), 30-46.

Chapter 2 – Validation of the modified flicker detection task as a test of hippocampal-dependent memory in monkeys

2.1 Introduction

Contextual cuing

Contextual cuing (see for review: (Le-Hoa Võ & Wolfe, 2015)) is when spatial configurations can contribute to improved search for an object – previously encountered patterns are implicitly remembered an used to influence later search. This effect has been demonstrated in (Chun & Jiang, 1998) where subjects had to search for a target object among an array of distractor objects. In this task, subjects were progressively faster in finding the target object, over repeated trials, when the position of target relative to the distractor objects remained consistent. The improved performance occurred independent of the subjects' ability to recognize the consistent configuration, suggesting that this was an implicit knowledge of target object position relative to other objects.

In follow up studies, the effect of consistent spatial configurations which was improving search duration, persisted up to 1 week later (Chua & Chun, 2003) and was replicated with 3d objects (Chun & Jiang, 2003). The contextual cueing effect has also been shown to influence eye movements (Peterson & Kramer, 2001), in that eye movement attends, with increasing probability, the location of the target object, based on contextual locations of the scene (here synthetic backgrounds). The eye movement pattern during context-facilitated search has been characterized as consisting of two phases, the monotonic and exploratory phase (Tseng & Li, 2004). The monotonic phase consists of a pattern of eye movements where each subsequent fixation is closer to the target location. The exploratory phase consists of subsequent fixations

that do move increasingly closer to the target location. The monotonic phase accompanies a decrease in search time, and occurs only after exploratory phases (consisting of more random search) have occurred. Though the makeup of these phases may change with age, the general effect of contextual cuing remains consistent between young and old groups (Wynn et al., 2015).

The effect of contextual cueing has been extended to search with naturalistic scenes (Brockmole & Henderson, 2006; Summerfield, Lepsien, Gitelman, Mesulam, & Nobre, 2006), extending the influence of contextual cueing, in that it likely plays a role in guiding search for relevant objects in complex scenes. The importance of the relationship between the object and scene was highlighted by a series of experiments in which memory performance was most accurate over repetition when target objects held a consistent position within scenes (Hollingworth, 2006). The importance of the contextual cuing effect has given rise to challenges against the classic image salience model for visual scene search, instead highlighting the importance of effects like contextual cuing, in understanding how visual scene search occurs (Tatler, Hayhoe, Land, & Ballard, 2010).

The role of the hippocampus in contextual cuing

The relationship between memory for object and scene was compared with a series of experiments in fornix transected and normal monkeys (Gaffan, 1994). The four experiments consisted of a typical contextual cuing task of responding to a object consistently placed among a background scene (object in scene), responding to an area in a scene (with no distinctive object), responding a particular object moved within a scene and responding to an object moved within a collection of scenes. Here, for the fornix transected group, the object in scene

task was most impaired, furthermore, learning objects among varying scenes was not impaired, suggesting an important role for the medial temporal brain regions for object in scene memory, but not object memory. More recently evidence for the role of hippocampus in object in scene search, comes from recording neuronal activity. Changes in single cell activity, in response to rapidly learning new scene-location associations, were observed in the macaque hippocampus, in that cells changed their stimulus-selective properties to become selective to particular scenes (Wirth, 2003). In humans, fMRI analysis has shown activity in the hippocampus during object in scene search, and this activity correlated with shorter trial durations (Summerfield et al., 2006). There has been a number of reviews written about the important role the hippocampus plays for recollection through the encoding and retrieval of contextual information (Aggleton, 2012; Diana, Yonelinas, & Ranganath, 2007; Eichenbaum, Yonelinas, & Ranganath, 2007) in the larger context of independent processing streams for familiarity vs recollection in the medial temporal lobe.

The strength of the contextual cuing effect, and the importance of the hippocampus for object in scene memory, would suggest that deficits should occur for hippocampal lesioned animals, in that trial durations will not reduce at the same rate as the control animals, over repetition of object in scene trials.

The flicker detection task.

The modified flicker detection task (also referred to in text as the change blindness task) has been shown to be sensitive to episodic memory, dependent on medial-temporal lobe integrity in a human patient, and superior to other tests where nonverbal report and single-trial learning are desirable (Chau, Murphy, Rosenbaum, Ryan & Hoffman, 2011).

The flicker detection task relies on contextual cuing, and as such, should be sensitive to proper hippocampal function. This previous work by Chau et al., however, did not address to what extent the hippocampus proper is required for the enhancement of performance that was associated with those trials labelled as remembered, nor was the effect tested for hippocampal dependence specifically in macaques. Establishing the role of the macaque hippocampus in this task is an important next step in assessing the validity of the modified flicker detection task as an assay of hippocampal-dependent episodic memory.

This current study reports the experimental results from comparing performance across days of the flicker detection task, between control and hippocampal-lesioned macaques. The results confirm that increases in performance attributed to learning were greater for the control group compared to the lesion group.

2.2 Methods

Subjects and apparatus.

Nine adult male rhesus monkeys (Macaca mulatta), (4 lesion, 5 control, all male) performed the task daily (see section: Task; figure 2), via individual testing rigs attached to each individual's home cage. Each rig included a laptop computer running a custom written task on NBS Presentation (Neurobehavioral Systems, Albany, CA), a 15-in. color LCD XGA (1024 pixel x 768 pixel) touch-sensitive screen (Elo TouchSystems, Menlo Park, CA), and an automatic food dispenser (Med Associates, St. Albans, VT) which delivered primate food pellets (Bio-Serv,

Frenchtown, NJ) below the screen. All procedures were conducted in accordance with the local ethics guidelines (IACUC).

Monkeys were pair-housed, had ad libitum access to water, and would participate in a testing period for 6-7 hours a day. Though multiple tasks were presented in a testing period, this task was always given first in the day. Animal pairs were separated by dividers that limited visual and physical contact between testing rigs. All subjects had prior experience with automated, touch-screen based, cognitive tests prior to the current experiment.

ID	Figure id	Group
AR		control
JC		control
L		control
R		control
S		control
AP		lesion
B		lesion
E		lesion
N		lesion

Table 1: Subject information.
Subject information for the 9 subjects. The figure id column references subject markers used in figure 3.

Lesions

MRI-guided, bilateral, excitotoxic lesions of the hippocampus were performed in six monkeys. See Hampton et al., 2004 for full details on the procedure, and figure 1 for post-surgery MRI images.

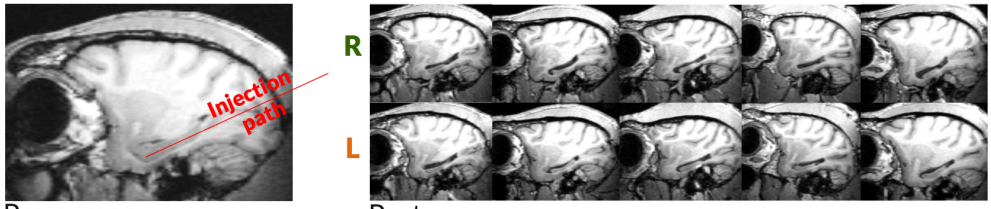

Figure 1: MRI -guided, bilateral , excitotoxic lesions of the hippocampus in five monkeys.

Task

A trial start screen appeared, with a green square on black background appearing in the middle lower portion of the screen. The subject would begin a trial by tapping this target.

The touchscreen variant of the flicker change-detection task required two taps on screen, in the target region, thereby indicating detection of a scene-unique target object. The target object was cued by appearing and disappearing within the scene in an alternating pattern every 500 ms, with an intervening 50 ms gray-screen gap that obscured the object change perceptually. Such tasks require effortful search to detect the changing part of the scene in humans and macaques (Chau et al., 2011). See previous reports (Chau et al., 2011; Hoffman et al., 2013) for more detailed descriptions of the change-detection task and its relation to hippocampal function. Shorter trial durations, after image repetition, is associated with remembering the target location (Chau et al., 2011).

Figure 2: Flicker change-detection task.

A, trial starts with black screen with green dot in lower center. Once this green square is tapped twice the visual search portion begins. The target object was cued by appearing and disappearing within the scene, in an alternating pattern, every 500 ms, with an intervening 50 ms gray-screen gap that obscured the object change perceptually. The visual search portion ends as soon as the target object is touched twice, consecutive touches, or after 30 seconds have elapsed. The Giveaway portion begins, where the scene is shown without the mask. Once the giveaway is complete, if the target object was touched twice (hit) a pellet reward was given. The trial ends with a 4 second black screen. B, each image was shown four times over 2 days. For analysis, these four presentations were coded as day of reputation (1 or 2; first row below images) plus within-day repetition (1 or 2; bottom row below images).

Each subject participated in 6 consecutive days consisting of 6 trial blocks each day. For day 1, blocks 1 and 2 consisted of 20 unique training images each (total of 40 unique training images).

Training images consisted of scenes with targets that were much larger than the rest of sets. The training images had targets that were on average 6.5 times larger than the testing sets. The control and lesion group found 98% and 97.5% respectively, of the targets in the

training images. Blocks 3 through 6 consisted of 15 new images, shown twice, plus 9 highly frequent (HF) images, for a total of 39 images per block. The HF images were not novel and a subset of which were randomly selected each day from a common pool of images.

Days 2 through 6 started with two repetition blocks, duplicates of blocks 3 and 4 from the previous day, though the HF images were randomized. Blocks 3-6 followed the same structure as day 1, each featuring 15 new images, shown twice, plus 9 HF images, for a total of 39 images per block.

For each subject, there were 360 unique images, 360 images presented twice (both on day n), 150 images presented three times, and 150 images presented four times (both on day n + 1).

For all images (presentations 1 through 4, and HF) the order was pseudo random, optimized so that target overlap was minimized across consecutive images (for every 10 consecutive images, the target locations are optimally separated using a brute force algorithm). No image ever had a target position that overlapped with the trial start target position. Three sessions were excluded for one subject due to experimenter error.

Statistics

Trial duration

Trial durations were predicted using a mixed effects multivariate linear regression (ordinary least squares algorithm), on group membership (control or lesion; coded 0,1 respectively), with subject term as mixed effects. Additional factors included in the model were image presentation number, coded by both day of image presentation (Day of Repeat; 1 or 2); and presentation number within day image was shown (Within Day Repeat; 1 or 2).

An interaction term between both of the factors coding image presentation number, and group membership (control or lesion) was included in order to determine to what extent trial durations change over image presentations, and if a change in durations, across days, is affected by group membership.

All p values associated with the estimates in the model have been corrected using the Bonferonni multiple comparisons method (7 pairwise comparisons, 5 main terms + 2 interactions).

Touch rate

A second model was built to predict touch rate based on group (control or lesion), and the image presentation number, coded by both day of image presentation (Day of Repeat; 1 or 2), and presentation number within day image was shown (Within Day Repeat; 1 or 2). See figure 2b (bottom) for an example of how the image presentation number was coded. An interaction term between both of the factors coding image presentation number, and group membership (control or lesion) was also added to the model. The interaction terms were added in order to test if the touch rate varied as a function of number of presentations of the image.

For group, control was coded as 0, and lesions as 1, so that results are expressed as effect of lesion in comparison to control.

All p values associated with the estimates in the model have been corrected using the Bonferonni multiple comparisons method (6 pairwise comparisons, 4 main terms + 2 interactions).

2.4 Results

In total, 8264 trials (control: 4484, lesion: 3780) consisting of image presentations 1 through 4, from 294 sessions (control: 162, lesion: 132) were included in the analysis.

Effect of lesions on trial performance

To understand if performance on the trial was different between groups (control vs. lesion), a multivariate regression model compared which factors affected trial performance (described as trial duration). Trial duration was predicted on group (control or lesion), touch rate, day of image (1 or 2), and presentation number within day image was shown (1 or 2), a mixed effects error term was added for subject id. Interaction terms were set between group and day of image, as well as group and repeat within day of image. The interaction terms are included to detect if performance between groups is differentially changing over repetitions.

Name	Estimate	CI	SE	t	p
(Intercept)	10.718	[8.84, 12.6]	0.960	11.168	6.55E-28
Group	-2.071	[-4.81, 0.66]	1.395	-1.484	n.s
Touch Rate	-0.062	[-0.22, 0.09]	0.079	-0.786	n.s
Day of Repeat	-1.461	[-1.95, -0.97]	0.249	-5.871	3.16E-08
WD Repeat	-3.028	[-3.47, -2.59]	0.226	-13.417	8.91E-40
Group x Day of Repeat	0.844	[0.12, 1.57]	0.369	2.287	n.s
Group x WD Repeat	2.129	[1.47, 2.78]	0.334	6.378	1.32E-09

Table 2: Regression results - Model predicts trial duration.

Fixed effect coeffeccients, with 95% Cis, for the random effects model. Both types of repeat predict shorter trial durations, with the largest effect for withing day repeats (WD), with a 3 second reduction in trial duration for the 2nd compare to 1st image presentation. The largest effect for differences between groups was for the interaction of group by within day repeat. On the 2nd repeat of the day, the hipocampal group averaged trial dirations 2.1 seconds longer than the control group. All p values corrected using the Bonferonni method. WD = Within Day. n.s = non significant p value.

Through the overall mean trial duration was 8.56s (95% bootstrap, n=10,000 ci: [8.32 8.80]) for the control group, and 7.78s [7.53 8.02] for lesion group. The Group x Within Day interaction term revealed a difference in trial duration, for both repeat types, when comparing lesion to control groups. Comparing duration of trial, across the two days an image was presented, on day 2 of image presentation, the trials were .95 seconds longer for the lesion group compared to the control group ($p<.05$; table 2**,** factor: Group x Day of Repeat). The trial duration was also longer for lesion groups, when comparing the image presentations within a day, where the 2nd image presentation in a day was 2.25 seconds longer for the lesion group compared to the control group.

Effects of image presentation on trial duration. Averaging across all other factors, on the second day of image presentation, trial duration is 1.5 seconds quicker ($p < 0.001$; table 2, factor: Day of Repeat). Furthermore, again averaging across all other factors, the second time an image is shown, the trial duration is 3 seconds quicker ($p < 0.001$; table 2, factor: Within Day Repeat).

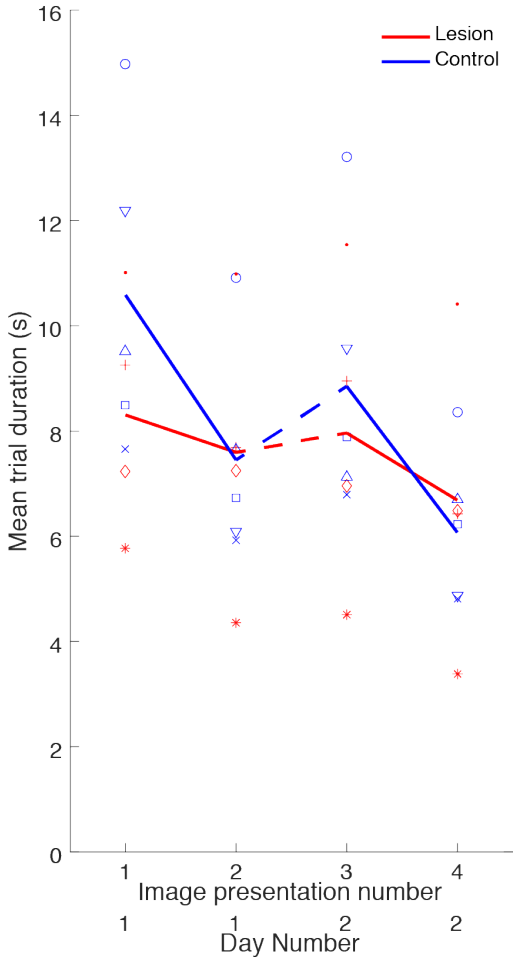

Figure 3: Mean trial durations for Lesion and Control groups.
Within day portions of trial shown in solid lines. Individual data points for each subject shown.

	Mean [ci]
Group	
control	8.56 [8.33 8.80]
lesion	7.78 [7.54 8.03]
Touch Rate	3.44 [3.40 3.47]
Within Day Repeat	
1	9.22 [8.96 9.48]
2	7.18 [6.97 7.40]
Day of Repeat	
1	8.52 [8.32 8.73]
2	7.40 [7.12 7.71]

Table 3: Summary of trial durations grouped by main effects.
Mean trial durations shown. Confidence intervals (ci) are bootstrapped mean values (10,000 permutations).

Group	Within Day 1	Within Day 2	Day 1	Day 2
control	10.08 [9.71 10.44]	7.05 [6.78 7.35]	9.01 [8.73 9.31]	7.46 [7.08 7.87]
lesion	8.21 [7.86 8.58]	7.34 [7.01 7.68]	7.95 [7.67 8.27]	7.33 [6.90 7.80]

Table 4: Summary of interaction terms in model.
Mean trial durations shown. Confidence intervals (ci) are bootstrapped mean values (10,000 permutations).

Touch rate

Hyperactive behavior has been found in bilateral hippocampal lesions in rats (Kimble 1963; Nadel 1968; Fanselow 2000). Because hyperactivity could act as a potential confound, it was important to determine if any such hyperactivity pattern existed between our groups, and if so, control for its effect. Additionally, it was important to establish if any other factors were predictive of touch rate, or if it was entirely attributable to group membership. As a behavioral comparison, the number of screen touches was compared between lesion and control groups using a linear regression model.

The touch rate was compared across groups, and image repetitions, using a regression model, in order to determine which factors affect touch rate. Touch rate (touch/second) was predicted on group (control or lesion), day of image (Day of Repeat; 1 or 2), and presentation number within day image was shown (Within Day Repeat; 1 or 2). Interaction terms were set between group and day of image, as well as, group and repeat within day of image. Of all terms, only group membership predicted a change in touch rate, 1.04 touch/second higher for the lesion group compared to the control group ($p < 4.35x10^{90}$). All other factors in the model were non-significant predictors of touch rate. See Appendix B for supplemental touch rate results and descriptive statistics.

	Estimate	SE	t	p
(Intercept)	2.9833	0.0347	86.02	0
Group	1.0440	0.0511	20.43	**4.35×10^{-89}**
Day of Repeat	-0.0959	0.0491	-1.95	n.s
Within Day Repeat	-0.0445	0.0446	-1.00	n.s
Group x Day of Repeat	0.0241	0.0729	0.33	n.s
Group x Within Day Repeat	0.1077	0.0660	1.63	n.s

Table 5: Regression results on touch rates.

Model predicts touch rate ($F(8258) = 226$, $p = 4.7 \times 10^{227}$). P values corrected using the Bonferonni method. The Lesion group is touching the screen, on average, 1 touch/second more than control group, this rate is not affected by day of repeat or number of repeat within day.

2.5 Discussion

Where the lesion group at first appears to complete trials faster overall, when controlling for effects of repetition and touch rate, the control group shows better performance after image repetition for both within day repetition factors. This effect can be seen in figure 3 – overall, the control groups rate of performance increase is higher. Put another way, though the hippocampal group has shorter trial durations on day 1, presentation number 1, they fail to improve at the same rate the control group does. The hippocampal group may be benefiting from hyperactive behavior initially, however fail to benefit from repetition in the same way the control group does. It may be that the hyperactive touching confers an initial advantage, where the target is found quickly, but not deliberately like the control group. In later trials, the lesioned animals must rely mostly on the hyperactive touching strategy, unable to rely on memory to the extent that the control animals do.

These results extend the findings from Chau et al. (2011). Though lesioned animals were still able to perform the task, that they did experience deficits when compared to the control group, confirms that the flicker detection task is indeed a memory task that is sensitive to hippocampal function in macaques.

In future work, it should be noted that hippocampal deficits may not be detectable if trial repeats are shown between-day only. It would be very interesting to see if this effect would gain more power if an analysis was done over multiple days, and to what extent the control group could end up ultimately out-performing the lesion group.

Finally, as a follow up to this work, it may be advisable to include restrictions or penalty associated with number of touches. However, this type of behavioral intervention during a task can introduce unforeseen training difficulties, and so the advantages should be carefully weighted before implementation.

2.5 References

Aggleton, J. P. (2012). Multiple anatomical systems embedded within the primate medial temporal lobe: Implications for hippocampal function. *Neuroscience and Biobehavioral Reviews*. https://doi.org/10.1016/j.neubiorev.2011.09.005

Brockmole, J. R., & Henderson, J. M. (2006). Using real-world scenes as contextual cues for search. *Visual Cognition*, *13*(1), 99–108. https://doi.org/10.1080/13506280500165188

Bonferroni, C. E., Teoria statistica delle classi e calcolo delle probabilità, Pubblicazioni del R Istituto Superiore di Scienze Economiche e Commerciali di Firenze 1936

Chau, V. L., Murphy, E. F., Rosenbaum, R. S., Ryan, J. D., & Hoffman, K. L. (2011). A Flicker Change Detection Task Reveals Object-in-Scene Memory Across Species. *Front Behav Neurosci, 5*, 58. doi:10.3389/fnbeh.2011.00058

Chua, K.-P., & Chun, M. M. (2003). Implicit scene learning is viewpoint dependent. *Perception & Psychophysics*, *65*(1), 72–80. https://doi.org/10.3758/BF03194784

Chun, M. M., & Jiang, Y. (1998). Contextual cueing: implicit learning and memory of visual context guides spatial attention. *Cognitive Psychology*, *36*(1), 28–71. https://doi.org/10.1006/cogp.1998.0681

Chun, M. M., & Jiang, Y. V. (2003). Implicit, long-term spatial contextual memory. *Journal of Experimental Psychology: Learning, Memory, and Cognition*, *29*(2), 224–234. https://doi.org/10.1037/0278-7393.29.2.224

Diana, R. A., Yonelinas, A. P., & Ranganath, C. (2007). Imaging recollection and familiarity in the medial temporal lobe: a three-component model. *Trends in Cognitive Sciences*, *11*(9), 379–386. https://doi.org/10.1016/j.tics.2007.08.001

Eichenbaum, H., Yonelinas, A. P., & Ranganath, C. (2007). The medial temporal lobe and recognition memory. *Annual Review of Neuroscience*, *30*, 123–52. https://doi.org/10.1146/annurev.neuro.30.051606.094328

Fanselow, M. S. (2000). Contextual fear, gestalt memories, and the hippocampus. In *Behavioural Brain Research* (Vol. 110, pp. 73–81). https://doi.org/10.1016/S0166-4328(99)00186-2

Gaffan, D. (1994). Scene-Specific Memory for Objects: A Model of Episodic Memory Impairment in Monkeys with Fornix Transection. *Journal of Cognitive Neuroscience*, *6*(4), 305–320. https://doi.org/10.1162/jocn.1994.6.4.305

Hampton, R. R., Buckmaster, C. A., Anuszkiewicz-Lundgren, D., & Murray, E. A. (2004). Method for making selective lesions of the hippocampus in Macaque monkeys using NMDA and a longitudinal surgical approach. Hippocampus, 14(1), 9–18. https://doi.org/10.1002/hipo.10150

Hollingworth, A. (2006). Scene and position specificity in visual memory for objects. *Journal of Experimental Psychology. Learning, Memory, and Cognition*, *32*(1), 58–69. https://doi.org/10.1037/0278-7393.32.1.58

Hoffman, K. L., Dragan, M. C., Leonard, T. K., Micheli, C., Montefusco-Siegmund, R., & Valiante, T. A. (2013). Saccades during visual exploration align hippocampal 3-8 Hz rhythms in human and non-human primates. *Frontiers in Systems Neuroscience*, *7*, 43. https://doi.org/10.3389/fnsys.2013.00043

Kimble, D. P. (1963). The effects of bilateral hippocampal lesions in rats. *Journal of Comparative and Physiological Psychology*, *56*(2), 273–283. https://doi.org/10.1037/h0048903

Le-Hoa Võ, M., & Wolfe, J. M. (2015). The role of memory for visual search in scenes. *Annals of the New York Academy of Sciences*, *1339*(1), 72–81. https://doi.org/10.1111/nyas.12667

Nadel, L. (1968). Dorsal and Ventral Hippocampal Lesions and Behavior'. *Physiology and Behavior*, *3*, 891–900. https://doi.org/10.1016/0031-9384(68)90174-1

Peterson, M. S., & Kramer, a F. (2001). Attentional guidance of the eyes by contextual information and abrupt onsets. *Perception & Psychophysics*, *63*(7), 1239–1249. https://doi.org/10.3758/BF03194537

Summerfield, J. J., Lepsien, J., Gitelman, D. R., Mesulam, M. M., & Nobre, A. C. (2006). Orienting attention based on long-term memory experience. *Neuron*, *49*(6), 905–916. https://doi.org/10.1016/j.neuron.2006.01.021

Tatler, B. W., Hayhoe, M. M., Land, M. F., & Ballard, D. H. (2010). Eye guidance in natural vision: reinterpreting salience. *Journal of Vision*, *11*(5), 5. https://doi.org/10.1167/11.5.5

Tseng, Y.-C., & Li, C.-S. R. (2004). Oculomotor correlates of context-guided learning in visual search. *Perception & Psychophysics*, *66*(8), 1363–1378. https://doi.org/10.3758/BF03195004

Wirth, S. (2003). Single Neurons in the Monkey Hippocampus and Learning of New Associations. *Science*, *300*(5625), 1578–1581. https://doi.org/10.1126/science.1084324

Wynn, J., Bone, M., Dragan, M., Hoffman, K., Buchsbaum, B., & Ryan, J. (2015). Selective scanpath repetition supports memory-guided visual search. *Journal of Vision*, *15*(12), 789. https://doi.org/10.1167/15.12.789

Chapter 3 - Sharp wave ripples during visual exploration in the primate hippocampus

This chapter is adapted from the following paper:

Leonard, T. K., Mikkila, J. M., Eskandar, E. N., Gerrard, J. L., Kaping, D., Patel, S. R., Hoffman, K. L. (2015). Sharp Wave Ripples during Visual Exploration in the Primate Hippocampus. *The Journal of Neuroscience : The Official Journal of the Society for Neuroscience*, *35*(44), 14771–82. https://doi.org/10.1523/JNEUROSCI.0864-15.2015

3.1 Preface

Hippocampal sharp wave ripples (SWRs) are highly synchronous oscillatory field potentials that are thought to facilitate memory consolidation. Sharp-wave ripples typically occur during quiescent states, when neural activity reflecting recent experience is replayed. In rodents, SWRs also occur during brief locomotor pauses in maze exploration, where they appear to support learning during experience. In this study, we detected SWRs that occurred during quiescent states, but also during goal-directed visual exploration in non-human primates (*Macaca mulatta*). The exploratory SWRs showed similar peak frequency bands to quiescent SWRs, and both types were inhibited at the onset of their respective behavioral epochs. In apparent contrast to rodent SWRs, these eexploratory SWRs occurred during active periods of exploration, e.g. while animals searched for a target object in a scene. SWRs were associated with smaller saccades, longer fixations, and when they coincided with target-object fixations during search, detection was more likely than if these events were decoupled. Although we observed high gamma-band field potentials of similar frequency to SWRs, only the SWRs accompanied greater spiking synchrony in neural populations. These results reveal that SWRs

are not limited to offline states as conventionally defined; rather, they occur during active and informative performance windows. The exploratory SWR in primates is an infrequent occurrence associated with active, attentive performance, which may indicate a new, extended role of SWRs during exploration in primates.

3.2 Significance statement

Sharp-wave ripples (SWRs) are high-frequency oscillations that generate highly-synchronized activity in neural populations. Their prevalence in sleep and quiet wakefulness, and the memory deficits that result from their interruption, suggest that SWRs contribute to memory consolidation during rest. Here, we report that SWRs from the monkey hippocampus occur not only during behavioral inactivity but also during successful visual exploration. SWRs were associated with attentive, focal search and appeared to enhance perception of locations viewed around the time of their occurrence. SWRs occurring in rest are noteworthy for their relation to heightened neural population activity, temporally-precise and widespread synchronization, and memory consolidation, therefore the SWRs reported here may have similar impact on neural populations, even as experiences unfold.

3.3 Introduction

The sharp wave ripple (SWR) is a highly synchronized hippocampal field potential complex that is associated with widespread activation of the neocortex (Chrobak, & Buzsáki, 1994; Siapas, & Wilson, 1998; Sirota et al., 2003; Battaglia et al., 2004; Isomura et al., 2006; Mölle et al., 2006; Logothetis et al., 2012). During SWRs, internally generated sequences of cell-specific firing (‘replay’) occur locally (Wilson, & Mcnaughton, 1994; Kudrimoti et al., 1999; Csicsvari et al., 2000; Gerrard et al., 2001; Louie, & Wilson, 2001; Foster, & Wilson, 2006), and

at remote neocortical sites (Qin et al., 1997; Ji, & Wilson, 2007; Peyrache et al., 2009; Benchenane et al., 2010). Both SWRs and these replay events, are most frequently observed during slow-wave sleep (SWS) and periods of waking immobility; furthermore, interruption of SWRs during these states leads to memory deficits (Girardeau et al., 2009; Ego-stengel, & Wilson, 2010). As a result, SWRs are widely considered to underlie memory consolidation during quiescence (Buzsáki, 1989; Buzsáki, 1996; Hoffman et al., 2007; Battaglia et al., 2011).

Sharp wave ripples, however, are also seen during active waking states, termed 'exploratory' SWRs or *eSWRs* (O'neill et al., 2006). In rats, their occurrence during goal-directed tasks predicts correct performance/memory (Dupret et al., 2010; Singer et al., 2013; Pfeiffer, & Foster, 2013) and their interruption during these active states impairs task performance (Jadhav et al., 2012). Detection criteria for eSWRs require low to no movement velocity, to prevent false-positive detection of theta-related high-frequency activity seen during running (but see (Kemere et al., 2013). Although eSWRs, by definition, occur during slow or no movement during the task, their occurrence during the task opens up a broader interpretation of SWRs, that includes a role in learning or recollection within epochs of exploration, decision making, and goal acquisition (O'neill et al., 2010; Carr et al., 2011; Girardeau, & Zugaro, 2011; Pezzulo et al., 2014; Yu, & Frank, 2015).

In humans and macaques, sharp wave ripples have only been described during inactive states, during extended periods of quiescence including slow-wave sleep (*qSWR:* quiescent state SWRs) or during inattentive, quiet wakefulness in an experimental booth or bedside – but in any case with relative inactivity and immobility during waking, termed *iSWR* in rats (*iSWR:* waking 'inactive' SWRs (Bragin et al., 1999; Skaggs et al., 2007; Axmacher et al., 2008; Le van

quyen et al., 2008; Le van quyen et al., 2010; Logothetis et al., 2012). It is as yet unclear whether or not SWRs also play a role in goal-directed visual exploration in primates, e.g. visual scanning behaviors observed as sequences of gaze fixations in which different parts of a scene are successively foveated. Such visual search comprises a major – even default – class of exploration that supports learning of one's surroundings and that generalizes across many primate species, including humans. If SWRs in primates occur as they do in rats, we expect that SWRs should occur during goal-directed visual exploration tasks.

Here, we set out to determine the behavioral states and behavioral correlates when primate SWRs occur and to compare characteristics of SWR events to those of high-gamma (~80-120 Hz) and high-frequency oscillations (HFOs: 110-160 Hz) that occur during exploration and other active waking behaviors (Csicsvari et al., 1999; Scheffer-teixeira et al., 2012; Tort et al., 2008; Sullivan et al., 2011; Jackson et al., 2011; Tort et al., 2013; Buzsáki, & Schomburg, 2015). Studies of SWRs in humans and monkeys have not evaluated the relationship between these high-frequency events and sharp-wave ripples with overlapping frequency bands, though conventional methods could falsely detect these events as SWRs. We found that SWRs differed from other high-frequency events, and that they appeared not only in quiescence, but also during goal-directed visual exploration, and at higher rates when coinciding with target fixations on successful trials.

3.4 Methods

Subjects and experimental design

Four adult macaques (*Macaca mulatta*; two female, and two male) completed visual target detection tasks during daily recording sessions. Each animal completed one of three

specific task variations, but all required the animals to find and select a correct target object from non-targets, within a visual array, for fluid reward. Cues that determined the correct visual target were photorealistic visual scenes for M1, M2 and M3 and simple color cues for M4. Both M1 and M2 performed a flicker change detection task, requiring that gaze remains in the target region for a prolonged (>800ms) 'selection' duration, thereby indicating detection of a scene-unique target object. The target object was cued by appearing and disappearing within the scene, in alternation, every 500ms, with an intervening 50ms gray screen gap that obscured the object change perceptually. Such tasks require effortful search to detect the changing part of the scene in humans and macaques (Chau et al., 2011). See previous reports (Chau et al., 2011; Hoffman et al., 2013) for more detailed descriptions of the change detection task and its relation to hippocampal function. M3 also learned scene-object associations, but the correct (i.e. fluid rewarded) response required manual selection of the correct response object from an array that followed scene presentation. Most of the scene-object location pairings were new each day, and learned by trial and error during the session, whereas a well-learned subset of pairings were repeated daily. M4 performed a task requiring visually-cued target selection (selective attention) that led to an additional conditional visuomotor response (Shen et al., 2015). The initial visual cue was a color indicating the correct target object to attend on that trial; changes in this target indicated the correct response location (the conditional visuomotor response), whereas changes in non-targets indicated alternate response locations. The conditional response – a saccade to the correct response location immediately following the target object change – disambiguated which target had been attended.

For all animals, an inter-trial interval (ITI) followed each trial. ITIs lasted 2-20s; both room and screen were darkened throughout the epoch. We took these periods as quiet waking 'inactive' behavioral epochs (iSWRs), as they follow immediately reward on correct trials, and marked a transition between the end of one trial and the beginning of the next, akin to startbox or reward locations in rat experiments. Finally, for M1, M2, and M3, the daily sessions began and ended with a period of at least 10 minutes when no stimulus was presented within the darkened booth and animals were allowed to sleep or sit quietly (quiescent period, for 'qSWRs').

Eye movements were recorded using video-based eye tracking (M1, M2: iViewX Hi-Speed Primate remote infrared eye tracker, SensoMotoric Instruments, SMI, Berlin, Germany; M3,M4: iScan, ISCAN Inc, Woburn, MA). Infrared tracking allows monitoring of eye movements only when the eye is open, calibrated to the display screen, therefore in the present study, signal is shown only in case of such eye movements. All experimental protocols were conducted with approval from the local ethics and animal care authorities.

Electrophysiological Recordings

Animals M1-3 were implanted chronically with platinum/tungsten multicore tetrodes (96 micron outer diameter; Thomas Recordings, Giessen, Germany) lowered into the CA3/DG region of hippocampus. M4 was recorded with 125 and 200 micron tungsten microelectrodes (FHC, Bowdoinham, ME) lowered daily, with trajectories aimed at CA3/DG and CA1/Subiculum. Locations are estimated from chamber insert locations in MR images (M4), from post-explant MR images (M1) and from MR/CT coregistration of electrode position (M2), and on functional characterization based on expected white/gray matter and ventricle transitions in depth during

lowering, followed by the appearance of SWRs (M1, M2, M3; Figure 1 a,b,e). We observed SWRs only in limited ranges of depth across the chronically implanted tetrodes, within which we encountered single units. These units were predominantly complex spiking, or 'bursting' cells, with proportions matching hippocampal distributions (88%) rather than the lower proportions characteristic of surrounding areas (Skaggs et al., 2007). Unlike rodent dorsal CA1, we did not observe sharp wave polarity reversals across the cell layer.

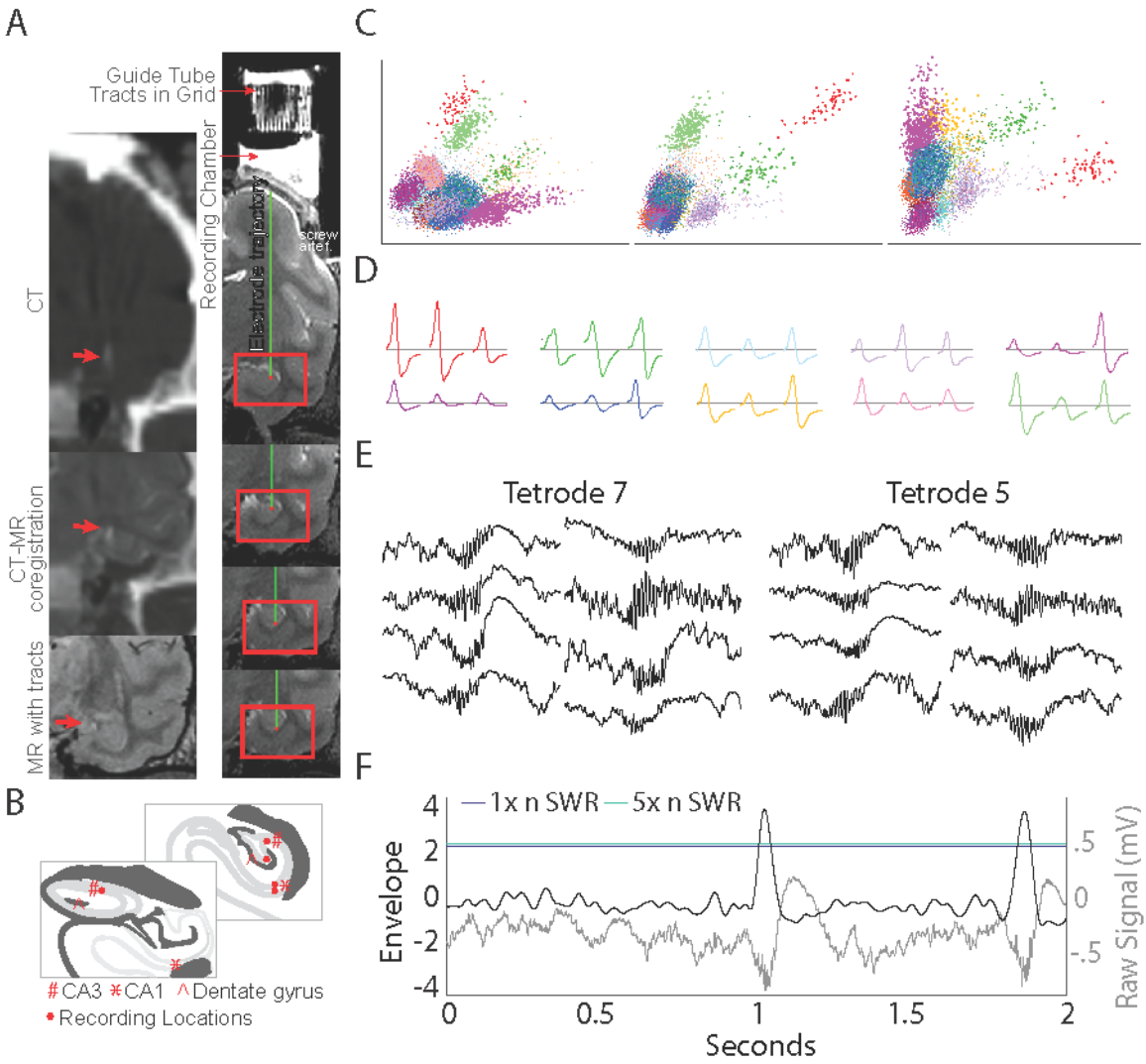

Figure 1: Electrophisological descriptions.

a. Coronal MR and CT images of hippocampal electrode trajectories. CT image of tract (top) coregistered and superimposed on MR image (middle) shows the electrode tip (white puff) registered to CA3/DG of hippocampus for

M3 (indicated in b), closely matching the MR with tracts seen for M1 (bottom). The top panel of the right series of MR images shows the location of the recording chamber on the skull for M4, with electrode grid locations (white vertical tracts). The reconstructed electrode trajectory (green) and tip locations (red) reveal the hippocampal recording sites, primarily in CA3/DG. **b**. Schematic drawings of coronal sections of the hippocampal formation. Red dot: recording locations; #: CA3; * CA1; ^ Dentate gyrus. Illustrations adapted from (Saleem, & Logothetis, 2012). **c.** Spike scatter plots from recordings on one tetrode based on energy (same tetrode and session as in d and e). **d.** Examples of the average waveforms of units isolated from one tetrode, during the same session in which SWRs were recorded (shown in e). Waveforms are shown inverted, by convention. **e.** Broadband traces of SWR events from m1. Tetrode 7 was used for SWR detection in this session; the simultaneously-recorded activity on Tetrode 5 is shown on the corresponding row. SWRs were observed in a limited range of depth across the chronically implanted tetrodes, where units were also observed (c and d). **f**. Illustration of the ripple envelope threshold method calculated for a single session and applied to an example segment of signal containing 2 SWRs. Shown in black is an example segment of the recorded signal that contains two ripples. The filtered signal envelope (final detection step) is shown in grey. An envelope zscore of 3 (original signal) is shown by a blue horizontal line, and the change in this threshold after simulating a 500% increase in SWR events is shown in green (see methods), revealing a relative tolerance of the threshold method to large changes in ripple rates.

For M4, local field potentials (LFPs) were digitally sampled at 1 kHz using a multichannel processor (Map System, Plexon, Inc., M2) and for M1-3 potentials were sampled at 32 kHz using a Digital Lynx acquisition system (Neuralynx, Inc., Bozeman, Montana, USA) and filtered between 0.5 Hz and 2 kHz. The recording chamber was used as reference for all but M1, who had a local reference at the end of the array 'bundle', ~5mm above the recording sites. Single unit activity was sampled at 32 kHz and filtered between 600 Hz and 6 kHz, recording the waveform for 1 ms around a threshold-triggered "spike" event. Single units were isolated using MClust software based on waveshape principle components, energy, peak/valley and width, across channels (Figure 1 c,d). Care was taken to include only cells that were well isolated, based on < 1% ISIs within 2ms and cross-correlograms between bursting cell pairs had to be free of burst-latency peaks (asymmetric, <10ms peak that could indicate the erroneous splitting of one complex spiking unit into two; see (Harris et al., 2000). The complex spiking (CS) group included bursting cells (ISI mode peak <10 ms, comprising >= 10% of ISIs, and with < 1 Hz overall

firing rate window). Putative interneurons were cells with > 1 Hz overall firing rate and no apparent burst mode (<10 ms) in the ISI histogram.

Hippocampal field potentials change with vigilance state and behaviors, though the patterns observed in human and monkeys (Bódizs et al., 2001; Uchida et al., 2001; Cantero et al., 2003; Moroni et al., 2007; Tamura et al., 2013) differ from those that are well-characterized in rats (Vanderwolf, 1969; Winson, 1972; Whishaw, & Vanderwolf, 1973; Buzsáki et al., 1983; Buzsáki, 1986; Blumberg, 1989). To replicate previous studies' characterization of hippocampal fields during different behavioral states (Clemens et al., 2013; Tamura et al., 2013), and to extend the observations to the present study's behavioral paradigm, we displayed examples of the spectral content of wideband LFP in 3s-second segments taken during search and rest, for the two animals (M1, M2) who had both extended search and quiescent epochs during recordings. Spectra were calculated from the short-time Fourier transform of 600ms segments, shifted in 6 ms increments, windowed with a Hamming window, 1/f normalized ('whitened'), and z-transformed. Traces, superimposed on onto each spectrogram, corresponding to the raw signal underlying each spectrogram, were taken from the z-score transform of the entire session from which each epoch was taken. (Figure 2). In addition, overall spectral power differences between epochs were calculated from the FFT transforms of the full duration of search and quiescent behavioral epochs, where the mean quiescent FFT epoch value was subtracted from the mean FFT search epoch value and min-max normalized (with a scale from 0 to 1), to compare to previously-reported differences in spectral content by behavioral/vigilance state (Figure 2b). Differences in spectral content are apparent across behavioral epochs, in both animals' recordings. Specifically, power in low frequencies, including 6-10 Hz 'theta', is stronger

during quiescent states than during active goal-directed behaviors, consistent with microelectrode recordings in macaques and macroelectrode recordings in humans, localized to the hippocampal formation (Clemens et al., 2013; Tamura et al., 2013).

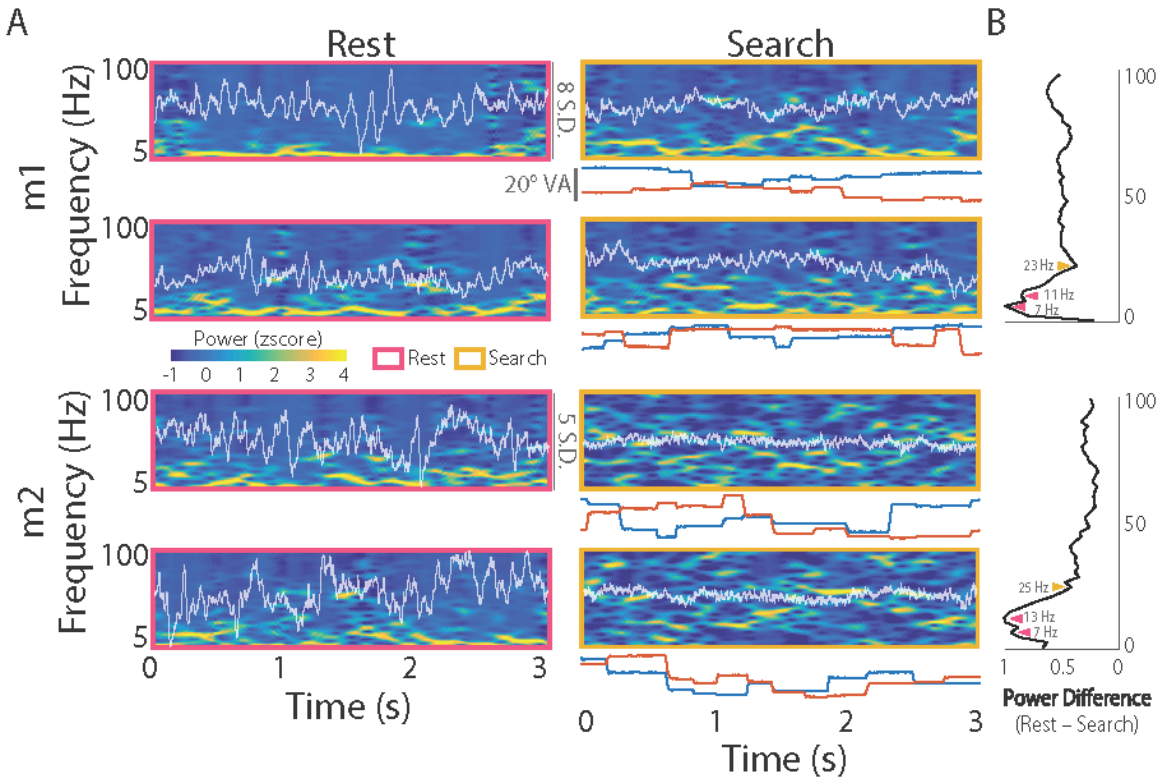

Figure 2: Hippocampal activity during different behavioral states

a. Hippocampal activity during different behavioral states, shown for example 3-second windows during rest epochs (pink outline; left column) and search epochs (orange outline; right column). Recordings from m1 shown in top two rows and from m2 on bottom two rows. Time-frequency resolved spectra were generated from 600ms segments, shifted in 6 ms increments, windowed with a Hamming window, 1/f normalized, and z-transformed. White trace, superimposed on the spectra, is the broadband LFP of the same 3 second window taken from a z-score transform of the entire session. The scale shown in standard deviations (SD) applies to all plots for a given animal. Below search epochs, the concurrent on-screen eye position (horizontal and vertical) are represented as degrees of visual angle (VA; the monitor encompasses 38.5° x 30.9° VA). **b.** Difference in grand average fft power across behavioral epochs. For each animal, the average FTTs of epochs for search vs. rest were calculated (M1: 66 rest epochs, 1258 search epochs; M2: 100 rest epochs 2584 search epochs). The average FFT for each epoch type was calculated, min-max normalized to a range of 0 to 1, and resultant rest values subtracted from the search values. First two peaks (rest > search) are highlighted with pink markers; the trough where search-epoch frequencies become prominent are highlighted with an orange marker.

Sharp-wave ripple, $\varepsilon_{80\text{-}120}$ and $\varepsilon_{110\text{-}160}$ event detection

SWR events were detected by selecting the tetrode/electrode channel with the most visibly apparent ripple activity, filtering that LFP signal (100-250 Hz), transforming to z-scores, rectifying, and band pass filtering the rectified signal from 1-20 Hz, approximating the envelope of the high-frequency signal (Skaggs et al., 2007). Ripple events were defined as threshold crossings 3 standard deviations (SD) above the mean, with a minimum duration of 50ms, beginning and ending at 1 SD.

The use of a variance-based threshold allows comparison to previous studies using this method, though such a threshold is expected to change at least nominally in response to an increase in SWR rate, assuming SWRs increase signal variance. In practice, the sparsity of SWRs relative to the ongoing continuously recorded signal render the impact of different ripple rates on the threshold negligible.

To quantify threshold changes as a function of changes in ripple rate, we selected a session of typical duration (64.27 minutes) with a typical number of SWR events (n=41 SWR events; total ripple duration of 3.31s; .09% of session occupied by SWR events). All ripples were removed and the zscore of 3 was calculated iteratively, as SWR events were added back into the signal, up to maximum of 5 times the original number of ripples in this session (205 swr events). In the present experiments, it would be unlikely to observe a doubling of ripples (200%), but even after after a 500% increase in ripple events, the underlying signal value for a zscore of 3 increased the zscore threshold value by .1, or 3.3% (Figure 1f), constituting a negligible impact on ripple rate overall, and no specific grounds that this would vary across statistical conditions.

Based on these criteria, M1 had 32 sessions with SWRs during both quiescence and task, M2 had 45 sessions with SWRs during both quiescence and task, M3 had 5 sessions with SWRs, only 3 of which had SWRs that occurred during the task, and M4 had 4 task-only sessions with SWRs.

Low epsilon band ($\varepsilon_{80\text{-}120}$; ε_L; 'high gamma'), and high-epsilon band ($\varepsilon_{110\text{-}160}$; ε_H; 'HFO') events were similarly identified, but with the filter criterion set at 80-120 Hz and 110-160 Hz, respectively, and in both cases identifying peaks as those > 1 SD. Duplicate epsilon and SWR events were labeled as SWRs. Events with a repetition rate < 125 ms were considered a single event.

Behavioral epoch and SWR rates

eSWRs, iSWRs and qSWRs (see Figure 3a for examples of each) were contrasted by comparing peak frequencies of SWR events from each behavioral state (Figure 3b). Peak SWR frequencies were calculated on a 200ms windows, centered on the SWR event, with a Hamming window. Peak value locations from the 3 groups were compared using a Kruskal-Wallis test (KW test). The KW test was used for omnibus tests whereas the assumption of homogeneity of variance was not met between groups.

To address whether or not elapsed time in a behavioral epoch (search or ITI) influenced the probability of observing SWRs, ripple rates for the first 20 seconds of these behavioral epochs were calculated, in 1 second bins, from all recording sessions with at least one ripple (Figure 3c). For search epochs, all periods, where the subject was not looking at the screen, were discarded. The 1 s rate bins were separated into 5 second groups (at 5s, 10s, 15s and 20s) and tested for significant group differences in ripple rate using a non-parametric omnibus test

(KW test). For each behavioral epoch, where the omnibus test was significant, paired comparisons were performed across the groups, using the Wilcoxon rank sum test (rank sum), and corrected for false discovery rate with the Benjamini–Hochberg procedure (Benjamini, & Hochberg, 1995); Figure 3d). The rank sum test was employed where paired comparisons on non-normally distributed data was required. For rank sum tests with large samples, the Z score is given as effect size, otherwise the Wilcoxon U-test statistic is given. For m4, the average SWR rate was calculated separately for the first 2s of the search epoch, as the average visual search trial duration was 2.99s (rate reported in results, not included in statistics or figures).

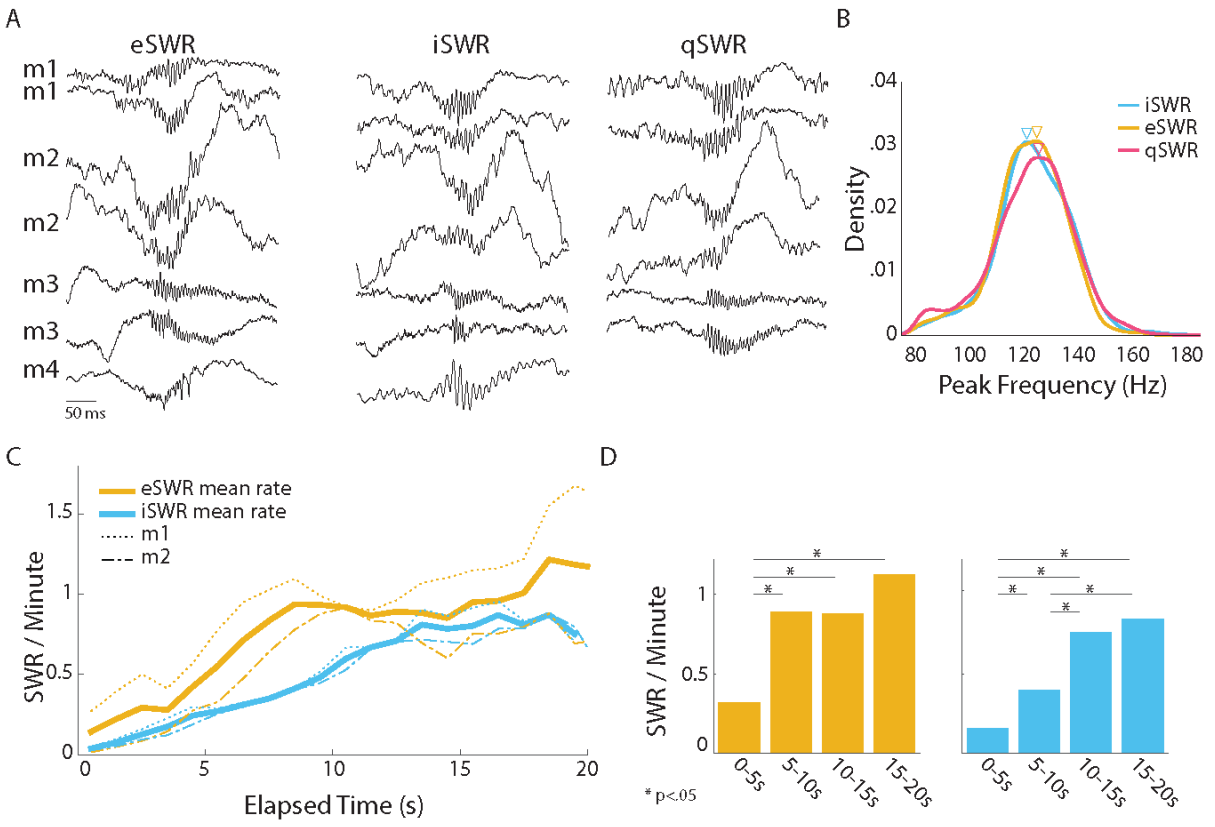

Figure 3: SWR Descriptions

a. Example SWRs during exploratory, inactive, and quiescent periods (eSWR left, iSWR middle, and qSWR right, respectively) in four macaques (m1-4). **b.** Kernel density plot comparing peak frequencies between e/i/qSWR events. Peak frequencies were calculated from 200ms windows centered on the SWR event, shown with open triangles. The

difference between peak frequencies across behavioral epochs was not significant. **c .** Overall mean SWR rate during search (eSWR) or inactive (iSWR) periods, relative to epoch onset, shown in thick lines, and individual mean rates shown in dashed lines. SWR rates were calculated for the first 20 seconds of these epochs, in 1 second bins, from all recording sessions with at least one ripple. For search, only periods with on screen looking is included. **d**. The SWR rates, shown in c, for search (left) and inactive (right) behavioral epochs, divided into 5s bins. An omnibus test showed rates vary with elapsed time for both search and inactive periods (eSWR: $\chi2(4) = 12.3$, $p = .006$; iSWR: $\chi2(4) = 16.62$, $p = .002$), results from the follow-up paired comparisons are shown here (for full results see Table 1 and 2).

Single unit analysis

We compared firing rates for CSs and putative interneurons (INs) over 28 sessions in which SWR events occurred, and cells could be isolated (Figure 4). We used a previously-established measure of population synchronization (Csicsvari et al., 1998), taking the probability of firing of a class of cells (CS/IN) in a 100ms window, centered on the SWR event, and comparing to the probability of firing in a 100ms window shifted to 1s after the SWR event. The mean rate represents the percentage of cells, in a given group, active during this window. Due to non-normality of data, a Wilcoxon signed-rank test was used to compare activation during SWRs and control windows, for both cell groups. Error bars are the 95% confidence interval generated from the bootstrapped mean (1000 permutations). This method was also used to compare cell firing rates across event types (SWR/$\varepsilon_{80\text{-}120}$/$\varepsilon_{110\text{-}160}$; Figure 6c).

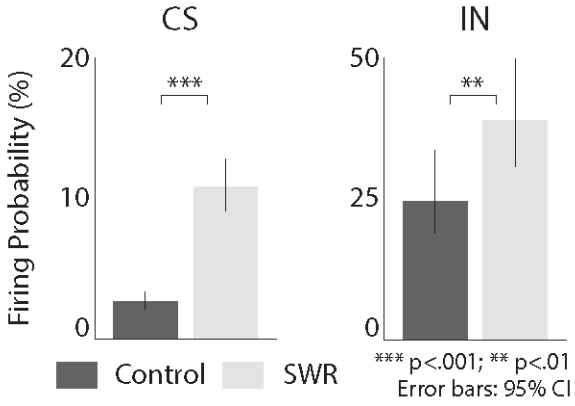

Figure 4: Changes in Spike Firing Probability

SWR events led to increased population synchrony for complex spiking units (CS) and putative interneurons (IN). Probability of firing of a class of cells (CS/IN) was taken from a 100ms window, centered on the ripple event (SWR: light grey), compared to the probability of firing in a 100ms window shifted to 1s after the SWR event (control: dark grey). Error bars are bootstrapped 95% confidence intervals.

Parameterization of visual exploration

We evaluated ripple occurrence during the task as a function of visual search. Search is comprised of 1. sequences of fixations, which are considered the active perceptual component of search, and 2. intervening ballistic movements of the eye (i.e. 'saccades') that enable changes in the visual-field content of fixations, for further analysis (Matin, 1974; Bridgeman et al., 1975; Mcconkie, & Currie, 1996). Because the visual field resolution is greatest at its center – corresponding to the foveal area of the retina – saccades are used to re-position the eye so that the fovea is directed towards places of interest in the environment. The sequence of these movements, or 'scanpath', during natural scene viewing can be divided into segments of 'looking at' (termed local or focal) with shorter saccades than segments of 'looking around' (termed ambient or global; (Velichkovsky et al., 2005). For target identification in a scene, global segments are also termed 'search and comparison' and local segments 'detection and verification' (Pomplun et al., 2001). Local segments of search are predictive of successful target detection and of subsequent memory (Henderson et al., 2005; Van der linde et al., 2009) and in humans these fixations are ~30ms longer duration than global fixations. Furthermore, local segments begin well in advance of target detection, and on scene locations other than the target, therefore they are considered part of extended, attentive search as opposed to an intrinsic part of detection itself (Scinto et al., 1986). Of importance to our evaluation of behavioral state in the present study, differences between local and global fixations durations

still fall within typical duration distributions (200-300ms in humans). In contrast, fixations that include outright cessation in performance ('staring') are unusually long, in excess of 2s (Tole et al., 1982), whereas lapses in attention during performance, e.g. 'mindless' scanning with failure to comprehend text during reading, are associated with shorter durations than expected, especially for fixations that are prolonged during attentive reading due to cognitive load (Schad et al., 2012).

We used these findings to guide search behavior analysis, including possible indicators of inattentive states during search. Specifically, we took as dependent measures for search: fixation duration, saccade amplitude, and fixations with gaze directed in the target location ('target fixations'). We note that previous studies have examined the relationship between spiking or LFPs from the temporal lobe and search/saccadic eye movements in macaques (Ringo et al., 1994; Sobotka et al., 1997; Sobotka et al., 2002; Purpura et al., 2003; Mruczek, & Sheinberg, 2007; Ibbotson et al., 2008; Ibbotson, & Krekelberg, 2011; Bartlett et al., 2011; Jutras et al., 2013; Hoffman et al., 2013) and in humans (Hoffman et al., 2013; Andrillon et al., 2015). In contrast, the present study will evaluate the as-yet-uncharacterized occurrence of SWRs in relation to visual search.

SWR rates and behavior

To assess whether SWRs were associated with changes in scanning behavior, including pauses in scanning, akin to the slow running or <2.5s pauses in movement used to define 'exploratory' eSWRs (O'neill et al., 2006); see Figure 5a for examples of SWRs during visual search), we first compared fixation durations during SWR events to all remaining fixations

during scene search using a rank sum test. We also compared saccade amplitudes flanking SWR-aligned fixations to those occurring at other times during search, again using the rank sum test. As a follow-up to probe possible interaction between these measures, a logistic regression model was used to identify significant predictors for the occurence of SWRs, based on fixation durations, saccade amplitudes, and the factor of subject id. A non-significant result on the Hosmer-Lemeshow goodness of fit test confirmed the model as a good fit.

To evaluate if exploratory SWRs coincide with changes in behavioral outcome, SWR rates were computed as a function of lag (number of fixations) from target fixation (Figure 5b). To account for SWR durations that could extend into the adjacent fixation, 'concurrent' SWRS are those whose peak time is within 1 fixation of the target fixation. These occurrences were subdivided by the outcome of the trial, that is, if the target detection was successful ('hit') or unsuccessful ('miss', in which the maximum trial time was reached without detection). Concurrent target fixation and SWR rates were compared for hits and misses, using a rank sum test. In addition, for a given detection type, the rates for non-concurrent SWRs (9 fixations before, and after, the fixation window) were collapsed and compared to the SWR rates concurrent with target fixations, using a rank sum test. All tests within a detection group were corrected for false discovery rate with the Benjamini–Hochberg procedure. A Chi-squared test was used to assess the probability of observing the frequency of trials which were hits or misses, for trials with both SWRs and fixations-in-target, and the probability of the observed frequency of these trials, which were hits or misses, for which SWRs and fixations-in-target coincided.

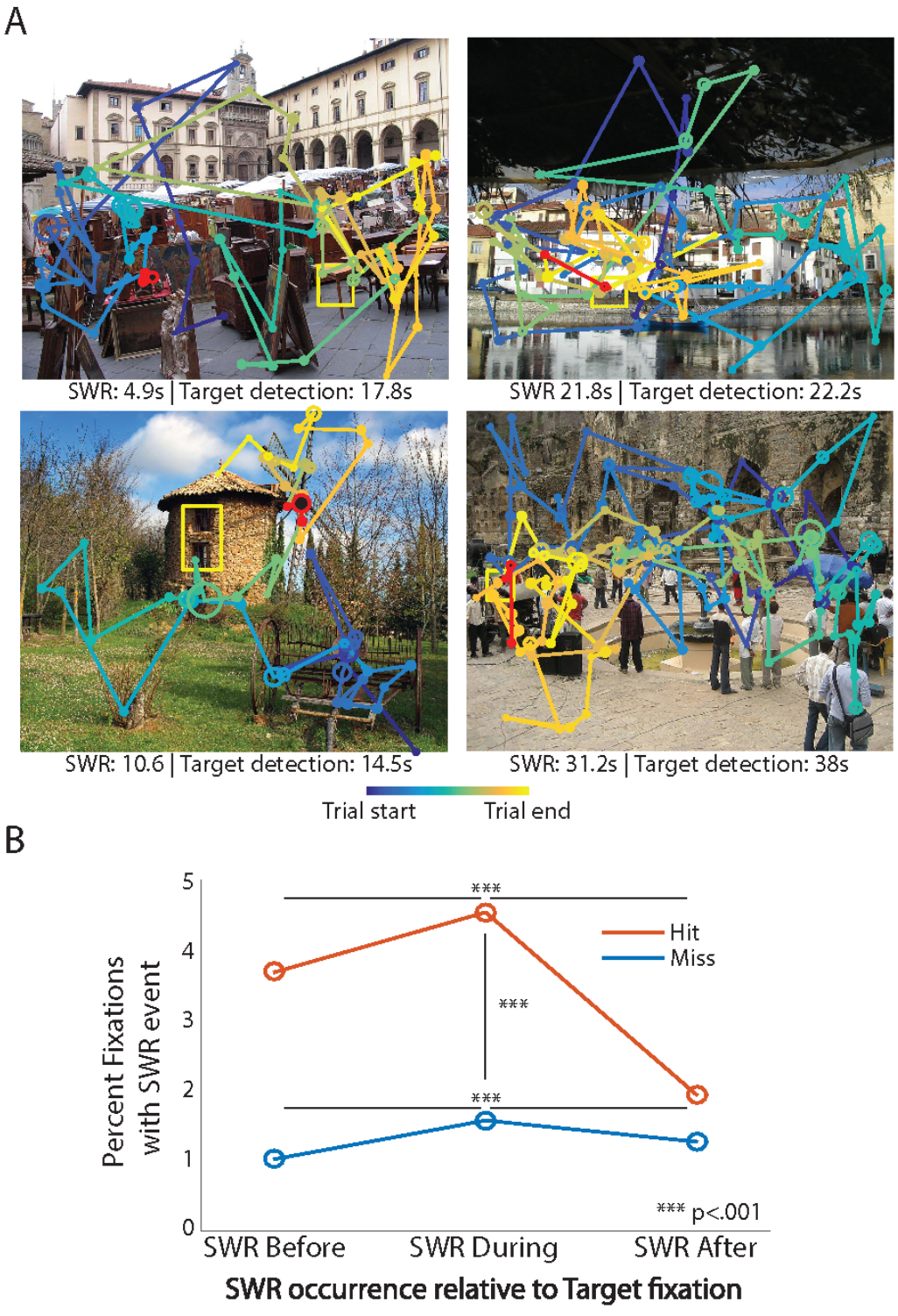

Figure 5: SWR during search

a. Four examples of scanpaths during search in successful trials containing SWRs. Fixation (circles) and saccades (lines) with graded coloring according to the scan path (blue: trial start; yellow: trial end), with fixation duration represented by circle size. The nearest fixation in time to the SWR event is shown in black outlined in red, with the flanking fixations, and saccades, only outlined in red. The elapsed search time when the SWR ocurred, and total

search time until the target was detected, are listed below each image. **b.** SWR occurrence, as a function of scanpath distance from fixations directed in the target location. Fractional occurrence is shown separately for trials that were successful or unsuccessful (Hits: red; Misses: blue, respectively). SWRs concurrent with target fixations, show in the middle group, had more hits than misses (vertical black significance bar). For a given detection type (Hit/Miss), the percent of non-concurrent SWRs (9 fixations preceeding, and 9 subsequent to, the target fixation window) were compared to the percent concurrent with target fixations (horizontal black significance bars).

Comparing SWRs to high-gamma oscillations and HFOs ($\varepsilon_{80\text{-}120}$, $\varepsilon_{110\text{-}160}$)

[analysis contributed by JMM] To explore whether ripple frequencies during SWRs overlap with theta-modulated gamma-band frequencies, we generated comodulograms using a modified version of (Tort et al., 2010) modulation index (MI; Figure 6b). The MI measures how the amplitude of one frequency band varies as a function of the phase of another band, expressed as divergence from uniformity, i.e., no relation between the two. The MI calculation takes the mean amplitude of a given narrowband signal for several equally sized phase bins over [0, 2π]. For each bin, a probability term is created, defined as the mean amplitude from one bin divided by the sum of mean amplitudes from all bins. The Kullback–Leibler divergence from a uniform probability distribution for normalization (NKLD) is calculated on these probability terms.

The modulation index requires sufficient phase bin sampling but the typical sharp-wave-ripple event is one 'sharp wave' cycle in duration, whereas our typical primate theta bursts are 3-10 cycles in duration. As a modification, we concatenated the amplitude means for each signal at the same respective phase bin across multiple signals within the same category into a phase-specific vector, and used the respective mean and sum of this vector for the NKLD. We then used the same general signal processing procedures and analytic parameters from (Tort et al., 2008), including bidirectional filtering and eegfilt MATLAB toolbox parameters. FIR design

parameters were (phase frequency: 2 Hz passband in 1 Hz increments from 1 – 30 Hz; amplitude frequency: 4 Hz passband in 2 Hz increments from 30 – 170 Hz; all with 3-cycle filter order of the lower passband cutoff frequency. For each SWR event we included 600 ms of centered processed signal, and 2000 ms of each theta bout event.

To extract features of the high-frequency events, we first applied a multi-resolution time-frequency analysis using a hamming window of three cycles (Shuren qin, 2004). For each event, spectrograms were generated from 50 - 180 Hz in 2 Hz non-overlapping frequency bins, and +/- 100ms intervals sliding in 1ms increments. To ensure that features from both higher and lower frequencies in the 50-180 Hz band could be detected, event spectrograms were min/max normalized separately for 50 - 110 Hz and 110 Hz - 180 Hz. The resulting patterns for each event comprised the inputs to the non-negative matrix factorization (NMF), to extract the largest features across SWR and Epsilon events (Lee, & Seung, 1999; Berry et al., 2007; Logothetis et al., 2012). Feature extraction used an alternating least squares algorithm to produce 80 component factors.

Events were clustered based on their NMF feature weights using a self-organizing map that had a 5 x 8 rectangular topology and used Euclidean distance as an error function for training. For illustration of differences across clusters (Figure 6d), we show the event with the lowest Mahalanobis distance to the centroid of each cluster.

This procedure effectively produces a time-frequency taxonomy of epsilon band activity. To further investigate whether the time-frequency content of SWR events is distinct from that of other epsilon band activity, we computed the group composition (SWR, $\varepsilon_{80\text{-}120}$, $\varepsilon_{110\text{-}160}$) for each of the 40 self-organizing map nodes and plotted them in a three-dimensional group-

membership space (Figure 6d). We then used a permutation label-swapping (2000 permutations) between SWR, $\varepsilon_{80\text{-}120}$ and $\varepsilon_{110\text{-}160}$ events to compute a series of one-tailed significance tests.

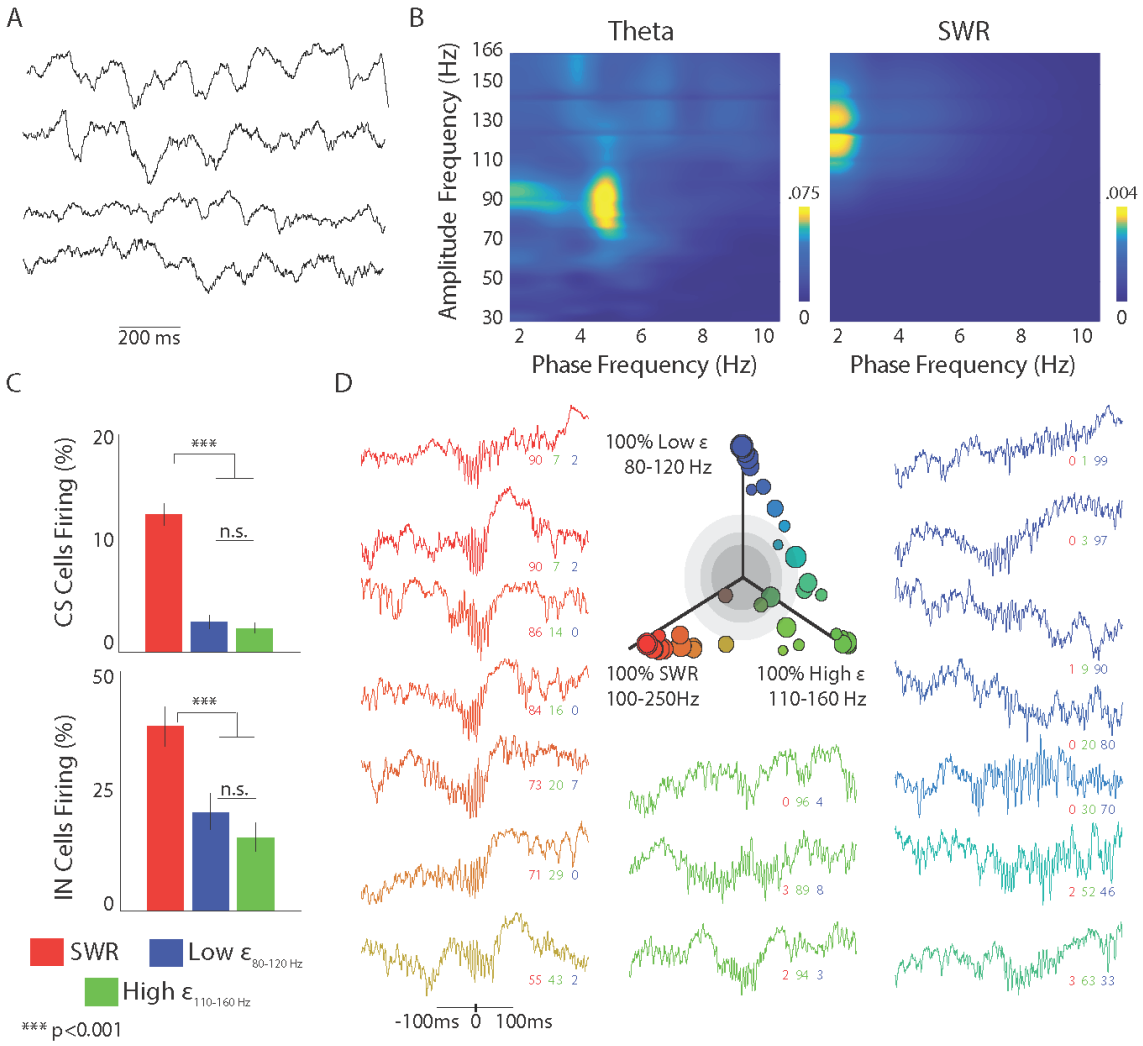

Figure 6: SWR vs Other High Frequency Activity

a. Example broadband LFP traces of theta oscillations for m1, used to generate comodulograms in b. **b.** Comodulogram showing the modulation index for each phase frequency by amplitude envelope frequency. The left plot used 2000ms segments of theta events; the right plot used 600 ms of signal around SWR events, concatenated across events for sufficient phase-bin sampling (see methods).[analysis contributed by JMM] **c.** The probability of spiking was greater for SWR than for ε events. Bars show firing probability during peak SWR, $\varepsilon_{80\text{-}120}$ and $\varepsilon_{110\text{-}160}$ windows, for CS and IN cells, following same methods as figure 4; SWR bars are also shown in Figure 4, duplicated here for comparison to ε events. **d.** Events were clustered based on their NMF feature weights (see methods). Middle plot shows the comparison of original group labels (SWR, high- and low-ε) by unsupervised clustering of all high-frequency events. Cluster position is defined by the % of members from each original group, with each group

assigned to one axis, RGB color-coded by axis position. Raw traces of the events that were closest to the center of their clusters are shown in the color corresponding to their cluster, with proportion of group representation shown below the trace. Dark grey, grey and light grey spheres correspond to $p<0.5$, $p<0.01$ and $p<0.001$ significance rate boundaries, respectively. [analysis contributed by JMM]

3.5 Results

Relation of SWR occurrence to behavioral states

Based on the ripple-band threshold criteria (see materials and methods), SWRs were observed during task performance in all four macaques (Figure 5a, M1-2). M1 had 32 sessions with SWRs during both quiescence and task, M2 had 45 sessions with SWRs during both quiescence and task, M3 had 5 sessions with SWRs, only 3 of which had SWRs that occurred during the task, and M4 had 4 task-only sessions with SWRs. The exploratory SWR (eSWR) oscillation's peak frequency did not differ from the peak frequencies of SWRs observed in the inter-trial interval, during inactivity (iSWRs) or during the start and end of the session quiescent states (qSWRs; $\chi^2(2) = 4.18$, $p = .124$; Figure 3b) suggesting eSWRs share similar characteristics to more commonly-described SWRs that occur during inactive states. In eSWR and iSWR epochs, SWRs occurred less frequently (i.e. lower rate) during the first 5 seconds of the epoch onset than at any other time point in the epoch (see table 1 and 2, Figure 3d). This pattern was similar to the comparatively low rate of SWRs seen in M4 during that animal's 2-second task epochs (search: 0.013 SWR/minute; rest: 0.011 SWR/minute). Finally, SWR events led to increased population synchrony (i.e. a decrease in firing sparsity) for both bursting complex spike (CS) cells and putative interneurons (CS: $w(28) = 26$, $p = 4.2 \times 10^{-7}$; IN: $w(12) = 10$, $p = .002$; Figure 4), similar to the increase observed in rodents (Csicsvari et al., 1998).

Relation of SWR occurrence to search behaviors

Within eSWR epochs, and contrary to expectation, SWRs occurred on-screen during scene search and occurred preferentially during active scanning strategies. Scanpath examples (Figure 5a) show saccades and fixation durations that were typical for this task, and allow comparison to those seen during SWRs. Fixation durations during SWRs were around 40ms longer than for non-SWR fixations (37.73 ms, $z(2590) = 9.3$, $p = 2.8 \times 10^{-20}$), which is within typical search fixation durations, and is more consistent with a local than a global search strategy. In addition, saccade amplitudes were smaller (-0.51° visual angle, $z(1049) = -3.3$, $p = .0009$), also consistent with local search. SWRs were therefore more closely associated with active local search strategies than with protracted lapses in scanning or brief 'inattentive' fixations. Using logistic regression to predict the occurrence of SWRs by fixation duration, saccade amplitude, and subject as a factor, we found that SWRs were predicted by the interaction of subject, saccade amplitude, and fixation duration, suggesting that (shorter) saccade amplitude and (longer) fixation duration contribute independently to SWR prediction, after accounting for subject. When all measures are held constant, there was a significant main effect of saccade amplitude, an interaction between saccade amplitude and subject, as well an interaction between saccade amplitude, fixation duration, and subject (see Table 3 for full results).

Although sharp wave ripples occurred during visual exploratory epochs, they may nevertheless signify brief *interruptions* in visual/perceptual processing, consistent with 'offline' states, albeit without interrupting search-related eye movements. Accordingly, if SWRs occurred when the target was fixated during search, perception of the target ('hits') should be impaired. Alternatively, if SWRs are part of active exploratory activity and not interruptions of

it, then their occurrence at times when the target is fixated may facilitate target detection. Finally, if the phenomenon is irrelevant to search, the timing of SWRs relative to target fixations should have no impact on target detection.

Overall, trials with at least one SWR and at least one target fixation during the search epoch were equally likely to be hits as misses (n_{hit}:150, n_{miss}: 153, $\chi^2(1) = .005$, $p = .909$). In contrast, the subset of these trials with *concurrent* SWRs and target fixations were about twice as likely to be hits than misses (χ^2 (1) = 9.2, p = .002; Table 4). Closer examination of the timing of SWRs relative to target fixations during successful search revealed a higher rate of SWRs when concurrent with target fixation than the SWR rate when they were non-concurrent with target fixations. (hits: z(2347) = -6.15, $p = 7.67 \times 10^{-10}$, misses: z(2656) = -5.08, $p = 3.71 \times 10^{-7}$; Figure 5b). Finally, the rate of coincidence was higher for trials that were hits than for misses (z(2347) -6.5, $p = 8.06 \times 10^{-11}$; Figure 5b), consistent with the success-rate measure described above. Target fixations and SWRs are both relatively infrequent events, nevertheless, when SWRs occur as targets are fixated, the target is more likely to be detected rather than overlooked, consistent with an association between SWRs and attentive perception.

Relation of SWRs to other high-frequency events

Prima facie, these results conflict with reports from rodent hippocampal physiology in which theta and various high gamma/epsilon band oscillations – not SWRs – dominate during active task behaviors. One alternative account for the present findings would be that SWR detection, which is based on thresholding the power envelope in the 100-250 Hz range, (see methods), erroneously identified waking gamma/epsilon activity as SWR events. In contrast to

SWRs, the $\varepsilon_{80\text{-}120}$ and $\varepsilon_{110\text{-}160}$ bands ('high-gamma' and 'HFOs') are expected to be weaker but more periodic, due to their modulation by theta oscillations (Scheffer-teixeira et al., 2012). We therefore conducted three tests to determine if the SWR events detected through conventional threshold methods might be more accurately described as theta-high frequency phenomena, or if they show distinct spectral properties. Theta phase-gamma amplitude modulation has not been established in macaque hippocampus. We therefore first selected bouts of low frequency activity during search and calculated the phase-amplitude modulation index for low frequency phase and high frequency amplitude modulations. This showed that ~5 Hz theta-band phase modulates high-gamma amplitude, consistent with previous reports from the rat (Tort et al., 2013). Furthermore, a lower frequency "phase modulation" (due to the sharp wave peak that manifests at 2 Hz) correlated with ripple amplitude variations, and the ripple frequency differed from the theta-modulated frequency. These results quantify that theta band phases are related to a segregated gamma frequency band that differs from the ripple frequency band that is modulated during the sharp wave (Figure 6b).

Second, we compared population synchrony across these high-frequency groups (Figure 6c). We found that synchrony (decreased probability of firing) was enhanced selectively for SWRs, both for complex spiking neurons (SWR/ε_H: $z(28) = 5.2$, $p = 5.9 \times 10^{-7}$; SWR/ε_L: $z(28) = 4.6$, $p = 1.5 \times 10^{-5}$) and putative interneurons (SWR/ε_H: $z(12) = 3.5$, $p = .0014$; SWR/ε_L: $z(12) = 3.0$, $p = .0073$), and was not different between epsilon bands (CS: $\varepsilon_H/\varepsilon_L$: $z(28) = -0.58$, $p = 1.7$; $\varepsilon_H/\varepsilon_L$: $z(12) = -1.1$, $p = .27$).

[analysis contributed by JMM] Finally, using these same group definitions of high frequency events (SWR, $\varepsilon_{80\text{-}120}$, $\varepsilon_{110\text{-}160}$) we visualized group differences, with a data-driven

feature extraction that spanned +/-100 ms across the 50-180 Hz frequency band of each event, irrespective of group label, and then clustered the events in feature space (see Methods and Materials). For visualization, we projected each cluster in a 3-D space according to the % membership from the original event labels; thus, the distance of a cluster from the center suggests non-random assignment into clusters. For example, if all events of a cluster came from the SWR group, it would appear at maximal eccentricity along the SWR axis (100, 0, 0). Most of the clusters (33/40) had at least 90% overlap with one of the original group labels (Figure 6d), suggesting that the high-frequency content alone within a small (200ms) window contains spectro-temporal features that separate ripples from other ($\varepsilon_{80\text{-}120}$, $\varepsilon_{110\text{-}160}$) high-frequency events.

3.6 Discussion

Sharp-wave ripples occurred during goal-directed visual behaviors in macaques, specifically, during visual exploration. These SWRs were similar in frequency and spectral content to those seen during periods of inactivity and sleep, but differed from rat 'eSWRs' in their apparent behavioral correlates during the task. Macaque SWRs, like their rodent counterparts, appeared during inactive states, but in addition, we observed SWRs during active visual search that was not associated with pauses in scanning. This raised two questions: 1) were these detected events 'true' SWRs, sharing the features of SWRs in inactive states and not high-frequency epsilon-band activity and 2) are these eSWRs related to search behaviors?

The comparison of SWR events to other high-frequency events revealed several differences among these groups. First, SWRs events had greater spiking probability than either high-gamma $\varepsilon_{80\text{-}120}$, or HFO $\varepsilon_{110\text{-}160}$ group, (Figure 6c). Second, isolated theta-band bouts

showed a theta modulation of high-gamma amplitude frequency (80-100 Hz) that differed from the sharp-wave-dependent amplitude frequency of SWRs (~125 Hz; Figure 6b; theta: left, swr: right.; (Tort et al., 2013). The separation of peaks between the two comodulograms suggests that eSWRs can be segregated from theta-gamma modulation. Third, the data-driven classification of high-frequency events yielded a clustering of those events that had been designated as SWRs using conventional criteria (Figure 6d). The clustering was non-random, and the SWR clusters had very little contamination by events that lacked the sharp-wave appearance and thus validated the accuracy of the SWR events we analyzed. Indeed, the few clusters that contained events from both SWR and high-epsilon-labeled groups appeared to be SWRs clusters, but with lower-amplitude members that were sub-threshold for inclusion as SWRs (i.e. false negatives). This method, therefore, may be useful for better signal detection and extraction of SWRs than conventional amplitude-envelope threshold methods, and for isolating consistent spectrotemporal classes of SWRs that may be produced by different underlying neural populations.

SWRs varied with behavioral states, more specifically, subsets of SWRs were linked to active scanning processes of the visual environment. Previous studies have shown that scan paths during image viewing can be divided into global and local categories based on saccade amplitude (Unema et al., 2005). Local fixations are associated with longer fixation durations and more effective encoding of the foveated part of the image (the center of gaze), leading to better subsequent memory (Velichkovsky et al., 2005; Van der linde et al., 2009). SWRs during visual search epochs were associated with smaller saccades and longer fixation durations, all of which are paradoxically more consistent with attentive processing of the scene than with

distracted or inactive behaviors. Whereas SWRs could occur while searching anywhere on the image, the target location is where the change lies and its fixation predicts successful detection. SWRs occurring concurrent with target fixations were more than twice as likely on successful as on unsuccessful trials. Successful trials also had higher SWR rate concurrent with target fixations than the SWR rate for the scanpath fixations well in advance of or following target fixations (Figure 5b). This finding suggests that the timing of SWRs relative to target fixations mattered. We speculate that SWRs did not impair processing of concurrently-viewed parts of the image; on the contrary, if SWRs and target fixations occurred during a trial, the SWRs 'on the target' facilitated detection.

A consideration about SWRs reported in this study, and of those reported in other studies, is the rate of SWR occurrences, which in primates, is on the order of several times a minute. In these difficult tasks, search could last tens of seconds, and up to 45 seconds. The elapsed time analysis indicated that SWRs may not occur in tasks lasting only a few seconds (possibly explaining their absence in (Skaggs et al., 2007). In our change detection task, SWRs were detected every few trials, on average: sometimes several per trial, but often none. As with eSWR occurrence during tasks in rodents, the SWRs may not occur for several trials, and performance (including learning) can occur without, or in-between, detected SWRs, therefore they cannot be considered critical mediators of task performance.

The rate of these phenomena, however, may be underestimated using current methods. SWRs in rats may occur independently along the septotemporal axis (Patel et al., 2013). The macaque hippocampal length along the long axis is manyfold greater than in rats and there is an elaboration of the anterior portion, along with a reduction in the hippocampal commissure,

all of which may produce substantially more independent SWR events than what is seen in the rat. In this study, we report SWRs recorded from one position per session, therefore non-locally generated SWRs could have gone undetected. Furthermore, the classification analysis clustered some events that appeared like SWRs, but were sub-threshold for the SWR detection procedure, therefore false negatives may also contribute to an underestimate of SWR rate. The reduction in SWR power with increased running speed, may exacerbate the false negatives for exploratory SWRs in rats (Kemere et al., 2013). Taken together, SWRs may be more frequent than currently reported, but should nevertheless be considered rare phenomena that carry considerable impact when they occur (Buzsáki, 2015; Chrobak, & Buzsáki, 1994; Siapas, & Wilson, 1998; Sirota et al., 2003; Battaglia et al., 2004; Isomura et al., 2006; Mölle et al., 2006; Logothetis et al., 2012).

We also note that our study does not resolve the direction of the relation between behavioral and eSWR events. Local search strategies may engender brain states conducive to SWR generation; likewise general brain states that lead to better search may also increase SWR rate. SWRs, therefore, may be a reflection of – rather than a facilitator of – successful search. The increased SWR rate specific to target fixations is more difficult to account for in this manner, but those events are only one subset of all SWRs observed.

Given the role of SWRs in large-scale neocortical synchrony, in synchronous hippocampal pyramidal cell reactivation and its posited role in 'offline' synaptic plasticity and memory consolidation (Buzsáki, 2015) the presence of SWRs in the midst of active search is somewhat surprising. Either these events allow for continued sensory processing as posited for encoding, or else the transition to/from 'offline' states is more nimble than previously

appreciated. Such rapid transitions are not unheard of in the hippocampus (Jezek et al., 2011; Kemere et al., 2013), and would allow eSWRs to provide a unique mechanism for timing long-range coordinated activity during experience (Hoffman, & Mcnaughton, 2002; Sirota et al., 2003; Battaglia et al., 2004; Battaglia et al., 2011; Logothetis et al., 2012; Womelsdorf, 2015). In primates, as in rodents, this may prove to be important for learning during exploration. Alternatively, these infrequent but powerful events may occasionally 'slip through' in active waking, and provide some as-yet-undescribed means of potentiating neurons selectively active when viewing the target location.

Either way, SWRs during visual task performance may have important consequences to single unit responses and BOLD activation in the hippocampus and neocortex. It is standard preprocessing in hippocampal physiology to filter for movement and/or theta-band LFP in rodent studies of place field activity, thereby avoiding contamination by SWR-related activation. If primates have SWRs during active portions of a task, the response selectivity ('place fields' or 'view cells') described in those segments may be artificially inflated by the SWR. For example, if SWRs occur with uneven sampling over the stimulus response space such as at goal locations in a scene or virtual environment, those regions may appear to have place/view fields. This scenario would also predict that population level activation measures like the hippocampal BOLD response could be affected by SWR occurrences as a function of task performance (Logothetis et al., 2012). These possibilities are purely speculative, but if several fold changes in ongoing signal occurs – as observed during SWRs – they could impact results and warrant consideration.

One of the most striking differences between studies of SWRs in primates and those in rats and mice is the behavioral methodology. The rat and mouse studies of SWRs use running to indicate active task behavior, and filter out fast movement epochs when detecting SWRs. In contrast, very few of the hippocampal-dependent tasks in humans and monkeys involve locomotion. Furthermore, memories that require hippocampal integrity do not need to be encoded or retrieved during self-movement through space. Imagine if memory for the personally-experienced past required this: our desks and blackboards in school, our TVs, movie screens and video-streaming laptops would need to be anchored to treadmills, or require that we watch as we walk. Indeed, humans and other primates extract much of what we know from our environment based on what we view, and not necessarily what we're actively ambulating toward or away from. That said, locomotion is an important aspect to hippocampal activity that may even be conserved across species, and hippocampal contributions to navigation may also be conserved. Yet, even if that is the case, we need an account for the memories we form that appear to be hippocampal-dependent and yet do not require locomotor or ambulatory movement. SWRs occurring during periods of active, attentive visual exploration may serve some role in memory independent of locomotion, suggesting a more general or widespread role than previously thought.

Group 1	Group 2	p (corrected)	U	n	Group 1 mean	Group 2 mean
5s	10s	0.032	16	5	0.159	0.397
5s	15s	0.032	15	5	0.159	0.759
5s	20s	0.032	15	5	0.159	0.841
10s	15s	0.032	16	5	0.397	0.759
10s	20s	0.032	15	5	0.397	0.841
15s	20s	0.651	25	5	0.759	0.841

Table 1: eSWR Rates

Paired comparisons for the SWR 5s rate bins, for exploratory behavioral epochs (eSWR). All p values corrected with Benkamini-Hochberg procedure.

Group 1	Group 2	p (corrected)	U	n	Group 1 mean	Group 2 mean
5s	10s	0.032	15	5	0.317	0.888
5s	15s	0.032	15	5	0.317	0.874
5s	20s	0.032	15	5	0.317	1.120
10s	15s	0.548	31	5	0.888	0.874
10s	20s	0.444	21	5	0.888	1.120
15s	20s	0.444	21	5	0.874	1.120

Table 2: iSWR Rates

Paired comparisons for the SWR 5s rate bins, for inactive behavioral epochs (iSWR). All p values corrected with Benkamini-Hochberg procedure.

	Z	P
Subject	-1.85	0.065
Saccade Amplitude	-2.74	0.006*
Fixation Duration	1.85	0.064
Subject X Fixation Duration	1.50	0.133
Subject X Saccade Amplitude	3.47	0.001*
Saccade Amplitude X Fixation Duration	1.22	0.221
Subject X Saccade Amplitude X Fixation Duration	-2.22	0.026*
57061 degrees of freedom		

Table 3: Logistic Regression Results

Results of logistic regression predicting the occurrence of SWRs from fixation duration, saccade amplitude, and subject as a factor.

	Hit	Miss	Total
Coincident	31	12	43
Non-Coincident	119	141	260
Total	150	153	

Table 4: Coincident Rates

Trials with at least one SWR and at least one target fixation during search. Coincident is when the SWR and target fixation occurred together. Hit and miss refer to, respectively, successful, or unsuccessful search.

3.7 References

Andrillon T, Nir Y, Cirelli C, Tononi G, Fried I (2015) Single-neuron activity and eye movements during human REM sleep and awake vision. Nature communications 6:7884.

Axmacher N, Elger CE, Fell J (2008) Ripples in the medial temporal lobe are relevant for human memory consolidation. Brain 131:1806-1817.

Bartlett AM, Ovaysikia S, Logothetis NK, Hoffman KL (2011) Saccades during Object Viewing Modulate Oscillatory Phase in the Superior Temporal Sulcus. J Neurosci 31:18423-18432.

Battaglia FP, Benchenane K, Sirota A, Pennartz CMA, Wiener SI (2011) The hippocampus: hub of brain network communication for memory. Trends Cogn Sci 15:310-318.

Battaglia FP, Sutherland GR, McNaughton BL (2004) Hippocampal sharp wave bursts coincide with neocortical "up-state" transitions. Learn Mem 11:697-704.

Benchenane K, Peyrache A, Khamassi M, Tierney PL, Gioanni Y, Battaglia FP, et al (2010) Coherent theta oscillations and reorganization of spike timing in the hippocampal- prefrontal network upon learning. Neuron 66:921-936.

Benjamini Y, Hochberg Y (1995) Controlling the False Discovery Rate: A Practical and Powerful Approach to Multiple Testing. Journal of the Royal Statistical Society. Series B (Methodological) 57:289-300.

Berry M, Browne M, Langville A, Pauca V, Plemmons R (2007) Algorithms and applications for approximate nonnegative matrix factorization. Computational Statistics and Data Analysis 52:155-173.

Blumberg MS (1989) An allometric analysis of the frequency of hippocampal theta: the significance of brain metabolic rate. Brain Behav Evol 34:351-356.

Bódizs R, Kántor S, Szabó G, Szûcs A, Erõss L, Halász P, et al (2001) Rhythmic hippocampal slow oscillation characterizes REM sleep in humans. Hippocampus 11:747-753.

Bragin A, Engel J, Wilson CL, Fried I, Buzsáki G (1999) High-frequency oscillations in human brain. Hippocampus 9:137-142.

Bridgeman B, Hendry D, Stark L (1975) Failure to detect displacement of the visual world during saccadic eye movements. Vision Res. 15:719-722.

Buzsáki G (1986) Hippocampal sharp waves: their origin and significance. Brain Res 398:242-252.

Buzsáki G (1989) Two-stage model of memory trace formation: a role for "noisy" brain states. Neuroscience 31:551-570.

Buzsáki G (1996) The hippocampo-neocortical dialogue. Cereb Cortex 6:81-92.

Buzsáki G, Leung LW, Vanderwolf CH (1983) Cellular bases of hippocampal EEG in the behaving rat. Brain Res 287:139-171.

Buzsáki G (2015) Hippocampal sharp wave-ripple: A cognitive biomarker for episodic memory and planning. Hippocampus

Buzsáki G, Schomburg EW (2015) What does gamma coherence tell us about inter-regional neural communication? Nat Neurosci 18:484-489.

Cantero JL, Atienza M, Stickgold R, Kahana MJ, Madsen JR, Kocsis B, et al (2003) Sleep-dependent theta oscillations in the human hippocampus and neocortex. J Neurosci 23:10897-10903.

Carr MF, Jadhav SP, Frank LM (2011) Hippocampal replay in the awake state: a potential substrate for memory consolidation and retrieval. Nat Neurosci 14:147-153.

Chau VL, Murphy EF, Rosenbaum RS, Ryan JD, Hoffman KL (2011) A Flicker Change Detection Task Reveals Object-in-Scene Memory Across Species. Front Behav Neurosci 5:58.

Chrobak JJ, Buzsáki G (1994) Selective activation of deep layer (V-VI) retrohippocampal cortical neurons during hippocampal sharp waves in the behaving rat. J Neurosci 14:6160-6170.

Clemens Z, Borbély C, Weiss B, Erőss L, Szűcs A, Kelemen A, et al (2013) Increased mesiotemporal delta activity characterizes virtual navigation in humans. Neurosci Res 76:67-75.

Csicsvari J, Hirase H, Czurko A, Buzsáki G (1998) Reliability and state dependence of pyramidal cell-interneuron synapses in the hippocampus: an ensemble approach in the behaving rat. Neuron 21:179-189.

Csicsvari J, Hirase H, Czurkó A, Mamiya A, Buzsáki G (1999) Fast network oscillations in the hippocampal CA1 region of the behaving rat. J Neurosci 19:RC20.

Csicsvari J, Hirase H, Mamiya A, Buzsáki G (2000) Ensemble patterns of hippocampal CA3-CA1 neurons during sharp wave-associated population events. Neuron 28:585-594.

Dupret D, O'Neill J, Pleydell-Bouverie B, Csicsvari J (2010) The reorganization and reactivation of hippocampal maps predict spatial memory performance. Nat Neurosci 13:995-1002.

Ego-Stengel V, Wilson MA (2010) Disruption of ripple-associated hippocampal activity during rest impairs spatial learning in the rat. Hippocampus 20:1-10.

Foster DJ, Wilson MA (2006) Reverse replay of behavioural sequences in hippocampal place cells during the awake state. Nature 440:680-683.

Gerrard JL, Kudrimoti H, McNaughton BL, Barnes CA (2001) Reactivation of hippocampal ensemble activity patterns in the aging rat. Behav Neurosci 115:1180-1192.

Girardeau G, Benchenane K, Wiener SI, Buzsáki G, Zugaro MB (2009) Selective suppression of hippocampal ripples impairs spatial memory. Nat Neurosci 12:1222-1223.

Girardeau G, Zugaro M (2011) Hippocampal ripples and memory consolidation. Curr Opin Neurobiol 21:452-459.

Harris KD, Henze DA, Csicsvari J, Hirase H, Buzsáki G (2000) Accuracy of tetrode spike separation as determined by simultaneous intracellular and extracellular measurements. J Neurophysiol 84:401-414.

Henderson JM, Williams CC, Falk RJ (2005) Eye movements are functional during face learning. Mem Cognit 33:98-106.

Hoffman KL, McNaughton BL (2002) Coordinated reactivation of distributed memory traces in primate neocortex. Science 297:2070-2073.

Hoffman KL, Battaglia FP, Harris K, MacLean JN, Marshall L, Mehta MR, et al (2007) The upshot of up states in the neocortex: from slow oscillations to memory formation. J Neurosci 27:11838-11841.

Hoffman KL, Dragan MC, Leonard TK, Micheli C, Montefusco-Siegmund R, Valiante TA, et al (2013) Saccades during visual exploration align hippocampal 3-8 Hz rhythms in human and non-human primates. Frontiers in systems neuroscience 7:43.

Ibbotson MR, Crowder NA, Cloherty SL, Price NSC, Mustari MJ (2008) Saccadic modulation of neural responses: possible roles in saccadic suppression, enhancement, and time compression. J Neurosci 28:10952-10960.

Ibbotson M, Krekelberg B (2011) Visual perception and saccadic eye movements. Curr Opin Neurobiol 21:553-558.

Isomura Y, Sirota A, Ozen S, Montgomery S, Mizuseki K, Henze DA, et al (2006) Integration and segregation of activity in entorhinal-hippocampal subregions by neocortical slow oscillations. Neuron 52:871-882.

Jackson J, Goutagny R, Williams S (2011) Fast and slow γ rhythms are intrinsically and independently generated in the subiculum. J Neurosci 31:12104-12117.

Jadhav SP, Kemere C, German PW, Frank LM (2012) Awake hippocampal sharp-wave ripples support spatial memory. Science 336:1454-1458.

Jezek K, Henriksen EJ, Treves A, Moser EI, Moser MB (2011) Theta-paced flickering between place-cell maps in the hippocampus. Nature 478:246-249.

Ji D, Wilson MA (2007) Coordinated memory replay in the visual cortex and hippocampus during sleep. Nat Neurosci 10:100-107.

Jutras MJ, Fries P, Buffalo EA (2013) Oscillatory activity in the monkey hippocampus during visual exploration and memory formation. Proceedings of the National Academy of Sciences 110:13144-13149.

Kemere C, Carr MF, Karlsson MP, Frank LM (2013) Rapid and continuous modulation of hippocampal network state during exploration of new places. PloS one 8:e73114.

Kudrimoti HS, Barnes CA, McNaughton BL (1999) Reactivation of hippocampal cell assemblies: effects of behavioral state, experience, and EEG dynamics. The Journal of neuroscience 19:4090-4101.

Le Van Quyen M, Bragin A, Staba R, Crépon B, Wilson CL, Engel J, et al (2008) Cell type-specific firing during ripple oscillations in the hippocampal formation of humans. J Neurosci 28:6104-6110.

Le Van Quyen M, Staba R, Bragin A, Dickson C, Valderrama M, Fried I, et al (2010) Large-scale microelectrode recordings of high-frequency gamma oscillations in human cortex during sleep. J Neurosci 30:7770-7782.

Lee DD, Seung HS (1999) Learning the parts of objects by non-negative matrix factorization. Nature 401:788-791.

Logothetis NK, Eschenko O, Murayama Y, Augath M, Steudel T, Evrard HC, et al (2012) Hippocampal-cortical interaction during periods of subcortical silence. Nature 491:547-553.

Louie K, Wilson MA (2001) Temporally structured replay of awake hippocampal ensemble activity during rapid eye movement sleep. Neuron 29:145-156.

Matin E (1974) Saccadic suppression: a review and an analysis. Psychol Bull. 81:899-917.

McConkie GW, Currie CB (1996) Visual stability across saccades while viewing complex pictures. J Exp Psychol Hum Percept Perform 22:563-581.

Mölle M, Yeshenko O, Marshall L, Sara SJ, Born J (2006) Hippocampal sharp wave-ripples linked to slow oscillations in rat slow-wave sleep. J Neurophysiol 96:62-70.

Moroni F, Nobili L, Curcio G, De Carli F, Fratello F, Marzano C, et al (2007) Sleep in the human hippocampus: a stereo-EEG study. PloS one 2:e867.

Mruczek RE, Sheinberg DL (2007) Activity of inferior temporal cortical neurons predicts recognition choice behavior and recognition time during visual search. Journal of Neuroscience 27:2825-2836.

O'Neill J, Pleydell-Bouverie B, Dupret D, Csicsvari J (2010) Play it again: reactivation of waking experience and memory. Trends Neurosci 33:220-229.

O'Neill J, Senior T, Csicsvari J (2006) Place-selective firing of CA1 pyramidal cells during sharp wave/ripple network patterns in exploratory behavior. Neuron 49:143-155.

Patel J, Schomburg EW, Berényi A, Fujisawa S, Buzsáki G (2013) Local generation and propagation of ripples along the septotemporal axis of the hippocampus. J Neurosci 33:17029-17041.

Peyrache A, Khamassi M, Benchenane K, Wiener SI, Battaglia FP (2009) Replay of rule-learning related neural patterns in the prefrontal cortex during sleep. Nat Neurosci 12:919-926.

Pezzulo G, van der Meer MAA, Lansink CS, Pennartz CMA (2014) Internally generated sequences in learning and executing goal-directed behavior. Trends Cogn Sci 18:647-657.

Pfeiffer BE, Foster DJ (2013) Hippocampal place-cell sequences depict future paths to remembered goals. Nature 497:74-79.

Pomplun M, Sichelschmidt L, Wagner K, Clermont T, Rickheit G, Ritter H, et al (2001) Comparative visual search: a difference that makes a difference. Cognitive Science 25:3-36.

Purpura KP, Kalik SF, Schiff ND (2003) Analysis of perisaccadic field potentials in the occipitotemporal pathway during active vision. J Neurophysiol 90:3455-3478.

Qin YL, McNaughton BL, Skaggs WE, Barnes CA (1997) Memory reprocessing in corticocortical and hippocampocortical neuronal ensembles. Philos Trans R Soc Lond B Biol Sci 352:1525-1533.

Ringo JL, Sobotka S, Diltz MD, Bunce CM (1994) Eye movements modulate activity in hippocampal, parahippocampal, and inferotemporal neurons. J Neurophysiol 71:1285-1288.

Schad DJ, Nuthmann A, Engbert R (2012) Your mind wanders weakly, your mind wanders deeply: objective measures reveal mindless reading at different levels. Cognition 125:179-194.

Scheffer-Teixeira R, Belchior H, Caixeta FV, Souza BC, Ribeiro S, Tort ABL, et al (2012) Theta phase modulates multiple layer-specific oscillations in the CA1 region. Cerebral Cortex 22:2404-2414.

Scinto LF, Pillalamarri R, Karsh R (1986) Cognitive strategies for visual search. Acta Psychol (Amst) 62:263-292.

Shen C, Ardid S, Kaping D, Westendorff S, Everling S, Womelsdorf T, et al (2015) Anterior Cingulate Cortex Cells Identify Process-Specific Errors of Attentional Control Prior to Transient Prefrontal-Cingulate Inhibition. Cerebral Cortex 25:2213-2228.

Shuren Qin ZJ (2004) Multi-Resolution Time-Frequency Analysis for Detection of Rhythms of EEG Signals. 2004 IEEE 11th Digital Signal Processing Workshop 4:0-7803.

Siapas AG, Wilson MA (1998) Coordinated interactions between hippocampal ripples and cortical spindles during slow-wave sleep. Neuron 21:1123-1128.

Singer AC, Carr MF, Karlsson MP, Frank LM (2013) Hippocampal SWR activity predicts correct decisions during the initial learning of an alternation task. Neuron 77:1163-1173.

Sirota A, Csicsvari J, Buhl D, Buzsáki G (2003) Communication between neocortex and hippocampus during sleep in rodents. Proc Natl Acad Sci U S A 100:2065-2069.

Skaggs WE, McNaughton BL, Permenter M, Archibeque M, Vogt J, Amaral DG, et al (2007) EEG sharp waves and sparse ensemble unit activity in the macaque hippocampus. J Neurophysiol 98:898-910.

Sobotka S, Zuo W, Ringo JL (2002) Is the functional connectivity within temporal lobe influenced by saccadic eye movements? J Neurophysiol 88:1675-1684.

Sobotka S, Nowicka A, Ringo JL (1997) Activity linked to externally cued saccades in single units recorded from hippocampal, parahippocampal, and inferotemporal areas of macaques. J Neurophysiol. 78:2156-2163.

Sullivan D, Csicsvari J, Mizuseki K, Montgomery S, Diba K, Buzsáki G, et al (2011) Relationships between hippocampal sharp waves, ripples, and fast gamma oscillation: influence of dentate and entorhinal cortical activity. J Neurosci 31:8605-8616.

Tamura R, Nishida H, Eifuku S, Fushiki H, Watanabe Y, Uchiyama K, et al (2013) Sleep-stage correlates of hippocampal electroencephalogram in primates. PloS one 8:e82994.

Tole JR, Stephens AT, Harris RL, Ephrath AR (1982) Visual scanning behavior and mental workload in aircraft pilots. Aviat Space Environ Med 53:54-61.

Tort ABL, Komorowski R, Eichenbaum H, Kopell N (2010) Measuring phase-amplitude coupling between neuronal oscillations of different frequencies. J Neurophysiol 104:1195-1210.

Tort ABL, Kramer MA, Thorn C, Gibson DJ, Kubota Y, Graybiel AM, et al (2008) Dynamic cross-frequency couplings of local field potential oscillations in rat striatum and hippocampus during performance of a T-maze task. Proc Natl Acad Sci U S A 105:20517-20522.

Tort ABL, Scheffer-Teixeira R, Souza BC, Draguhn A, Brankačk J (2013) Theta-associated high-frequency oscillations (110-160Hz) in the hippocampus and neocortex. Prog Neurobiol 100:1-14.

Uchida S, Maehara T, Hirai N, Okubo Y, Shimizu H (2001) Cortical oscillations in human medial temporal lobe during wakefulness and all-night sleep. Brain Res 891:7-19.

Unema PJ, Pannasch S, Joos M, Velichkovsky BM (2005) Time course of information processing during scene perception: The relationship between saccade amplitude and fixation duration. Visual Cognition 12:473-494.

van der Linde I, Rajashekar U, Bovik AC, Cormack LK (2009) Visual memory for fixated regions of natural images dissociates attraction and recognition. Perception 38:1152-1171.

Vanderwolf CH (1969) Hippocampal electrical activity and voluntary movement in the rat. Electroencephalogr Clin Neurophysiol 26:407-418.

89. Bara BG, Barsalou L, Bucciarelli M editor. Two visual systems and their eye movements: Evidence from static and dynamic scene perception. Proceedings of the XXVII conference of the Cognitive Science Society; 2005; Lawrence Erlbaum Associates, Inc.; 2005. 2283 p.

Whishaw IQ, Vanderwolf CH (1973) Hippocampal EEG and behavior: changes in amplitude and frequency of RSA (theta rhythm) associated with spontaneous and learned movement patterns in rats and cats. Behav Biol 8:461-484.

Wilson MA, McNaughton BL (1994) Reactivation of hippocampal ensemble memories during sleep. Science 265:676-679.

Winson J (1972) Interspecies differences in the occurrence of theta. Behav Biol 7:479-487.

Womelsdorf T (2015) Long-Range Attention Networks: Circuit Motifs Underlying Endogenously Controlled Stimulus Selection. Trends in Neuroscience

Yu JY, Frank LM (2015) Hippocampal-cortical interaction in decision making. Neurobiol Learn Mem 117:34-41.

Chapter 4 - Sharp-wave ripples in primates are enhanced near remembered visual objects

This chapter is adapted from the following paper:

T. K. Leonard, K. L. Hoffman (2016) Sharp-wave ripples in primates are enhanced near remembered visual objects. Current Biology. (in press)

4.1 Summary

The hippocampus plays an important role in memory for events that are distinct in space and time. One of the strongest, most synchronous neural signals produced by the hippocampus is the sharp-wave ripple (SWR), observed in a variety of mammalian species during offline behaviors such as slow-wave sleep (Buzsáki, 2015; Le Van Quyen et al., 2010; Buzsáki, 1986) and quiescent waking and pauses in exploration (O'Neill, Senior & Csicsvari, 2006; O'Keefe, 1976; Skaggs et al., 2007; Suzuki & Smith, 1985; Buzsáki, Leung & Vanderwolf, 1983), leading to longstanding and widespread theories of their contribution to plasticity and memory during these inactive or immobile states (Ylinen et al., 1995; Buzsáki, 1989; Roumis & Frank, 2015; O'Neill, Pleydell-Bouverie, Dupret & Csicsvari, 2010; Girardeau & Zugaro, 2011; Carr, Jadhav & Frank, 2011). Indeed, during sleep and waking inactivity, hippocampal SWRs in rodents appear to support spatial long-term and working memory (O'Neill, Senior & Csicsvari, 2006; Girardeau, Benchenane, Wiener, Buzsáki & Zugaro, 2009; Ego-Stengel & Wilson, 2010; Dupret, O'Neill, Pleydell-Bouverie & Csicsvari, 2010; Jadhav, Kemere, German & Frank, 2012; Singer, Carr, Karlsson & Frank, 2013; Pfeiffer & Foster, 2013; Jackson, Johnson & Redish, 2006; Eschenko, Ramadan, Mölle, Born & Sara, 2008; Girardeau, Cei & Zugaro, 2014), but so far, they have not been linked to memory in primates. More recently, SWRs have been observed during

active, visual scene exploration in macaques (Leonard et al., 2015), opening up the possibility that these active-state ripples in the primate hippocampus are linked to memory for objects embedded in scenes. By measuring hippocampal SWRs in macaques during search for scene-contextualized objects, we found that SWR rate increased with repeated presentations. Furthermore, gaze during SWRs was more likely to be near the target object on repeated than on novel presentations, even after accounting for overall differences in gaze location with scene repetition. This proximity bias with repetition occurred near the time of target object detection for remembered targets. The increase in ripple likelihood near remembered visual objects suggests a link between ripples and memory in primates; specifically, SWRs may reflect part of a mechanism supporting the guidance of search based on past experience.

4.2 Results and Discussion

Results:

Two adult macaques searched for target objects embedded in photographic scenes, comprising unique object-scene pairs (Figure 1A, B). They showed faster detection – speeded search – with stimulus repetition (Figure 1C; $Z(1218) = -13.438$, $P < 3.5989e\text{-}41$), indicating relational/episodic-like memory for the target objects-in-context (Chau, Murphy, Rosenbaum, Ryan & Hoffman, 2011; Hollingworth, 2006; Gaffan, 1994; Dragan et al., 2016). Hippocampal recordings were obtained during task performance using depth-adjustable indwelling tetrodes (Leonard et al., 2015; Hoffman et al., 2013; Talakoub, Gomez Palacio Schjetnan, Valiante, Popovic & Hoffman, 2016). Recordings showed that sharp-wave ripples (SWRs) occurred at higher rates on repeated trials than on novel trials (Figure 2A; $p <= 0.0001$, permutation test). To determine when the repetition-related enhancement emerges in the trial, we calculated

ripple rates at increasing delays from scene onset, by novel and repeated trial repetition group (Figure 2B; gray lines indicate different rates between trial groups; permutation test, n = 10000). Repeated trials had higher ripple rates beginning shortly into the trial, and were not restricted to narrow temporal windows from trial onset.

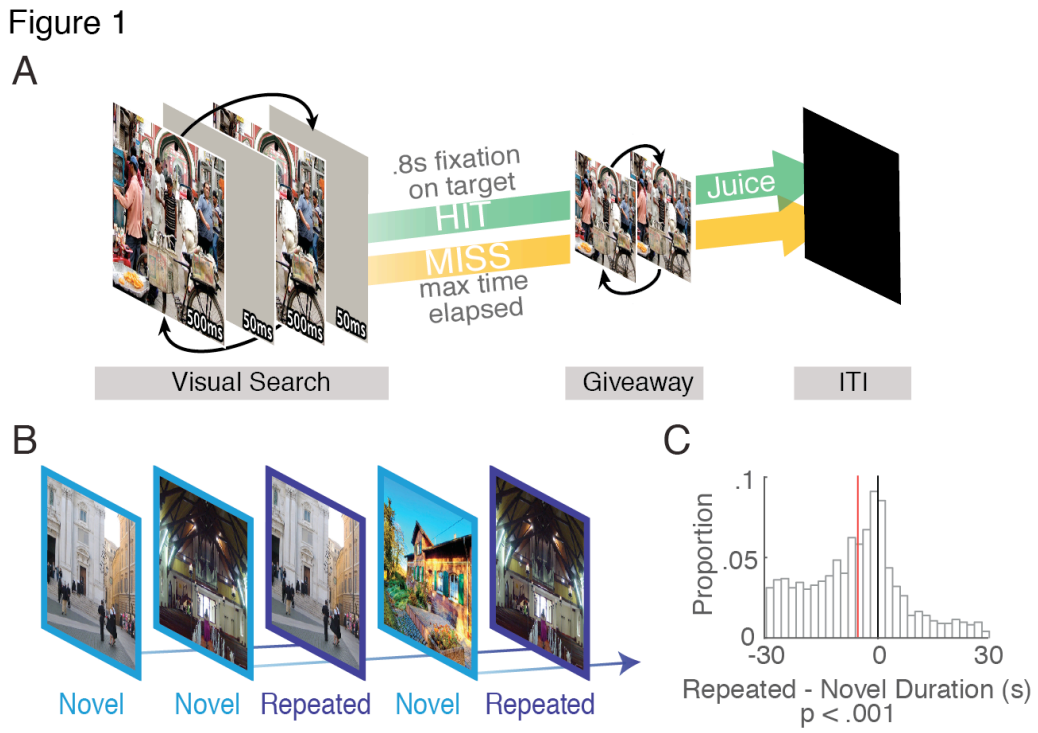

Figure 1. Memory-guided visual search task

(A) Trial structure. Left: an original and target-modified scene are presented in alternation, with a brief mask presented in between, requiring protracted visual search on the image to detect the changing target ('flicker change detection'). Visual search ends after the target is fixated for .8 seconds or the maximum on-screen search time is reached. Following visual search is the 'giveaway' (middle), consisting of an alternation between the two scenes, without mask, revealing the changed location, and ending with an inter trial interval (ITI) black screen period (right). (See methods, [24,29], Supplemental Experimental Procedures for more details).

(B) A sequence of flicker scene pairs are presented in blocks of 30 trials. Novel-trial scenes were never presented to that animal before, and these comprised 12/30 trials per block, distributed evenly across first and second halves of the blocks to prevent order effects. Each novel-trial scene was repeated after at least 1 but not more than 36 intervening trials, such that repetitions occurred either within a single block or in the next trial block.

(C) Histogram of trial duration changes with scene repetition. Difference in duration for 1218 unique image trial pairs, each pair consisting of a novel trial duration minus a repeated trial duration. Targets are typically found faster on repeated trials of a scene than on novel presentations (i.e. trial durations are shorter) indicated by the leftward, negative bias; red line indicates the median difference value (-5.35 s).

In rodents, ripple-related replay predicts the animal's navigation to learned locations (Singer, Carr, Karlsson & Frank, 2013; Pfeiffer & Foster, 2013; Diba & Buzsáki, 2007), and ripple occurrence is associated with learning goal locations when rats are stopped near those goals (Dupret, O'Neill, Pleydell-Bouverie & Csicsvari, 2010), therefore we reasoned that ripples in macaques may show a visuospatial homolog of the locomotor spatial navigation effects described in rodents. Because visual scan paths are known to change with trial repetition (Wynn et al., 2015; Summerfield, Lepsien, Gitelman, Mesulam & Nobre, 2006; Le-Hoa Võ & Wolfe, 2015; Brockmole & Henderson, 2006; Tatler, Hayhoe, Land & Ballard, 2011), we reasoned that ripples occurring during repeated-scene search may be more frequent when gaze is focused near the target object than any such effect seen during novel trials. Figure 3A shows example SWR local field potential (LFP) traces from both monkeys, some occurring when gaze was near the target object. Figure 3B shows an example sequence of fixations ('scan path') on a repeated trial that contained a ripple near the target location (see supplemental video for an example from the other subject). To quantify this, we took the gaze location at the time of each ripple during search and measured the distance to the scene's target object ('proximity'), yielding two distributions of proximity values: one for SWRs from novel trials and the other from repeated trials. We predicted that there would be a greater likelihood of SWR-locked fixations near the target on repeated than on novel trials. In Figure 3C, the probability distribution of SWR-locked gaze proximity for repeated trials is expressed as a proportion of the novel-trial distribution ('SWR', purple line). Repeated trials had a greater likelihood of SWR-locked fixations near the target than novel trials had (e.g. at 6 DVA; degrees visual angle). Critically, the prior distribution of fixation distances to targets may be biased, and could vary

with trial repetition. As an extreme example, if all fixations were closer to the target on repeated trials than on novel trials, then the subset of fixations that co-occur with SWRs would also, by definition, be closer, and not due to any relation to the SWR. We therefore obtained the prior probabilities, i.e. the proximity distributions for all non-SWR-locked fixations by trial type, and again calculated the likelihood index (here, the likelihood of a given non-SWR-locked proximity value for repeated distribution / the likelihood of that value for the novel distribution). The repeated-trial bias in proximity – attraction of gaze to the repeated-trial target – was specific to SWR-locked fixations. To compare SWR-locked and non-SWR-locked proximity changes with repetition, repeated-trial distances were mean-subtracted from the novel-trial distances in each group (SWR/No-SWR) and compared using a ranksum test, revealing a significant effect (figure 3D; z(2386, 217) = 3.856, p=.000116; SWR means: novel = 14.49 DVA, repeated = 13.70 DVA; No-SWR means: novel = 13.60 DVA, repeated = 14.72 DVA). The repeated-trial proximity bias was greater (repeated fixations were closer) for SWR-locked fixations compared to non-SWR-locked fixations.

Figure 2

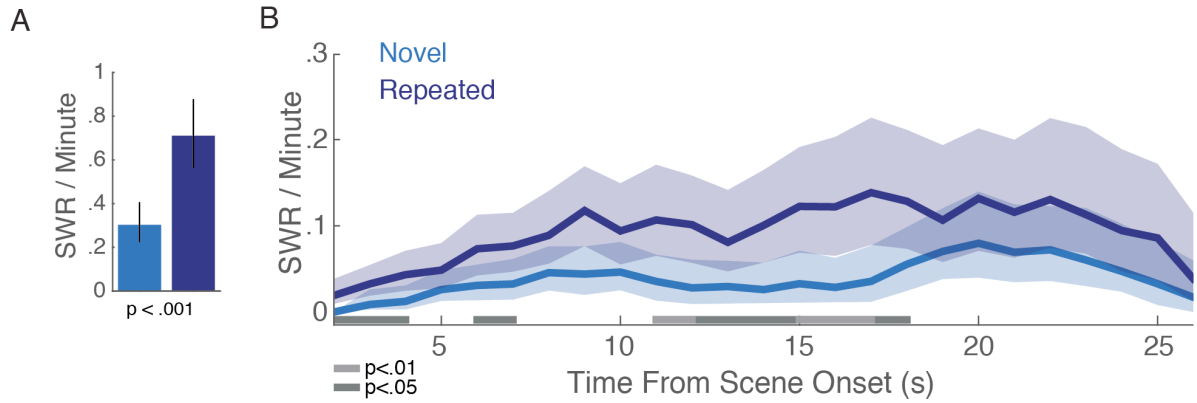

Figure 2. Ripple (SWR) occurrence increases with trial repetition

(A) Mean SWR rates differ for novel (blue) and repeated (purple) trials (P<0.001). Error bars represent 95% bootstrap confidence intervals.

(B) SWR rates over time from scene onset, for Novel and Repeated trials. Shaded portions represent 95% bootstrap confidence intervals. Periods in which rates differ, after multiple comparison correction, are highlighted in grey with their corresponding p value (see methods).

Figure 3

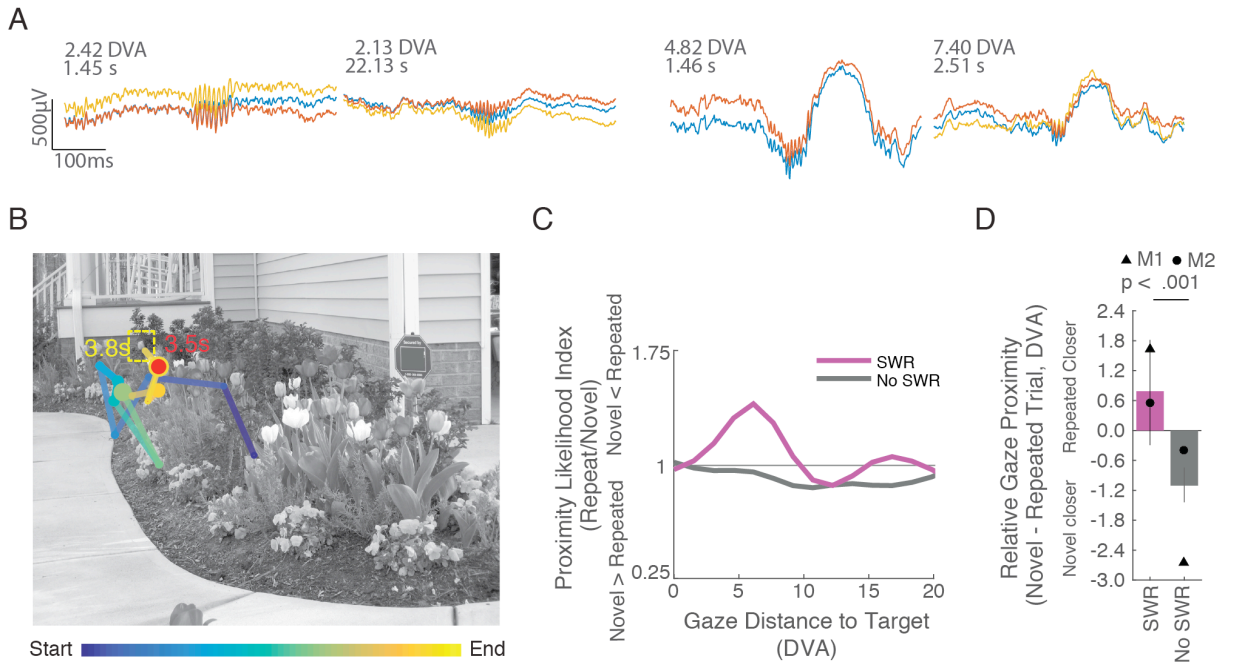

Figure 3. Relation between ripples (SWRs) and gaze location with trial repetition

(A) Example SWRs from both subjects. Left, two examples from M1, and right, two examples from M2. For a given example, multiple channels from same tetrode are shown. Above each example, the distance of the SWR-locked fixation to the target edge is shown in degrees visual angle (DVA), and the time remaining until the target is detected is shown in seconds.

(B) Example scan path to a remembered target. The scan path is color coded for elapsed time (early = blue; late = yellow). The fixation location at the time of the ripple is highlighted in red. The image is shown as grayscale here for scanpath clarity, and the target location box ('AOI', yellow dashed square) has been added. The onset of gaze within the AOI that exceeded the detection threshold ('detection time') occurred 3.8s after scene onset; the ripple occurred 300ms before the detection onset, i.e. 3.5s after scene onset. See supplementary video for scan path example from the other subject.

(C) Probability distributions of all fixation distances to the target ('proximity likelihood'), expressed as a ratio of novel/repeated trial distributions. Separate ratios were calculated for fixations that did/did not accompany SWRs, to explore whether memory-related changes in fixations may be associated with SWR occurrence. For fixations accompanied by SWRs (purple line), the likelihood of a given distance from fixation to target is shown as ratio of Novel/Repeated fixations at given distance; thus, a proximity likelihood ratio > 1 indicates a greater likelihood on repeated trials at that distance. The ratios obtained from non-SWR-locked fixations are shown in gray ('No-SWR').

(D) Comparison of fixation distances to target, for fixations accompanied by SWRs and those occurring in the absence of SWRs. Fixations from repeated trials were normalized by mean-subtracting novel fixation distances, for each group (SWR and no SWR), plotted with 95% confidence intervals, and separated by animal: filled triangle (M1) and circle (M2). Relative to the distances at the time of encoding, SWR-locked fixations (purple) are closer to the target than non SWR-locked fixations (gray; p<.001, ranksum test; SWR N=217, No SWR N=2386).

As illustrated in Figure 3B, proximity of SWR-locked gaze to the target may precede or facilitate target detection. If so, the gaze proximity results of figure 3C, D, may be related to remaining time-to-detection. We measured the proximity of SWR-locked fixations occurring at fixed time intervals leading up to detection, for novel and repeated trials, where memory-guided effects could only be occurring in the repeated-trial group. SWR-locked fixations were closer to the target than SWR-locked novel trial fixations in the seconds leading up to target detection (see figure 4A for p values, permutation test, n=10000). In contrast, among fixations unaccompanied by SWRs, the repeated trial fixations were consistently farther from the target than novel fixations in the seconds leading up to target detection (see figure 4A for p values, permutation test, n=10000).

To better understand the interaction between SWRs and repeated target detection, the difference in novel – repeated distances was compared for SWR-locked fixations and non-SWR locked fixations (figure 4B). Here, from 1 to 9 seconds before the trial ends, SWR-locked and non-SWR locked fixations differed in their proximity bias with trial repetition. Specifically, SWR-locked fixations near the end of the trial are closer to repeated than to novel targets, and this change in proximity is greater than what is observed for non-SWR-locked fixations (see figure 4B for p values, permutation test, n=10000).

Figure 4

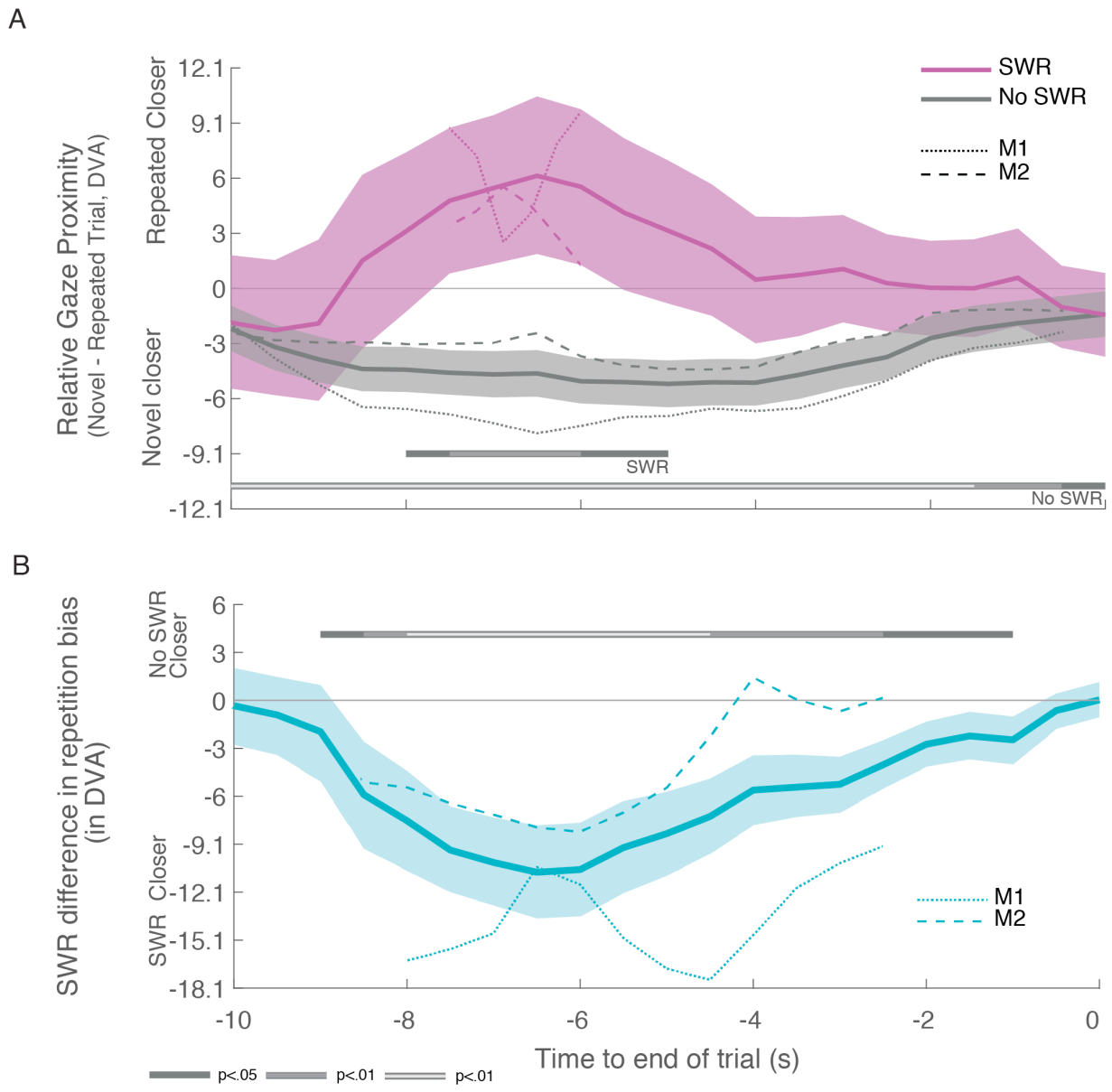

Figure 4. SWR-locked and non-SWR locked fixations differ in proximity bias

(A) Mean difference in gaze distance to target with trial repetition (in DVA), measured as a function of time prior to target detection. Distances on repeated trials subtracted from those on novel trials shown for fixations that were accompanied by SWRs (purple) and those not accompanied by SWRs (grey), both surrounded by shading indicating 95% bootstrap confidence intervals. For all significant effects, each subject's mean difference is also shown with dotted (M1) or dashed (M2) lines. P values (permutation test; multiple comparison corrected), for the mean difference within category, for each window, are shown on bottom portion of plot. Top p value bars: novel minus repeated distance for SWR-locked fixations. Bottom p value bar: novel minus repeated distances for non-SWR locked fixations. Grey reference line included at distance = 0.

(B) SWR difference in repetition bias (in DVA), aligned in time relative to end of trial. Difference between the repetition-fixation bias with SWRs and the repetition-fixation bias without SWRs (i.e. 4a gray line – purple line) shown here with solid light blue line surrounded by shading indicating 95% bootstrap confidence intervals. Individual

subject mean differences shown with dotted (M1) or dashed (M2) lines. P values (permutation test; multiple comparison corrected), for the mean difference, collapsed across subjects, for each window, are shown on bottom portion of plot. $P<0.05$ indicates [[novel - repeated non-SWR-locked fixations] - [novel - repeated SWR-locked fixations]] $\neq 0$. Grey reference line included at distance = 0.

Discussion:

In the present study, we measured hippocampal sharp-wave ripples (SWRs) that appeared as macaques searched for target objects naturally embedded in photographic scenes, comprising unique events. With repetition, ripples became more frequent near the target object in time and space, demonstrating a link between ripples and memory in primates.

In rats, goals are over-represented in both the preponderance of SWRs and as representations in ripple-associated internally-generated sequences (Dupret, O'Neill, Pleydell-Bouverie & Csicsvari, 2010; Pfeiffer & Foster, 2013), putatively through NMDA-R-dependent processes (Dupret, O'Neill, Pleydell-Bouverie & Csicsvari, 2010). During sequence replay of location representations, specific cell firing can be biased by current in-field cells (Pfeiffer & Foster, 2013; Diba & Buzsáki, 2007) see also (Jackson, Johnson & Redish, 2006). Although speculative, such a bias in the present study could increase view-selective firing near the target, facilitating later recall of the target location.

In addition to the local neuronal populations modulated during SWRs, SWR-associated population bursts can have widespread effects on neocortical and subcortical structures (Le Van Quyen et al., 2010; Siapas & Wilson, 1998; Sirota, Csicsvari, Buhl & Buzsáki, 2003; Battaglia, Sutherland & McNaughton, 2004; Peyrache, Khamassi, Benchenane, Wiener & Battaglia, 2009; Kaplan et al., 2016; Logothetis et al., 2012), while targeting specific subsets of cells in select target areas (Jadhav, Rothschild, Roumis & Frank, 2016; Ciocchi, Passecker, Malagon-Vina,

Mikus & Klausberger, 2015). Thus, the role of SWRs in waking tasks may relate to memory retrieval and generation of goal trajectories (Roumis & Frank, 2015) affecting extra-hippocampal systems (Jadhav, Rothschild, Roumis & Frank, 2016; Maingret, Girardeau, Todorova, Goutierre & Zugaro, 2016).

Ripples are detected relatively infrequently in vivo, and particularly in primates (Bragin, Engel, Wilson, Fried & Mathern, 1999; Talakoub, Gomez Palacio Schjetnan, Valiante, Popovic & Hoffman, 2016; Le Van Quyen et al., 2008; Axmacher, Elger & Fell, 2008); nevertheless, we observed that they occur reliably during visual task performance, session after session (Leonard et al., 2015). The rates observed are likely lower bounds, due to the limited sampling across subfields and along the septotemporal axis, typically in one hemisphere, and the amplitude threshold detection methods are susceptible to false negatives. This is true across species but likely to be exacerbated when sampling reflects a smaller proportion of area, as in the many-fold larger hippocampi of macaques and humans compared to rats and mice. Even with these considerations, SWRs/IGSs do not appear to occur with each instance of learning or recall in rodents, and as such, they may be conceived as modulators rather than mediators of these processes [see (Carr, Jadhav & Frank, 2011; Girardeau, Benchenane, Wiener, Buzsáki & Zugaro, 2009; Girardeau & Zugaro, 2011; O'Neill, Pleydell-Bouverie, Dupret & Csicsvari, 2010)]. The results in macaques are in line with these reports in rodents, with the note that SWRs appear in macaques both in quiescence and pauses in exploration, but also during active exploration (Leonard et al., 2015). Further, the present results suggest a juxtaposition of two different, associated activities seen in the rat hippocampus: IGSs during task performance, on one hand, and SWRs and IGSs at trial end/the search goal, on the other.

'Vicarious trial and error' is behavior seen in rodents during exploration and decision making, and is associated with strong, protracted theta-band activity (Redish, 2016). Whereas some aspects of behavior during exploration of visual images in macaques may map on to VTE, the theta rhythm is relatively weak and transient compared to its appearance during rest and offline epochs (Leonard et al., 2015). It's unclear if the computations attributed to VTE could be conveyed through ripples in primates.

Alternatively, although highly speculative, SWR rates may be related to changes in reward anticipation. Broadly supporting this, reward consumption leads to increased SWR rates in rats (Dupret, O'Neill, Pleydell-Bouverie & Csicsvari, 2010), and changing reward rate is 'tracked' by SWR and associated patterned replay (Shen, Bezgin, Selvam, McIntosh & Ryan, 2016). In the present study, perceived likelihood of reward can change with gaze location and as a function of trial repetition, similar to SWRs rates. On novel trials, it is unclear whether the animal will find the difficult target. Indeed, in some cases gaze may land right on the target without recognition. Proximity to the target is unknown during search on novel trials. On repeated trials, the situation changes. Particularly for object/scene exemplars that are not immediately recognized, it may take some 'looking around' before finding a cue that aids recall, at which point the animal has a rapid change in anticipated reward. Even if the exact target location or stimulus content is unclear, they may recognize that they are in the correct region (e.g. part of a landscape, or, in Figure 3a, set of tulips). This would be distinct from well-learned scene-target associations for which reward is correctly anticipated from the outset. During search, typical saccade sizes overlap with image content in patches within the scene, thus patches of scene near the target are more likely to be similar in content, i.e. predictive of the

target in space, visual similarity, and temporal order. Over trials, this may have produced a bias in SWR occurrence on repeated trials near the target, in space and time, within ~8 degree swaths of the target and within the final 1-9 seconds of search.

This is only one of many possible accounts, and could be properly tested with different experiments in which rate of reward was varied in predictable ways (e.g. by location or image type), cueing of the target was systematically varied (controlling sampling during encoding and cueing during recall) and through task responses that indicate reward prediction (e.g. anticipatory lipping responses).

In general, the interest in SWRs lies in their reflection of strong local population synchrony and selective activation, and their ability to alter activity in distant structures. These properties were considered useful during 'offline' epochs, when stimulus-related processing would not be corrupted by such activity. Although speculative, the increased incidence of SWRs near visual goal detection, suggests that one consequence of SWR-activity may be to exert a memory-related top-down influence on neural systems that guide behavior, including the oculomotor system (Shen, Bezgin, Selvam, McIntosh & Ryan, 2016). In sum, the SWR-mediated mechanisms that support route finding and spatial decision-making in rodents may be co-opted in primates to support non-ambulatory visual, and episodic-like learning, using past experience to guide visual search towards goals.

4.3 Experimental Procedures

Detailed experimental procedures are available in the Supplemental Experimental Procedures.

Experimental Design

All procedures were conducted with approval from the local ethics and animal care authorities (Animal Care Committee, Canadian Council on Animal Care). Two adult female rhesus macaques, *M. mulatta*, performed a memory-guided visual target detection task thought to require hippocampal function in primates (Chau, Murphy, Rosenbaum, Ryan & Hoffman, 2011). The modified flicker change detection task is shown in Figure 1 and consisted of an original scene that alternated with an object-manipulated scene, with a short mask (grey screen) shown between each image presentation, making the changing object difficult to identify without prior experience with that flicker scene. Found targets were rewarded with delivery of a preferred juice. The data presented here were included in part in previous publications, addressing questions related to saccades and visual search, but not memory (Leonard et al., 2015; Hoffman et al., 2013).

Electrophysiological preparation and recordings

The surgical and experimental procedures are described in detail in Leonard et al., (Leonard et al., 2015); M1 and M2 . Tetrodes (Thomas Recordings, Giessen, Germany) or electrodes were placed in the CA3/DG region of the hippocampus to record local field potentials (LFPs). SWR events were identified as events which registered 3 SD above the mean ripple-band envelope. Supplemental Experimental Procedures describe the detection in more detail.

Statistical Procedures

Novel-Repeated SWR Rate comparisons

Sharp-wave ripple rates were compared for 584 novel and 749 repeated trials, where both novel and repeated trial durations were under 30 seconds ('hits'). We compared the observed mean rate difference between novel and repeated conditions (Novel mean SWR/min: .306; Repeated mean SWR/min: .708) to 10000 mean rate differences generated by randomly swapping condition labels for the trial duration, and SWR occurrence (see Figure 2A).

Rates as a function of time from scene onset

Using a sliding window (width 4s, steps 1s) SWR rate was calculated as the number of SWR events divided by all trial durations which fell into that window. Differences in rates were tested using a permutation test for Novel vs. Repeated rates for each sliding window, corrected using the positive false discovery rate method (pFDR (Storey, 2002)). Figure 2B shows bootstrap-estimated variability for each window of each condition.

Visual distance between fixation and target during SWRs

For all fixations during scene search, the distance between fixation and target edge was calculated. For both SWR-locked and non-locked fixations, repeated distances were subtracted from the mean novel distances, shown in figure 3D, expressed in degrees visual angle (DVA), with 95% bootstrap confidence intervals (n=10000). Positive values represent larger novel distances (i.e. repeated trial fixations had the 'proximity bias' meaning that they were closer), where negative values represent larger repeated distances (i.e. a novel trials has a proximity bias). These distances were compared with a Wilcoxon Rank Sum test.

For both SWR-locked fixations and non-SWR locked fixations, the frequency distribution of distances from fixation to target edge was calculated using a kernel density function. The density for each repeated bin was then divided by the corresponding novel bin, to establish a repeated/novel ratio, describing the relative change in SWR likelihood at various distances from the target (figure 3C, purple). The ratio was also calculated for non-SWR locked fixations (figure 3C, grey), indicating changes in fixation distances with repetition, outside of SWR co-occurrences.

Distance between fixation and target over time

In Figure 4A, for SWR-locked fixations and non-SWR locked fixations, the difference in gaze distance from target was calculated, in a given 4-second window. Positive values reflect shorter repeated distances than novel ('proximity bias'), and negative values reflect shorter novel distances than repeated. In figure 4B, the mean difference between SWR-locked fixations and non-SWR locked fixations, were calculated, in a given window. In both cases, a label swap procedure was run for each window, establishing the probability of the observed difference distances, corrected using the positive false discovery rate method (Figure 4; pFDR (Storey, 2002)).

4.4 Supplemental Experimental Procedures

Experimental Design

In the visual target detection task (modified flicker change detection) visual search on the flickering scene (Described in Figure 1) lasted until the changing object was viewed for at least .8 s (target found; 'hit') or a total search time maximum was reached (target not found; 'miss'). Maxima were 45s for M1, and 30s for M2, therefore analysis was restricted to search

times under 30s for M1, for similar comparison across animals. Found targets were rewarded with delivery of a preferred juice, and all trials entered a black-screen inter-trial interval before the next trial started (ITI: 20s, M1; 8s, M2). Trials were shown in blocks of 30 trials, with the novel trials distributed evenly in first and second halves of the block, and where half of novel trials were repeated in that block and the remaining half in the next block (such that a minimum of 1 and maximum of 36 trials intervened between the novel and repeat presentations). If the subject looked off screen, the trial was paused. If the amount of off-screen looking exceeded the total trial duration (all off-screen and on-screen looking) by 50% that trial was removed from analysis.

Novel-Repeated paired search durations

Novel image trials were matched to their repeated image counterparts from all sessions with SWR events (M1: 36 daily sessions, M2: 45 daily sessions). Where an image was repeated twice, each repetition is paired with the novel trial duration. This resulted in 1218 novel/repeated trial pairs consisting of 591 novel presentations with 761 counterparts. Repeated trial durations (mean 10.121, std 10.214) were subtracted from the trial duration for the corresponding novel images (mean 16.404, std 11.203). Because these difference values were non-normally distributed (One sample KS test; $KS(1218) = 0.5859$, $P < 0.001$, two-tail), a non-parametric paired-samples test (Wilcoxon signed-rank test, two tailed) was used to test if the repeated and novel difference in durations deviated from 0. Note that the histogram occurrences near zero (Figure 1C) include trial-pairs in which both novel and repeated targets are undetected, registering both trial pairs with same 'maximum time'. Although infrequent

overall, these trials contribute disproportionately to the difference histogram due to their temporal precision compared to other trial performance types.

Electrophysiological preparation and recordings

The monkeys were implanted with depth-adjustable, indwelling platinum/tungsten multicore tetrodes (Thomas Recordings, Giessen, Germany), lowered into the CA3/DG region of hippocampus. Location was based on MR images (M1), on MR/CT coregistration of electrode position (M2), and on functional characterization based on expected white/gray matter and ventricle transitions in depth during lowering. In addition, we observed SWRs only in limited ranges of depth, often near single and multi-unit activity.

Neural recordings for field potentials were referenced to local guide tube tips (M1) or the titanium chamber (M2) and digitally sampled at 32 kHz using a Digital Lynx acquisition system (Neuralynx, Inc., Bozeman, Montana, USA), filtered between 0.5 Hz and 2 kHz.

SWR events were detected by an observer selecting the tetrode and channel with the clearest ripple activity, filtering that LFP signal (100-250 Hz), transforming to z-scores, rectifying, and band pass filtering 1-20 Hz. Events which registered 3 SD above the mean, with a minimum duration of 50ms beginning and ending at 1 SD, were identified as ripples. Unlike ripple detection procedures in rodents, this method does not need to account for strong theta oscillations as there was no sustained peak in the theta frequency band observed in these recording sites during search, for both animals. Additional example ripples and frequency power spectra from search are previously published in both animals used in this study, showing the drop in theta-band activity during search in this task (Leonard 2015).

Statistical Procedures

Novel-Repeated SWR Rate comparisons

We compared sharp-wave ripple rates using a label-swap permutation test, with a two-tail design. Rates are calculated from trial durations and numbers of SWRs per condition (N=145 SWRs). The observed mean rate difference between novel and repeated conditions (Novel mean SWR/min: .306; Repeated mean SWR/min: .708) were compared to 10000 mean rate label-swapped differences.

Rates as a function of time from scene onset

For all periods of on screen search behavior (all off-screen looking behavior removed), the SWR rate was calculated using a sliding window (width 4s, steps 1s; range 0 to 30s; 27 windows for each condition). The rate was calculated, in a given window, as the number of SWR events divided by all trial durations which fell into that window.

Differences in rates were tested using a permutation test, comparing the differences distribution for Novel vs. Repeated rates for each sliding window. To statistically test differences in rates between conditions, tests were run with 10,000 permutations, for each window, establishing the probability of the observed difference in novel vs. repeated rate having occurred, using a two tail design. These permutation test values were then corrected using the positive false discovery rate method (pFDR (Storey 2002)).

Figure 2B shows variability estimated for each window of each condition with the bootstrap method (sampling with replacement), whereas the permutation test statistic was the mean difference between conditions, generated with a label swap procedure (sampling without replacement). Because the significance test measures mean differences between conditions,

and the confidence intervals reflect variability within conditions, the 95% bootstrap confidence intervals may overlap where permutation test shows significance.

Visual distance between fixation and target during SWRs

Fixations within +- 250 ms of the middle of a SWR were labelled as SWR-locked fixations (novel trial fixations: N=178; repeated trial fixations: N=217). Fixations greater than +/- 2500 ms away from a SWR event, including fixations from trials without SWR events, were labelled as non-SWR locked fixations (novel trial fixations: N=2625; repeated trial fixations: N=2386). For both SWR-locked fixations and non-SWR locked fixations, the frequency distribution ('smoothed histogram') of distances from fixation to target edge was calculated using a kernel density function (kernel bandwidth: 2.39DVA; step size: 1.51DVA), thereby normalizing for differences in sample size across distributions. The density for each repeated bin was then divided by the corresponding novel bin, to establish a repeated/novel ratio. This ratio describes the relative change in SWR likelihood at various distances from the target. Values > 1 indicate the likelihood at that distance was greater for repeated-trial SWRs than novel-trial SWRs and values <1 indicate the likelihood is greater for novel trials (figure 3C, purple).

We then compared the distance between fixation and target for the SWR-locked fixations and non-SWR locked fixations. For both SWR locked and non-locked fixations, repeated distances were subtracted from the mean novel distance (SWR group: 14.49 DVA, no SWR group: 13.6 DVA). These distances are shown in figure 3D, expressed in DVA, with 95% bootstrap confidence intervals (n=10000). These distances were compared between SWR-locked fixations and non-SWR locked fixations with a Wilcoxon Rank Sum test.

Distance between fixation and target over time

Due to the two-way nature of the data (Novel/Repeated vs SWR-locked fixations/non-SWR locked fixations), two calculations were performed in sequence. The first compared novel to repeated distances (distance from fixation to target edge for both conditions, 'relative gaze proximity'), for the SWR-locked fixations (figure 4A, purple) and non-SWR locked fixations separately (figure 4A, grey). The second measure calculates the difference in the resultant relative gaze proximity between SWR-locked fixations and non-SWR locked fixations (figure 4B, light blue). In both cases, a moving window was used (width 4s; steps .5s), on all SWR-locked fixations and non-SWR locked fixations from periods of on screen search behavior, all aligned to trial end when the target was successfully detected.

In figure 4A, for SWR-locked fixations and non-SWR locked fixations, the difference in distance was calculated, in a given window, as the mean novel fixation distances minus the mean repeated fixation distances. SWR: mean distance for novel fixations with SWR minus mean distance for repeated fixations with SWR. No SWR: mean distance for novel fixations with no SWR minus mean distance for repeated fixations with no SWR. Where values differ from zero, positive values reflect shorter repeated distances than novel ('proximity bias'), and negative values reflect shorter novel distances than repeated.

In figure 4B, the mean difference between SWR-locked fixations and non-SWR locked fixations, were calculated, in a given window. Where values differ from zero, positive values reflect periods where SWR-locked fixations were farther from target, and negative values reflect periods where the SWR-locked group had fixations closer to target.

To statistically test differences are not equal to 0, a label swap procedure was run with 10,000 permutations, for each window and subsequently adjusted using the positive false

discovery rate method (figure 4; pFDR (Storey 2002)). Additionally, a 95% bootstrap confidence intervals (10,000 permutations) were calculated for each window.

4.5 References

Axmacher, N., Elger, C. E., & Fell, J. (2008). Ripples in the medial temporal lobe are relevant for human memory consolidation. *Brain, 131*(Pt 7), 1806-1817. doi:10.1093/brain/awn103

Battaglia, F. P., Sutherland, G. R., & McNaughton, B. L. (2004). Hippocampal sharp wave bursts coincide with neocortical "up-state" transitions. *Learn Mem, 11*(6), 697-704. doi:10.1101/lm.73504

Bragin, A., Engel, J., Wilson, C., Fried, I., & Mathern, G. (1999). Hippocampal and entorhinal cortex high-frequency oscillations (100--500 Hz) in human epileptic brain and in kainic acid--treated rats with chronic seizures. *Epilepsia., 40*(2), 127-137.

Brockmole, J. R., & Henderson, J. M. (2006). Using real-world scenes as contextual cues for search. *Endocrinol Metab Clin North Am, 13*(1), 99-108.

Buzsáki, G. (1986). Hippocampal sharp waves: their origin and significance. *Brain Res, 398*(2), 242-252.

Buzsáki, G. (1989). Two-stage model of memory trace formation: a role for "noisy" brain states. *Neuroscience, 31*(3), 551-570.

Buzsáki, G., Leung, L. W., & Vanderwolf, C. H. (1983). Cellular bases of hippocampal EEG in the behaving rat. *Brain Res, 287*(2), 139-171.

Buzsáki, G. (2015). Hippocampal sharp wave-ripple: A cognitive biomarker for episodic memory and planning. *Hippocampus, 25*(10), 1073-1188.

Carr, M. F., Jadhav, S. P., & Frank, L. M. (2011). Hippocampal replay in the awake state: a potential substrate for memory consolidation and retrieval. *Nat Neurosci, 14*(2), 147-153. doi:10.1038/nn.2732

Chau, V. L., Murphy, E. F., Rosenbaum, R. S., Ryan, J. D., & Hoffman, K. L. (2011). A Flicker Change Detection Task Reveals Object-in-Scene Memory Across Species. *Front Behav Neurosci, 5*, 58. doi:10.3389/fnbeh.2011.00058

Ciocchi, S., Passecker, J., Malagon-Vina, H., Mikus, N., & Klausberger, T. (2015). Brain computation. Selective information routing by ventral hippocampal CA1 projection neurons. *Science, 348*(6234), 560-563. doi:10.1126/science.aaa3245

Diba, K., & Buzsáki, G. (2007). Forward and reverse hippocampal place-cell sequences during ripples. *Nat Neurosci, 10*(10), 1241-1242. doi:10.1038/nn1961

Dragan, M. C., Leonard, T. K., Lozano, A. M., McAndrews, M. P., Ng, K., & Ryan, J. D., et al. (2016). Pupillary responses and memory-guided visual search reveal age-related and Alzheimer's-related memory decline. *Behav Brain Res, , in press* doi:10.1016/j.bbr.2016.09.014

Dupret, D., O'Neill, J., Pleydell-Bouverie, B., & Csicsvari, J. (2010). The reorganization and reactivation of hippocampal maps predict spatial memory performance. *Nat Neurosci, 13*(8), 995-1002. doi:10.1038/nn.2599

Ego-Stengel, V., & Wilson, M. A. (2010). Disruption of ripple-associated hippocampal activity during rest impairs spatial learning in the rat. *Hippocampus, 20*(1), 1-10. doi:10.1002/hipo.20707

Eschenko, O., Ramadan, W., Mölle, M., Born, J., & Sara, S. J. (2008). Sustained increase in hippocampal sharp-wave ripple activity during slow-wave sleep after learning. *Learning & Memory, 15*(4), 222-228. doi:10.1101/lm.726008

Gaffan, D. (1994). Scene-Specific Memory for Objects: A Model of Episodic Memory Impairment in Monkeys with Fornix Transection. *J Cogn Neurosci, 6*(4), 305-320. doi:10.1162/jocn.1994.6.4.305

Girardeau, G., Cei, A., & Zugaro, M. (2014). Learning-induced plasticity regulates hippocampal sharp wave-ripple drive. *J Neurosci, 34*(15), 5176-5183. doi:10.1523/JNEUROSCI.4288-13.2014

Girardeau, G., Benchenane, K., Wiener, S. I., Buzsáki, G., & Zugaro, M. B. (2009). Selective suppression of hippocampal ripples impairs spatial memory. *Nat Neurosci, 12*(10), 1222-1223. doi:10.1038/nn.2384

Girardeau, G., & Zugaro, M. (2011). Hippocampal ripples and memory consolidation. *Curr Opin Neurobiol, 21*(3), 452-459. doi:10.1016/j.conb.2011.02.005

Hoffman, K. L., Dragan, M. C., Leonard, T. K., Micheli, C., Montefusco-Siegmund, R., & Valiante, T. A., et al. (2013). Saccades during visual exploration align hippocampal 3-8 Hz rhythms in human and non-human primates. *Frontiers in systems neuroscience, 7*, 43. doi:10.3389/fnsys.2013.00043

Hollingworth, A. (2006). Scene and position specificity in visual memory for objects. *J Exp Psychol Learn Mem Cogn, 32*(1), 58-69. doi:10.1037/0278-7393.32.1.58

Jackson, J. C., Johnson, A., & Redish, A. D. (2006). Hippocampal sharp waves and reactivation during awake states depend on repeated sequential experience. *J Neurosci, 26*(48), 12415-12426. doi:10.1523/JNEUROSCI.4118-06.2006

Jadhav, S. P., Kemere, C., German, P. W., & Frank, L. M. (2012). Awake hippocampal sharp-wave ripples support spatial memory. *Science, 336*(6087), 1454-1458. doi:10.1126/science.1217230

Jadhav, S. P., Rothschild, G., Roumis, D. K., & Frank, L. M. (2016). Coordinated Excitation and Inhibition of Prefrontal Ensembles during Awake Hippocampal Sharp-Wave Ripple Events. *Neuron, 90*(1), 113-127.

Kaplan, R., Adhikari, M. H., Hindriks, R., Mantini, D., Murayama, Y., & Logothetis, N. K., et al. (2016). Hippocampal Sharp-Wave Ripples Influence Selective Activation of the Default Mode Network. *Curr Biol, 26*(5), 686-691. doi:10.1016/j.cub.2016.01.017

Le Van Quyen, M., Bragin, A., Staba, R., Crépon, B., Wilson, C. L., & Engel, J., et al. (2008). Cell type-specific firing during ripple oscillations in the hippocampal formation of humans. *J Neurosci, 28*(24), 6104-6110. doi:10.1523/JNEUROSCI.0437-08.2008

Le Van Quyen, M., Staba, R., Bragin, A., Dickson, C., Valderrama, M., & Fried, I., et al. (2010). Large-scale microelectrode recordings of high-frequency gamma oscillations in human cortex during sleep. *J Neurosci, 30*(23), 7770-7782. doi:10.1523/JNEUROSCI.5049-09.2010

Le-Hoa Võ, M., & Wolfe, J. M. (2015). The role of memory for visual search in scenes. *Ann N Y Acad Sci, 1339*(1), 72-81.

Leonard, T. K., Mikkila, J. M., Eskandar, E. N., Gerrard, J. L., Kaping, D., & Patel, S. R., et al. (2015). Sharp Wave Ripples during Visual Exploration in the Primate Hippocampus. *J Neurosci, 35*(44), 14771-14782. doi:10.1523/JNEUROSCI.0864-15.2015

Logothetis, N. K., Eschenko, O., Murayama, Y., Augath, M., Steudel, T., & Evrard, H. C., et al. (2012). Hippocampal-cortical interaction during periods of subcortical silence. *Nature, 491*(7425), 547-553. doi:10.1038/nature11618

Maingret, N., Girardeau, G., Todorova, R., Goutierre, M., & Zugaro, M. (2016). Hippocampo-cortical coupling mediates memory consolidation during sleep. *Nat Neurosci, 19*(7), 959-964. doi:10.1038/nn.4304

O'Keefe, J. (1976). Place units in the hippocampus of the freely moving rat. *Exp Neurol, 51*(1), 78-109.

O'Neill, J., Pleydell-Bouverie, B., Dupret, D., & Csicsvari, J. (2010). Play it again: reactivation of waking experience and memory. *Trends Neurosci, 33*(5), 220-229. doi:10.1016/j.tins.2010.01.006

O'Neill, J., Senior, T., & Csicsvari, J. (2006). Place-selective firing of CA1 pyramidal cells during sharp wave/ripple network patterns in exploratory behavior. *Neuron, 49*(1), 143-155. doi:10.1016/j.neuron.2005.10.037

Peyrache, A., Khamassi, M., Benchenane, K., Wiener, S. I., & Battaglia, F. P. (2009). Replay of rule-learning related neural patterns in the prefrontal cortex during sleep. *Nat Neurosci, 12*(7), 919-926. doi:10.1038/nn.2337

Pfeiffer, B. E., & Foster, D. J. (2013). Hippocampal place-cell sequences depict future paths to remembered goals. *Nature, 497*(7447), 74-79. doi:10.1038/nature12112

Redish, A. D. (2016). Vicarious trial and error. *Nat Rev Neurosci, 17*(3), 147-159. doi:10.1038/nrn.2015.30

Roumis, D. K., & Frank, L. M. (2015). Hippocampal sharp-wave ripples in waking and sleeping states. *Curr Opin Neurobiol, 35*(Complete), 6-12.

Shen, K., Bezgin, G., Selvam, R., McIntosh, A. R., & Ryan, J. D. (2016). An Anatomical Interface between Memory and Oculomotor Systems. *J Cogn Neurosci, 44*, 1-12. doi:10.1162/jocn_a_01007

Siapas, A. G., & Wilson, M. A. (1998). Coordinated interactions between hippocampal ripples and cortical spindles during slow-wave sleep. *Neuron, 21*(5), 1123-1128.

Singer, A. C., Carr, M. F., Karlsson, M. P., & Frank, L. M. (2013). Hippocampal SWR activity predicts correct decisions during the initial learning of an alternation task. *Neuron, 77*(6), 1163-1173. doi:10.1016/j.neuron.2013.01.027

Sirota, A., Csicsvari, J., Buhl, D., & Buzsáki, G. (2003). Communication between neocortex and hippocampus during sleep in rodents. *Proc Natl Acad Sci U S A, 100*(4), 2065-2069. doi:10.1073/pnas.0437938100

Skaggs, W. E., McNaughton, B. L., Permenter, M., Archibeque, M., Vogt, J., & Amaral, D. G., et al. (2007). EEG sharp waves and sparse ensemble unit activity in the macaque hippocampus. *J Neurophysiol, 98*(2), 898-910. doi:10.1152/jn.00401.2007

Storey, J. D. (2002). A direct approach to false discovery rates. *Journal Of The Royal Statistical Society Series B, 64*(3), 479-498.

Summerfield, J. J., Lepsien, J., Gitelman, D. R., Mesulam, M. M., & Nobre, A. C. (2006). Orienting attention based on long-term memory experience. *Neuron, 49*(6), 905-916.

Suzuki, S. S., & Smith, G. K. (1985). Single-cell activity and synchronous bursting in the rat hippocampus during waking behavior and sleep. *Exp Neurol, 89*(1), 71-89.

Talakoub, O., Gomez Palacio Schjetnan, A., Valiante, T. A., Popovic, M. R., & Hoffman, K. L. (2016). Closed-Loop Interruption of Hippocampal Ripples through Fornix Stimulation in the Non-Human Primate. *Brain Stimulation,* , . doi:10.1016/j.brs.2016.07.010

Tatler, B. W., Hayhoe, M. M., Land, M. F., & Ballard, D. H. (2011). Eye guidance in natural vision: reinterpreting salience. *J Vis, 11*(5), 5. doi:10.1167/11.5.5

Wynn, J., Bone, M., Dragan, M., Hoffman, K., Buchsbaum, B., & Ryan, J., et al. (2015). Selective scanpath repetition supports memory-guided visual search. *J Vis, 15*(12), 789. doi:10.1167/15.12.789

Ylinen, A., Bragin, A., Nádasdy, Z., Jandó, G., Szabó, I., & Sik, A., et al. (1995). Sharp wave-associated high-frequency oscillation (200 Hz) in the intact hippocampus: network and intracellular mechanisms. *J Neurosci, 15*(1 Pt 1), 30-46.

Chapter 5 – Discussion

5.1 Summary of findings

Overall, this work demonstrates that SWRs in macaque are implicated in new memory formation. However, despite this result, the criticism remains that these SWR events are relatively uncommon (1-2 times per minute during activity). Given that SWR events are sparse, it may seem that SWRs are not an ideal candidate to study in trying to understand memory formation. However, despite the sparsity of SWR events, their influence has been observed throughout the cortex, suggesting the possibility for considerable impact in spite of their relative sparsity.

There is no other event in the brain (in healthy populations) that impacts such a far reaching and vast area of the cortex. Though originating in the hippocampus CA3 network (Buzsáki, Leung & Vanderwolf, 1983; Buzsáki, 1986) SWRs have been shown to be biased by neocortical slow oscillations (Siapas & Wilson, 1998; Sirota, Csicsvari, Buhl & Buzsáki, 2003; Battaglia, Sutherland & McNaughton, 2004; Wolansky, Clement, Peters, Palczak & Dickson, 2006; Isomura et al., 2006; Mölle, Yeshenko, Marshall, Sara & Born, 2006; Clemens et al., 2007; Wierzynski, Lubenov, Gu & Siapas, 2009), SWR events are correlated with spindles in both somatosensory and visual areas (Ji & Wilson, 2007), SWR events are correlated with reward-related activity in the striatum (Lansink, Goltstein, Lankelma, McNaughton & Pennartz, 2009) and SWR events are correlated with rule learning in the prefrontal cortex (Wierzynski, Lubenov, Gu & Siapas, 2009; Peyrache, Khamassi, Benchenane, Wiener & Battaglia, 2009).

In addition to impact throughout the cortex, SWR are an important topic of study as there exists a great deal of evidence linking their occurrence with memory formation. For

example, waking state SWRs increase in rate with experience (Jackson, Johnson & Redish, 2006), after learning (Axmacher, Elger & Fell, 2008), and following reward (Ramadan, Eschenko & Sara, 2009; Singer & Frank, 2009). More dramatically, interruption of SWRs during sleep or wake impairs memory (Girardeau, Benchenane, Wiener, Buzsáki & Zugaro, 2009; Ego-Stengel & Wilson, 2010), (Jadhav, Kemere, German & Frank, 2012).

Though the mechanisms of how SWRs impact memory are not fully characterized, the impact of SWR has been shown to be substantial. At the minimum, tracking SWR events act as a tractable proxy for the actual mechanisms behind new memory formation, and at maximum (though completely unsubstantiated) SWRs could be directly responsible for new memory formation. Even given the bare minimum assumption, that SWRs are a proxy to the events that lead to new memory formation, understanding their role during active behavior gives a glimpse into the important moments when the hippocampus is encoding information to remember.

5.2 Parallels in hippocampal activity during primate visual search compared to rodent locomotion

In the waking rat, during rodent locomotion, the theta frequency (6-10HZ) dominates the LFP of CA1 (Grastyán, Lissák, Madarász, & Donhoffer, 1959; Vanderwolf, 1969) and is characterized as part of a theta-SWR dichotomy, in that SWR and theta are generated by competing mechanisms, and in the rodent are not found to co-occur (Buzsáki, Lai-Wo S., & Vanderwolf, 1983). In the macaque, theta appears during image viewing (Jutras, Fries, & Buffalo, 2013), and least frequently occurs during periods where SWR events are present (Leonard et al., 2015). Furthermore, in human and macaque, saccadic eye movement acts to align hippocampal theta rhythms (Hoffman et al., 2014).

In the rodent, place cells, which are reliably activated as an area in an environment is consistently encountered, fire most consistently during locomotion (Foster, Castro, & McNaughton, 1989). Though the presence of place cells has been investigated in the macaque hippocampus (Chapter 13; Mizumori, 2008), their existence has yet to be confirmed. Where place cells were expected to be found, “view cells” were identified instead. View cells fire in response to gaze being directed to a particular part of the environment, and consistently fire in response to gaze and not location due to locomotion (Georges-François, Rolls, & Robertson, 1999).

Though parallels exist between theta during movement, and consistency in place and view cell firing exist, it is unclear if hippocampal functions remain consistent across species for space processing. In particular, to what extent place cells, which have been well characterized in the rat (O’Keefe & Dostrovsky, 1971) match the mechanisms at work in the primate hippocampus. Edmund T Rolls concludes that the difference in place cell findings, between the research on rodent compared to macaque space processing "[...] may not indicate fundamentally different computations by the hippocampus, but rather may result from different combinations of information passed on to the hippocampus, information that is dictated by the task conditions." (pg.24, Mizumori, 2008).

The visual cell literature and theta-band activity in visual research in primates suggests a possible homologue to rodent movement through space, but there are considerable differences in these types of exploration possibly rendering comparisons to be unfair. Specifically, the present findings revealed a role for SWR in visual search in primates that may have originated in part because of their lack of locomotion during the visual search task. To distinguish the role of

locomotion from exploration, future experiments could run tasks in primates requiring a locomotor component, such as walking to goal locations, or in rodents, tasks requiring non-locomotive exploration such as stationary sampling of visual, auditory or olfactory space. However, despite the task differences between species, this work provides an exciting first step in establishing that macaque SWRs play a role in memory just as SWRs do in rodent.

5.3 Limitations and retrospective

Chapter 2

The data collection and analysis, comparing hippocampal lesioned animals to controls, was quite challenging. The lab with lesioned animals had previously found it difficult to show deficits between the lesion and control group, across the array of tasks they had tried. This was our motivation in introducing the flicker detection task (Change Blindness task) to this experimental group. We anticipated the Change Blindness task would be more sensitive than the previous tasks, which up to this point, had failed to show difference in performance between control and lesion groups.

In retrospect, the behavioral differences between lesion and control groups was substantial, resulting in differing behavioral strategies between the groups. As demonstrated in Chapter 2, the touch rate was much higher for the lesion group, attributable to hyperactivity, which when comparing main effects between groups, gives the initial overall impression that the lesion group is performing better than the control (shorter task durations for lesion group). Not having anticipated the possible existence of such a large behavioral difference between

groups made the analysis quite difficult, until the possible confound behavioral differences, such as touch rate, came into focus.

Another behavioral difference, not covered in chapter 2, was an alternative strategy readily employed by the lesion group, and not the control group. In an earlier version of the experiment, a significant number of targets (targets in which the animals had to touch to end the trial) overlapped in area with the location of the green start square area (target the animals had to touch to start the trial). The trial started when the green start square was pressed, and where the control group would go on to search for the target, the lesion group quickly learned to continue pressing the area in which the green square had appeared. Although this strategy did not work on every trial, it was successful enough that the lesion group employed it consistently throughout an earlier version of this experiment, opting to not search for the target at all. The effect was trial distribution with a bimodal shape (either very fast or very slow) for the lesion group — a very perplexing effect at first. After some deep analysis, the overlap of target areas was discovered, and a subsequent version of the task prepared. This revision (the final version of task which appears in chapter 2) removed all trials with targets that overlapped the green start square, and explicitly controlled for target location by shuffling trial order based on target location, so to minimize target location overlap between trials. This was an important first step in designing the task to constrain possible behavioral strategies for obtaining reward.

Having a better idea of how hippocampal lesions would manifest in behavioral differences between the groups would have greatly streamlined the process of experimental design, data collection, and analysis. However, the data available on such groups (hippocampal lesioned macaques) is limited, and so pre-developed conclusions are not always possible. This is

an interesting anecdote nonetheless that nicely illustrates how unintended consequences (in this case differences in behavioral strategies) between groups can appear to reverse the effect of interest (in this case making it appear lesion group was performing better overall), and the importance of gaining a deep understanding when working with behaviorally based data.

Chapter 3

This paper was the first our lab had published on SWRs in macaques, and the first time any lab had reported SWR during visual exploration (in any species). Earlier versions of the manuscript included just one subject (n =1) - the only animal in which we had observed SWR events up to this point in time. The events were robust, clearly not artifact, established as stereotypical SWR events, and unarguably occurring during exploration, however, the lack of data from another animal was a concern. As we had no other data at this point (plans were in motion for our next implant, but still far off) we turned to other labs which had anecdotally reported the existence of SWRs within their data, which had been reported to be occurring during exploration and/or quiescent states. This meant integrating data from two additional labs into the initial analysis from our lab. Given that all three data sets employed different tasks, encoded into different types of behavioral data structures and schema, and recorded from subjects with different electrophysiology methods, this process quickly became a huge undertaking. At this point, the lab barely had a pipeline in place for processing our own data, and now two additional pipelines had to be built to ingest data from two other labs. Once all the behavioral task data was interpreted and distilled into common data structures, and all the electrode data converted and parsed by behavioral epochs, there still remained the task of detecting SWR events. In one case, the SWR events were extremely sparse, and in the other,

high frequency noise dominated parts of the signal. As SWR detection depends on a power threshold to identify SWR events, both of these situations create confounding situations for detection. In both cases, a substantial amount of time had to be spent looking through many hours of brain signal, to establish where automated tools would work, and where they would fail. After all this work, it was ultimately the addition of a second animal (and SWR data) from our lab, that showed almost identical SWR activity as our first animal that allowed us to publish.

In retrospect, the data from the additional labs did not pay off in terms of time spent (better part of a year), having completed the task did enrich our understanding of SWR in the macaque, in that the data is included in the publication. It is also an illustration of the difficulties of electrophysiology research in primates – if an effect needs to be replicated, one can't simply prepare an additional subject overnight. Mining data from other labs was the seemingly best solution at the time, and this decision would likely be repeated given similar circumstances.

Chapter 4

Showing that there is a memory effect for SWR events in the macaque was a challenging undertaking. There are a two main factors working against this type of analysis – SWR occurrence is sparse (1-2 times a minute during task), and SWR rate of occurrence is confounded by time (more time elapsed increases likelihood of SWR). To compare the time-course of an effect, between conditions, ultimately required complex statistical approaches. The statistical analysis in chapter 4 (shown in figure 3 and figure 4) was developed over many iterations. The moving window approach, combined with permutation testing, is a powerful way to compare time series data, but it is not a straightforward analysis to implement

(especially in the case of testing interactions). Because of the time that it takes to implement such an analysis, there was a trade-off between deciding between using more traditional but more easily implemented statistics, to describe the effect, or to use the more descriptive, but complex methods, to implement moving window approach. Ultimately, earlier versions of the paper chose a hybrid of these options – opting for a moving window in one analysis (for SWR rate), along with more traditional statistical designs for the remainder of the paper (for proximity of eye to target). However, given this version of analysis, a common reviewer complaint was a disjoint between statistical approaches. Ultimately, as a final major revision, the moving window approach was employed to describe the effects throughout the paper.

In retrospect, it seems that the complex but powerful statistical approach should have been used from the start. However, return on investment in time is an important consideration for research, and not every effect can have a nuanced statistical analysis custom designed for it. Starting analysis with descriptive statistics, then moving to the appropriate inferential statistic is not always a straightforward process in research. This highlights how easy it can be to do the technically correct statistics, but still lack explanatory power. In the future, given a time course analysis, the moving window approach will be much higher up on the priority list, given the techniques strong explanatory power in describing the evolution of an effect between groups over time.

5.2 Closing Remarks

The chapter 2 results extend the findings from Chau et al. (2011), establishing a sensitivity of the task to hippocampal lesioned macaques. Lesioned animals were able to perform the task without dramatic deficit on the first day of trial repetition. However, when

compared to the control group, for trials repeated on a second day, the rate of improvement was not equivalent between groups. This confirms that the flicker detection task is indeed a memory task that is sensitive to hippocampal function in macaques.

Chapter 3 established that need exists for research to account for the memories formed, that appear to be hippocampal-dependent, and yet do not require locomotor or ambulatory movement — that is, enriching the literature beyond the traditional SWR work featuring rodent locomotion. SWRs may play a more general or widespread role than previously thought and attentive visual exploration may serve some role in memory independent of locomotion. Showing that SWRs occur during waking experience and visual search is an important contribution to the literature.

Directly following up on chapter 3, chapter 4 shows an increased incidence of SWRs near visual goal detection. This suggests that one consequence of SWR-activity may be to exert a memory-related top-down influence on neural systems that guide behavior. Importantly, it is shown that SWR-mediated mechanisms in primates may support non-ambulatory visual, and episodic-like learning, using past experience to guide visual search towards goals.

5.3 References

Axmacher, N., Elger, C. E., & Fell, J. (2008). Ripples in the medial temporal lobe are relevant for human memory consolidation. *Brain, 131*(Pt 7), 1806-1817. doi:10.1093/brain/awn103

Battaglia, F. P., Sutherland, G. R., & McNaughton, B. L. (2004). Hippocampal sharp wave bursts coincide with neocortical "up-state" transitions. *Learn Mem, 11*(6), 697-704. doi:10.1101/lm.73504

Buzsáki, G., Leung, L. W., & Vanderwolf, C. H. (1983). Cellular bases of hippocampal EEG in the behaving rat. *Brain Res, 287*(2), 139-171.

Buzsáki, G. (1986). Hippocampal sharp waves: their origin and significance. *Brain Res, 398*(2), 242-252.

Clemens, Z., Molle, M., Eross, L., Barsi, P., Halasz, P., & Born, J., et al. (2007). Temporal coupling of parahippocampal ripples, sleep spindles and slow oscillations in humans. *Brain, 130*(11), 2868-2878. doi:10.1093/brain/awm146

Ego-Stengel, V., & Wilson, M. A. (2010). Disruption of ripple-associated hippocampal activity during rest impairs spatial learning in the rat. *Hippocampus, 20*(1), 1-10. doi:10.1002/hipo.20707

Foster, T. C., Castro, C. a, & McNaughton, B. L. (1989). Spatial selectivity of rat hippocampal neurons: dependence on preparedness for movement. *Science (New York, N.Y.)*, *244*, 1580–1582. https://doi.org/10.1126/science.2740902

Georges-François, P., Rolls, E. T., & Robertson, R. G. (1999). Spatial view cells in the primate hippocampus: Allocentric view not head direction or eye position or place. *Cerebral Cortex*, *9*(3), 197–212. https://doi.org/10.1093/cercor/9.3.197

Girardeau, G., Benchenane, K., Wiener, S. I., Buzsáki, G., & Zugaro, M. B. (2009). Selective suppression of hippocampal ripples impairs spatial memory. *Nat Neurosci, 12*(10), 1222-1223. doi:10.1038/nn.2384

Grastyán, E., Lissák, K., Madarász, I., & Donhoffer, H. (1959). Hippocampal electrical activity during the development of conditioned reflexes. *Electroencephalography and Clinical Neurophysiology*, *11*(3), 409–430. https://doi.org/10.1016/0013-4694(59)90040-9

Hoffman, K. L., Dragan, M. C., Leonard, T. K., Micheli, C., Montefusco-Siegmund, R., & Valiante, T. A. (2014). Saccades during visual exploration align hippocampal 3--8 Hz rhythms in human and non-human primates. *Eye Movement-Related Brain Activity during Perceptual and Cognitive Processing*, 80.

Isomura, Y., Sirota, A., Özen, S., Montgomery, S., Mizuseki, K., & Henze, D. A., et al. (2006). Integration and segregation of activity in entorhinal-hippocampal subregions by neocortical slow oscillations. *Neuron, 52*(5), 871-882. doi:10.1016/j.neuron.2006.10.023

Jackson, J. C., Johnson, A., & Redish, A. D. (2006). Hippocampal sharp waves and reactivation during awake states depend on repeated sequential experience. *J Neurosci, 26*(48), 12415-12426. doi:10.1523/JNEUROSCI.4118-06.2006

Jadhav, S. P., Kemere, C., German, P. W., & Frank, L. M. (2012). Awake hippocampal sharp-wave ripples support spatial memory. *Science, 336*(6087), 1454-1458. doi:10.1126/science.1217230

Ji, D., & Wilson, M. A. (2007). Coordinated memory replay in the visual cortex and hippocampus during sleep. *Nat Neurosci, 10*(1), 100-107. doi:10.1038/nn1825

Jutras, M., Fries, P., & Buffalo, E. (2013). Oscillatory activity in the monkey hippocampus during visual exploration and memory formation. *Proceedings of the National …*, *110*(32), 13144–9. https://doi.org/10.1073/pnas.1302351110

Kucewicz, M. T., Cimbalnik, J., Matsumoto, J. Y., Brinkmann, B. H., Bower, M. R., Vasoli, V., … Worrell, G. A. (2014). High frequency oscillations are associated with cognitive processing in human recognition memory. *Brain : A Journal of Neurology*, *137*(Pt 8), 2231–44. https://doi.org/10.1093/brain/awu149

Lansink, C. S., Goltstein, P. M., Lankelma, J. V., McNaughton, B. L., & Pennartz, C. M. A. (2009). Hippocampus leads ventral striatum in replay of place-reward information. *PLoS Biol, 7*(8)

Leonard, T. K., Mikkila, J. M., Eskandar, E. N., Gerrard, J. L., Kaping, D., Patel, S. R., … Hoffman, K. L. (2015). Sharp Wave Ripples during Visual Exploration in the Primate Hippocampus. *The Journal of Neuroscience : The Official Journal of the Society for Neuroscience*, *35*(44), 14771–82. https://doi.org/10.1523/JNEUROSCI.0864-15.2015

Mizumori, S. J. Y. (2008). *Hippocampal Place Fields: Relevance to Learning and Memory*. *Hippocampal Place Fields: Relevance to Learning and Memory*. https://doi.org/10.1093/acprof:oso/9780195323245.001.0001

Mölle, M., Yeshenko, O., Marshall, L., Sara, S. J., & Born, J. (2006). Hippocampal sharp wave-ripples linked to slow oscillations in rat slow-wave sleep. *J Neurophysiol, 96*(1), 62-70. doi:10.1152/jn.00014.2006

O'Keefe, J., & Dostrovsky, J. (1971). The hippocampus as a spatial map. Preliminary evidence from unit activity in the freely-moving rat. *Brain Research*, *34*(1), 171–175.

Peyrache, A., Khamassi, M., Benchenane, K., Wiener, S. I., & Battaglia, F. P. (2009). Replay of rule-learning related neural patterns in the prefrontal cortex during sleep. *Nat Neurosci, 12*(7), 919-926. doi:10.1038/nn.2337

Ramadan, W., Eschenko, O., & Sara, S. J. (2009). Hippocampal sharp wave/ripples during sleep for consolidation of associative memory. *PloS one, 4*(8), e6697. doi:10.1371/journal.pone.0006697

927–932. https://doi.org/10.1111/j.1467-9280.2007.02003.x.Gamma

Siapas, A. G., & Wilson, M. A. (1998). Coordinated interactions between hippocampal ripples and cortical spindles during slow-wave sleep. *Neuron, 21*(5), 1123-1128.

Singer, A. C., & Frank, L. M. (2009). Rewarded outcomes enhance reactivation of experience in the hippocampus. *Neuron, 64*(6), 910-921. doi:10.1016/j.neuron.2009.11.016

Sirota, A., Csicsvari, J., Buhl, D., & Buzsáki, G. (2003). Communication between neocortex and hippocampus during sleep in rodents. *Proc Natl Acad Sci U S A, 100*(4), 2065-2069. doi:10.1073/pnas.0437938100

Vanderwolf, C. H. (1969). Hippocampal electrical activity and voluntary movement in the rat. *Electroencephalography and Clinical Neurophysiology*, *26*(4), 407–418. https://doi.org/10.1016/0013-4694(69)90092-3

Wierzynski, C. M., Lubenov, E. V., Gu, M., & Siapas, A. G. (2009). State-Dependent Spike-Timing Relationships between Hippocampal and Prefrontal Circuits during Sleep. *Neuron, 61*(4), 587-596.

Wolansky, T., Clement, E. A., Peters, S. R., Palczak, M. A., & Dickson, C. T. (2006). Hippocampal Slow Oscillation: A Novel EEG State and Its Coordination with Ongoing Neocortical Activity. *Endocrinol Metab Clin North Am, 26*(23), 6213-6229.

Appendix A - Collaborative contributions to this work

Chapter 2:
Data collected by Tom Hassett, Tara Dove-VanWormer, lesions performed, under supervision of Robert Hampton

Chapter 3:
Jonathan M. Mikkila: Analyzed data (Section: Comparing SWRs to high-gamma oscillations and HFOs (ε80-120, ε110-160))
Emad Eskandar: Contributed unpublished data (M2)
Jason L. Gerrard: Designed research, performed research, contributed unpublished data (M2)
Shaun R. Patel: Performed research, contributed unpublished data (M2)
Daniel Kaping,: Performed research (M3)
Thilo Womelsdorf: Designed research, performed research, analyzed data (M3)
Kari L. Hoffman: Designed research, Performed research, (M1) Analyzed data

This chapter was reprinted, with permission, from:
Leonard, T. K., Mikkila, J. M., Eskandar, E. N., Gerrard, J. L., Kaping, D., Patel, S. R., Hoffman, K. L. (2015). Sharp Wave Ripples during Visual Exploration in the Primate Hippocampus. *The Journal of Neuroscience : The Official Journal of the Society for Neuroscience*, *35*(44), 14771–82.

Chapter 4:
Kari L. Hoffman contributed to the conceptualization, investigation, and writing of this manuscript, with Tim Leonard conducting the formal analysis under the supervision of Kari L. Hoffman

This chapter was reprinted, with permission, from:
T. K. Leonard, K. L. Hoffman (2016) Sharp-wave ripples in primates are enhanced near remembered visual objects. *Current Biology.* (Dec. 29 2016)

Funding Acknowledgements:
Krembil Foundation, NSERC Discovery Grant, NSERC CREATE VSA, OGS QEII-GSST, Brain Canada, Canada Foundation for Innovation, Alfred P. Sloan Foundation

As per FGS regulations, I (Tim Leonard) certify the information on this page is valid and correct.

Appendix B – Chapter 2 supplementary materials

Supplementary touch rate information

Methods

Touch rate ranksum

As validation against the touch rate regression test, the main effect was also tested using a non-parametric approach, as the distribution of residuals from the regression results were non-normal.

The touch rate was calculated, for each trial, as number of touches, divided by duration of trial. Significance testing between the median rate for the lesion group was compared to control group using a ranksum test. This test was chosen due to the non-normal distribution of the trial rates.

Touch rate regression

The touch rate was compared across groups, and image repetitions, using a regression model, in order to determine which factors affect touch rate. Touch rate (touch/second) was predicted on group (control or lesion), day of image (Day of Repeat; 1 or 2), and presentation number within day image was shown (Within Day Repeat; 1 or 2). Interaction terms were set between group and day of image, as well as, group and repeat within day of image.

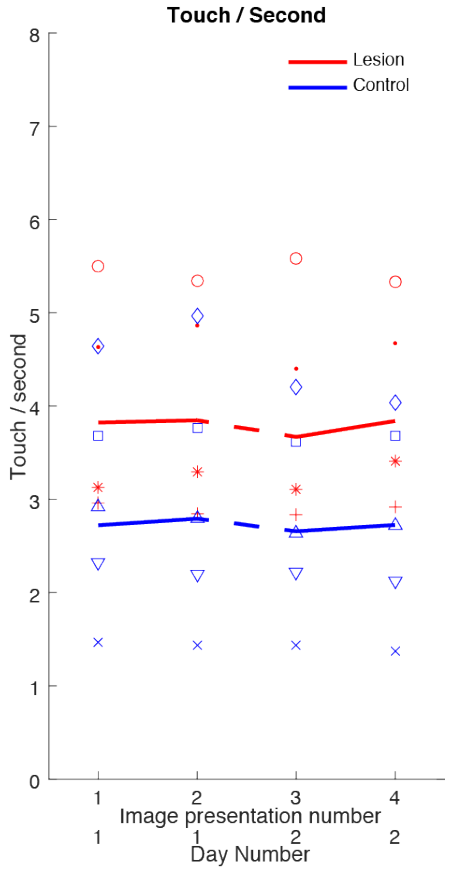

Figure 1: Mean touch rates.

Mean number of screen touches per second, is higher for the lesion group compared to the control group (see results). Within day portions of trial shown in solid lines. Individual data points for each subject shown.

Results

Touch rate ranksum results

The touch rate (touches/second) was higher for the lesion group (mean: 4.04 [3.99 4.09]) compared to the control group (mean: 2.93[2.89 2.98]; ranksum test, z(control: 4485, lesion: 3780) = 33.45, $p < 2.9x10^{245}$).

	Mean [ci]
Group	
control	2.93[2.89 2.98]
lesion	4.04[3.99 4.09]
Within Day Repeat	
1	3.44[3.39 3.49]
2	3.44[3.39 3.49]
Day of Repeat	
1	3.47[3.43 3.51]
2	3.37[3.31 3.43]

Table 1: Touch rate regression model - Summary of main effects rate.

Touch rate (touch/second) predicted on factors listed.

Group	Within Day 1	Within Day 2	Day 1	Day 2
control	2.96 [2.89 3.02]	2.91 [2.85 2.97]	2.96 [2.91 3.01]	2.87 [2.79 2.95]
lesion	4.01 [3.94 4.08]	4.07 [4.00 4.14]	4.06 [4.01 4.11]	3.99 [3.90 4.08]

Table 2: Touch rate regression model - Summary of interaction terms

Mean touches per second shown. Confidence intervals (ci) are bootstrapped mean values (10,000 permutations).

Appendix C – Chapter 3 supplementary materials

Validating SWR detection methodology

The use of a variance-based threshold allows comparison to the rest of the research in SWR detection, which uses this standard, though, such a threshold may be affected by variance. Simply put, an increase in SWR rate may affect the threshold, increase the number of false negative SWRs detected. In order to address this possible confound, the following analysis was performed.

If SWRs increase variance then an increase in their occurrence can be expected to also increase this threshold; however, due to their sparsity relative to the ongoing continuously recorded signal, the impact of different ripple rates on the threshold is actually quite small. For typical-duration sessions with typical ripple counts, ripples occupy around 1/1000th of the continuously-recorded signal (for the session described below, it was 0.09% or 3.3s / 3,856.2s). This already gives a general sense of how buffered the threshold is against differences in SWR count.

To illustrate the impact of SWR rate on the detection threshold more directly, we selected an LFP channel with a typical number of ripples from a session of typical duration and removed all detected ripples. The underlying value of the filtered signal corresponding to a zscore of 3 was calculated (this value was 0.0851 mV). The pool of extracted SWR events were then systematically added back into the signal, and the new threshold was calculated with each additional ripple. Based on that threshold value, we asked how many of the original ripples would have been below the threshold based on the simulated ripple rate. Although it would be

remarkable to observe double the number of ripples in a session, we didn't see any change in ripple detection with twice the ripple rate. By increasing the rate further, we found that it wasn't until a *fourfold increase* in ripple rate, when a single ripple fell under that threshold value. After a 5x increase in ripple events, the underlying signal value corresponding to the threshold rose from 0.0851 to 0.0894 mV, raising the zscore threshold value by .1, or 3.3% (the effect of this threshold change is shown for two ripples in figure 1b, top).

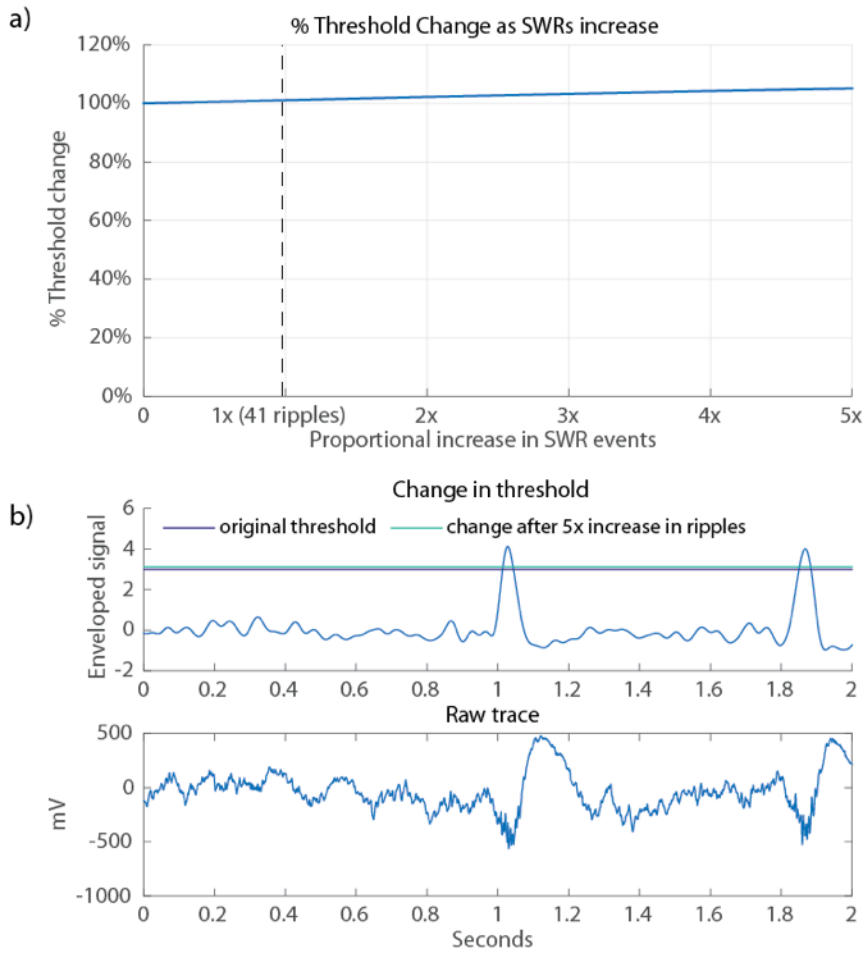

Figure 1: Effect of SWR Rate on Threshold Sensitivity

a. Change in the underlying filtered signal value corresponding to a zscore of 3 as the number of SWR increases up to 5 times the original numbers of ripples. b. Top, an example of two ripples, here the envelope values (final detection step) are shown. A zscore of 3 (original signal - 41 events) is shown by a blue horizontal line, the change after 5x increase in SWR events is shown in green. Bottom, the raw trace is shown for both events.

Clustering Local vs. Global Saccades

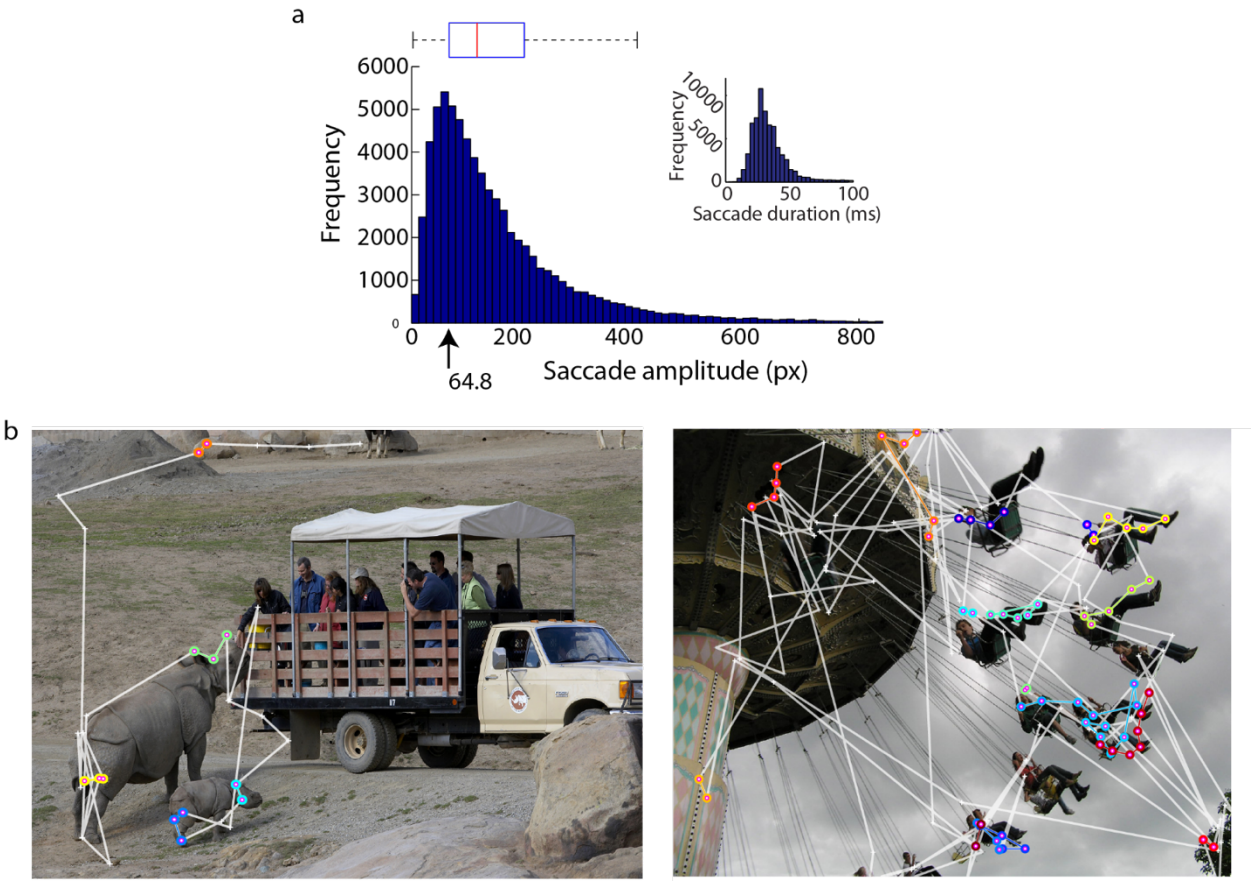

Figure 2: Grouping Fixations Based on Saccade Amplitude.

a. Distribution of all saccade amplitudes during active exploration trials (Distribution of all saccade durations, inset). Top, edges of blue box represents first and third quartile, middle red line is the median. Bottom, arrow at first quartile, the threshold used for grouping saccade distances. b. Examples of saccade grouping based on contiguous saccades shorter than first quartile of all saccade distances. Here, local search fixations are highlighted with colored dots. Each group of local fixations is separately colored. Non-local search fixations represented with white +.

Appendix D - Additional research contributions

Leonard, T. K., & Hoffman, K. L. (2016). Sharp-wave ripples in primates are enhanced near remembered visual objects. *Current Biology*, *(in press)*.

Leonard, T. K., Mikkila, J. M., Eskandar, E. N., Gerrard, J. L., Kaping, D., Patel, S. R., … Hoffman, K. L. (2015). Sharp Wave Ripples during Visual Exploration in the Primate Hippocampus. *The Journal of Neuroscience : The Official Journal of the Society for Neuroscience*, *35*(44), 14771–82. https://doi.org/10.1523/JNEUROSCI.0864-15.2015

Dragan, M. C., **Leonard, T. K**., Lozano, A. M., McAndrews, M. P., Ng, K., Ryan, J. D., … Hoffman, K. L. (2016). Pupillary responses and memory-guided visual search reveal age-related and Alzheimer's-related memory decline. *Behavioural Brain Research*. article.

Montefusco-Siegmund, R., **Leonard, T.K**., and Hoffman, K.L. Hippocampal gamma band synchrony and pupillary responses index memory during visual search, 2016. doi: http://dx.doi.org/10.1002/hipo.22702. In Press

Hoffman, K. L., Dragan, M. C., **Leonard, T. K**., Micheli, C., Montefusco-Siegmund, R., & Valiante, T. A. (2014). Saccades during visual exploration align hippocampal 3--8 Hz rhythms in human and non-human primates. *Eye Movement-Related Brain Activity during Perceptual and Cognitive Processing*, 80. article.